Adsorptive Removal of Fluoride from Contaminated Water Using Ceramic Materials

A Dissertation Submitted to

the Graduate School of Life and Environmental Sciences,

the University of Tsukuba

in Partial Fulfillment of the Requirements

for the Degree of Doctor of Environmental Studies

(Doctoral Program in Sustainable Environmental Studies)

Nan CHEN

Abstract

High fluoride levels in drinking water has become one of the most critical health hazards and more and more people have been drawn attention to this problem. Fluoride in nature exists as mineral deposits and, naturally, contaminates our ground water resources. Besides, surface water is also being polluted by fluoride due to various anthropogenic activities. Fluoride is very toxic, when it is taken in excess (3.18mg/L), leading to inhibition of infant's brain/mind development. This results abnormal behaviors and reduce IQ in children. The permissible limit of fluoride concentration in drinking water is 1.5mg/L according to WHO guidelines. And fluoride contamination in groundwater is a worldwide problem and many regions have fluoride concentration higher than prescribed by WHO, which is a serious threat to flora and fauna including humans. The adsorption method is an attractive alternative to other treatment because of its environmental respectability and ease of operation.

In recent years, considerable attention has been focused on the study of fluoride removal using natural, synthetic and biomass materials. They have shown a certain degree of fluoride adsorption capacities but some of them can only be used in a narrow pH range (5-6) and some of them are too expensive to be considered for full-scale water treatment. Furthermore, most of them are fine particles or powders which would be suspended in water, making separation difficult and blocking flumes. Therefore, an effective and low-cost adsorbent with coarse particles is desired as an efficient treatment technology for fluoride in large-scale water samples. We have

successfully combined Kanuma mud, with starch, zeolite and $FeSO_4 \cdot 7H_2O$ salts to calcine ceramic materials and investigated the fluoride adsorption capability of these adsorbents. BET, SEM, XRD, FTIR and EDS were used to characterize the physical attributes (particle size, pore size and distribution, surface roughness) of the granular ceramics. Fluoride adsorption characteristics were studied in a batch system with respect to changes in initial concentration of fluoride, initial pH of solution, adsorbent dose and co-existing ions. Fluoride adsorption was found to be pH dependent and the maximum removal of fluoride was obtained at pH 4.0-9.0. The equilibrium data have been analyzed by the Langmuir and Freundlich isotherm models. The adsorption kinetics also investigated by the pseudo-first-order and pseudo-second-order kinetic models. The intra-particle diffusion was indicated to play a major role in fluoride uptake in the adsorption process. The presence of nitrate and sulfate did not interfere much with fluoride adsorption while chloride had a slightly negative influence. However, carbonate and phosphate showed extremely negative effect for fluoride removal efficiency. Regeneration of these granular ceramic adsorbents was done with 0.1 M HCl as eluent. The regenerated adsorbents were shown to be effective even after 4 cycles.

On the other hand, this research has developed another kind of adsorbent, which was prepared by mixing Knar clay/King Kong clay, zeolite and starch with mass ratio 1:1:1. Porous granular ceramic adsorbents that contain dispersed aluminum and iron oxides have been synthesized by impregnating with salt solutions followed by precipitation at 600 °C. This adsorbent was sphere in shape, 2~3 mm in particle size,

Contents

Tables

Figures

Chapter 1 Introduction

Fluoride is a common element, but it occurs as fluorides in nature because of its high activity. It accounts for about 0.3 g/kg of the Earth's crust and exists in the form of fluorides in a number of minerals, of which fluorspar, cryolite and fluorapatite are the most common. Fluorine is highly reactive and is found naturally as CaF_2. It is an essential constituent in minerals like topaz, fluorite, fluorapatite, cryolite, phosphorite, theorapatite, etc. (Singn and Maheshwari, 2001). The oxidation state of the fluoride ion is -1. Inorganic fluorine compounds was mainly used in industry such as for aluminum production, flux in the steel and glass fiber industries. They can also be released to the environment during the production of phosphate fertilizer (which contain an average of 3.8% fluorine), bricks, tiles and ceramics. Fluorosilicic acid, sodium hexafluorosilicate and sodium fluoride are used in municipal water fluoridation schemes (IARC, 1982; IPCS, 2002).

Although fluoride was an essential element for humans (mainly in tooth and skeleton), it was limited in a very narrow range. The World Health Organization has suggested a value below 1 mg/L to 1.5 mg/L for areas with warm climates (WHO). Fluoride is known to cross cell membranes and to enter soft tissues. Impairment of soft-tissue function has been demonstrated in fluoride-intoxicated animals. In blood, brain, and liver of animals, various changes occur after chronic administration of fluoride. These include abnormal behavior patterns, altered neuronal cerebrovascular integrity, and metabolic lesions. Generation of free radicals, lipid peroxidation, and

altered antioxidant defense systems are considered to play important roles in producing toxic effects of fluoride. No matter the fluoride exist in the air or water, once human ingest it from environment over the value, it will be toxic to human, even may lead to fluorosis.

Endemic fluorosis is widely distributed throughout the world, covering over forty countries such as India, Mexico and Africa etc (Tan, 1990; Misra and Mishra, 2007; Grimaldo et al., 1995; Malde et al., 1997). It is also extensively distributed in China except Shanghai and Hainan province, and more than 1.34 million patients who are distributed in 1115 countries, has suffered from skeletal fluorosis due to high fluoride drinking water in 2006. In China, however, in addition to cases of endemic fluorosis from drinking water, there are other two types of endemic fluorosis, which are caused by the pollution from local coal burning and by drinking brick tea with high fluoride concentration (Wang and Huang, 1995; Li et al., 2009). It has been found that drinking brick tea type fluorosis is prevalent mainly among the minority inhabitants in the west of China, and the prevalence of fluorosis provoked by brick tea drinking has attracted more and more attention (Wang, 1993; Cao et al., 1997). It has been observed that low calcium and high bicarbonate alkalinity favor high fluoride content in groundwater (Bulusu and Pathak, 1980; Hem, 1959). Water with high fluoride content is generally soft, has high pH and contains large amount of silica. In groundwater, the natural concentration of fluoride depends on the geological, chemical and physical characteristics of the aquifer, the porosity and acidity of the soil and rocks, temperature, the action of other chemicals and the depth of wells. Due

to large number of variables, the fluoride concentration in groundwater range from well number under 1.0 mg/L to more than 35 mg/L (IPCS, 1984).

Because of its health risks, defluoridation of drinking water is the best practicable option to overcome the problem of excessive fluoride in drinking water, where alternate source is not available. During the years following the discovery of fluoride as the cause of fluorosis, extensive research has been done on various methods for removal of fluoride from water and wastewater. These methods are based on the principle of adsorption (Raichur and Basu, 2001), ion-exchange (Singh et al., 1999), precipitation-coagulation (Saha, 1993), membrane separation process (Dieye et al., 1998), electrodialysis (Hichour et al., 1999), etc.

1.1. Iron-exchange treatment methods

Fluoride can be removed from water supplies with a strongly basic anion-exchange resin containing quarternary ammonium functional groups. The removal takes place according to the following reaction:

$$\text{Matrix} - NR_3^+Cl^- + F^- \rightarrow \text{Matrix} - NR_3^+F^- + Cl^- \qquad (1.1)$$

The fluoride ions replace the chloride ions of the resin. This process continues until all the sites on the resin are occupied. The resin is then backwashed with water that is supersaturated with dissolved sodium chloride salt. New chloride ions then replace the fluoride ions leading to recharge of the resin and starting the process again. The driving force for the replacement of chloride ions from the resin is the stronger electronegativity of the fluoride ions. The advantages of this method are high fluoride

removal efficiency (90-95%) and can retain the taste and color of water intact. There are also a lot of limitations in this method. The fluoride removal efficiency will reduce in the presence of sulfate, carbonate, phosphate ions etc. The regeneration of resin is a problem because it leads to fluoride rich waste, which has to be treated separately before final disposal. Besides, the treated water has a very low pH and high levels of chloride (Meenakshi and Maheshwari, 2006).

1.2. Coagulation-precipitation treatment methods

This method always used lime and alum as the coagulants. Addition of lime leads to precipitation of fluoride as insoluble calcium fluoride and raises the pH value of water up to 11-12.

$$Ca(OH)_2 + 2F^- \rightarrow CaF_2 + 2OH^- \quad (1.2)$$

As lime leaves a residue of 8.0 mg/L, it is used only in conjunction with alum treatment to ensure the proper fluoride removal (Culp and Stolenberg, 1958; Parker and Fong, 1975). The Nalgonda technique of defluoridation is based on combined use of alum and lime in a two-step process and has been claimed as the most effective technique for fluoride removal (Nawalakhe et al., 1974). However, in the precipitation process, chemical precipitants, coagulants, and flocculantation are used to increase particle size through aggregation. The precipitation process can generate very fine particles that are held in suspension by electrostatic surface charges. These charges cause clouds of counter-ions to form around the particles, giving rise to repulsive forces that prevent aggregation and reduce the effectiveness of subsequent solid-liquid

separation processes. Therefore, chemical coagulants are often added to overcome the repulsive forces of the particles. The three main types of coagulants are inorganic electrolytes (such as alum, lime, ferric chloride, and ferrous sulfate), organic polymers, and synthetic polyelectrolytes with anionic or cationic functional groups. The addition of coagulants is followed by low-sheer mixing in a flocculator to promote contact between the particles, allowing particle growth through the sedimentation phenomenon called flocculant settling. The cogulation-precipitation process only can remove 18%-33% fluoride in the form of precipitates and converts 67%-82% ionic fluoride into soluble aluminum fluoride complex ion. Since the soluble aluminum fluoride complex is itself toxin, this method is also not quite desirable (Apparao and Kartikeyan, 1986). Besides, the maintenance cost of plant by this method is very high and silicates also have adverse effect on defluoridation.

1.3. Membrane process treatment methods

Membrane processing is a technique that permits concentration and separation without the use of heat. Particles are separated on the basis of their molecular size and shape with the use of pressure and specially designed semi-permeable membranes. Reverse osmosis (RO) designates a membrane separation process, driven by a pressure gradient, in which the membrane separates the solvent (generally water) from other components of a solution. The membrane configuration is usually cross-flow. With reverse osmosis, the membrane pore size is very small allowing only small amounts of very low molecular weight solutes to pass through the membranes. In the

resent years, RO membrane process has emerged as a preferred alternative to provide safe drinking water without posing the problem associated with other conventional methods. RO membrane rejects ions based on size and electrical charge. The factors influencing the membrane selection are cost, recovery, rejection, raw water characteristics and pretreatment. Efficiency of the process is governed by different factors such as raw water characteristics, pressure, temperature and regular monitoring and maintenance, etc.

The process of this method is highly effective for fluoride removal and can permit the treatment and disinfection of water in one step. It also can work under a wide pH range, and no interference by other ions is observed. However, this process would remove all the ions present in water, though some minerals are essential for proper growth, remineralization is required after treatment. The process is also very expensive and lots of water gets wasted as brine.

1.4. Electrodialysis process treatment methods

Electrodialysis (ED) is used to transport salt ions from one solution through ion-exchange membranes to another solution under the influence of an applied electric potential difference. This is done in a configuration called an electrodialysis cell. The cell consists of a feed (dilute) compartment and a concentrate (brine) compartment formed by an anion exchange membrane and a cation exchange membrane placed between two electrodes. In almost all practical electrodialysis processes, multiple electrodialysis cells are arranged into a configuration called an

electrodialysis stack, with alternating anion and cation exchange membranes forming the multiple electrodialysis cells. Electrodialysis processes are different compared to distillation techniques and other membrane based processes (such as reverse osmosis) in that dissolved species are moved away from the feed stream rather than the reverse. Because the quantity of dissolved species in the feed stream is far less than that of the fluid, electrodialysis offers the practical advantage of much higher feed recovery in many applications. Electrodialysis has inherent limitations, working best at removing low molecular weight ionic components from a feed stream. Non-charged, higher molecular weight, and less mobile ionic species will not typically be significantly removed. Also, in contrast to RO, electrodialysis becomes less economical when extremely low salt concentrations in the product are required and with sparingly conductive feeds: current density becomes limited and current utilization efficiency typically decreases as the feed salt concentration becomes lower, and with fewer ions in solution to carry current, both ion transport and energy efficiently greatly declines. Consequently, comparatively large membrane areas are required to satisfy capacity requirements for low concentration (and sparingly conductive) feed solutions. Innovative systems overcoming the inherent limitations of electrodialysis are available; these integrated systems work synergistically, with each sub-system operating in its optimal range, providing the least overall operating and capital costs for a particular application. As with RO, electrodialysis systems require feed pretreatment to remove species that coat, precipitate onto, or otherwise "foul" the surface of the ion exchange membranes. This fouling decreases the efficiency of the

electrodialysis system. Species of concern include calcium and magnesium hardness, suspended solids, silica, and organic compounds. Water softening can be used to remove hardness, and micrometre or multimedia filtration can be used to remove suspended solids. Hardness in particular is a concern since scaling can build up on the membranes. Various chemicals are also available to help prevent scaling. Also, electrodialysis reversal systems seek to minimize scaling by periodically reversing the flows of dilute and concentrate and polarity of the electrodes.

1.5. Adsorption process treatment methods

Adsorption is the adhesion of molecules of gas, liquid, or dissolved solids to a surface (Brandt et al., 1993). This process creates a film of the adsorbate (the molecules or atoms being accumulated) on the surface of the adsorbent. It differs from absorption, in which a fluid permeates or is dissolved by a liquid or solid. The term sorption encompasses both processes, while desorption is the reverse of adsorption. Similar to surface tension, adsorption is a consequence of surface energy. In a bulk material, all the bonding requirements (be they ionic, covalent, or metallic) of the constituent atoms of the material are filled by other atoms in the material. However, atoms on the surface of the adsorbent are not wholly surrounded by other adsorbent atoms and therefore can attract adsorbates. The exact nature of the bonding depends on the details of the species involved, but the adsorption process is generally classified as physisorption (characteristic of weak van der Waals forces) or chemisorption (characteristic of covalent bonding). Adsorption is present in many

natural physical, biological, and chemical systems, and is widely used in industrial applications such as activated charcoal, capturing and using waste heat to provide cold water for air conditioning and other process requirements (adsorption chillers), synthetic resins, increase storage capacity of carbide-derived carbons for tunable nanoporous carbon, and water purification. Adsorption, ion exchange, and chromatography are sorption processes in which certain adsorbates are selectively transferred from the fluid phase to the surface of insoluble, rigid particles suspended in a vessel or packed in a column.

Several adsorbent materials have been tried in the past to find out an efficient and economical material. Activated alumina, activated carbon, activated aluminum coated silica gel, calcite, fly ash, bone charcoal, laterite, red mud, etc., are different adsorbent materials reported in the literature (Barbier and Mazounie, 1984; Muthukumaran et al., 1995; Wang et al., 1995; Min et al., 1999; Mckee and Johnston, 1999; Sarkar et al., 2006; Tor et al., 2009). The most commonly used adsorbents are activated alumina and activated carbon. The fluoride removing efficiency of activated alumina gets affected by hardness and surface loading. Chloride does not affect the defluoridation capacity of activated alumina. The process is pH specific, so pH of the solution should be between 5.0 and 6.0 because at pH>7, silicate and hydroxide become stronger competitor of the fluoride ions for exchange sites on activated alumina and at pH less than 5. Activated alumina technique for defluoridation is being propagated in several villages by the voluntary organizations funded by UNICEF or other agencies to provide safe drinking water. The adsorption process can remove fluoride up to 90%

and the treatment is very cost-effective. Therefore, adsorption is the most widely used method in the world. However, this method can be improved by developing some novel, efficiency, low cost adsorbents in practical application.

1.6. The originality and objective of the study

1.6.1. The originality and objective

From the review of numerous studies in fluoride removal by adsorption method, applications of the adsorption method are limited mainly due to the narrow pH range, high concentration of total dissolved salts (TDS) which will result in fouling of the alumina bed, low capacity and poor integrity. Therefore, in the present study, the focal points are to develop a novel adsorbent which can overcome disadvantages of the above. The originalities are such follows,

1) Performing batch studies to examine fluoride adsorption using Kanuma mud (only spreading in Japan) (effect of initial fluoride concentration and pH, adsorption isotherm and kinetics). Designing the column studies to investigate the fluoride uptake characteristics of the Kanuma mud under different flow rates, bed depths and influent fluoride concentrations.
2) Combining the Kanuma mud which is widespread in Japan with starch, natural zeolite and $FeSO_4 \cdot 7H_2O$ to calcine ceramic materials which are robust, porous, effectively to remove fluoride and also can avoid clogging during field applications.
3) Investigating the adsorption feasibility of this adsorbent for fluoride under

different parameters such as contact time, pH, adsorbent dose, initial fluoride concentration etc, and discussing the possible mechanism of fluoride onto these ceramic materials.

4) Combining the Knar clay, starch and zeolite to prepare the ceramics with the mass ratio of 1:1:1. Then the granular ceramic were impregnated by Fe/Al salt solutions and investigate the adsorption feasibility of this adsorbent for fluoride and discussed the possible mechanism of fluoride onto these prepared materials.

5) Combining the King Kong clay, starch and zeolite to prepare the ceramics with the mass ratio of 1:1:1 and then to develop a novel iron (III)-aluminum (III) impregnated granular ceramic adsorbent. Performing a batch study to investigate fluoride adsorption ability by using these prepared adsorbents.

1.6.2. Content of the study

During the fluoride adsorption process by using the prepared adsorbents, the following factors were investigated,

(1) Selection of suitable fluoride adsorption granular ceramics;

(2) Effect of contact time;

(3) Effect of initial solution pH;

(4) Effect of adsorbent dose;

(5) Effect of co-existing anions;

(6) Adsorption isotherms;

(7) Adsorption kinetics;

(8) Intra-particle diffusion model;

(9) The possible adsorption mechanism;

(10) Column studies (flow rate, bed depth, and influent fluoride concentration)

The results of this study are divided into six parts so as to present the experiments results clearly, and every part of the experiment can be individually understood without reading other parts.

In the first part of this study (Chapter 2), we investigated the fluoride adsorption ability using one kind of natural mud in a batch study. Kanuma mud, a geomaterial, is used as an adsorbent for the removal of fluoride from water. The influences of contact time, solution pH, adsorbent dosage, initial fluoride concentration and co-existing ions were investigated by batch equilibration studies.

In the second part of study (Chapter 3), we investigated the fluoride adsorption ability using Kanuma mud in a batch (different from Chapter 2) and column study. The removal of fluoride from water by Kanuma mud using batch and fixed-bed column adsorption techniques was investigated.

In the third part of this study (Chapter 4), we investigated the fluoride adsorption process by using one kind of prepared granular ceramics. A new media, granular ceramic, has been developed for fluoride removal from water. Granular ceramic is a solid phase media that produces a stable Al-Fe surface complex for fluoride adsorption. BET, SEM and EDS were used to characterize the physical attributes (particle size, pore size and distribution, surface roughness) of the granular ceramic. Fluoride adsorption characteristics were studied in a batch system with respect to

changes in initial concentration of fluoride, pH of solution and co-existing ions.

In the fourth part of this study (Chapter 5), we compared two kinds of different granular ceramic materials in the fluoride adsorption process. This study evaluated the effectiveness of iron-impregnated granular ceramics in removing fluoride from aqueous solution. Kanuma mud, zeolite, starch and $FeSO_4 \cdot 7H_2O/Fe_2O_3$ mixed to prepare granular ceramic at room temperature by granulation procedure with the mass ratio of 4:3:2:1. Both the adsorbents were characterized by SEM, EDS and BET surface area. The various experimental parameters investigated for fluoride adsorption from aqueous solution were: contact time, initial pH, initial fluoride concentration and temperature.

In the fifth part of this study (Chapter 6), we developed a new kind of granular ceramic adsorbent by mixing the Knar clay, zeolite and starch. Porous granular ceramic adsorbents containing dispersed aluminum and iron oxides have been synthesized by impregnating with salt solutions followed by precipitation at 600 °C. In the present work detailed studies were carried out to understand the effect of contact time, adsorbent dose, initial solution pH and co-existing anions. Characterisation studies on the adsorbent by SEM, XRD, EDS, and BET analysis were carried out to understand the adsorption mechanism.

In the sixth part of this study (Chapter 7), we investigated another kind of granular ceramic adsorbent by mixing the King Kong clay, zeolite and starch. A novel iron (III)-aluminum (III) impregnated granular ceramic adsorbent has been developed for fluoride removal from aqueous solution. Batch experiments were performed to study

the effect of various experimental parameters such as contact time, initial pH, adsorbent dose and the presence of competing anions on the adsorption of fluoride.

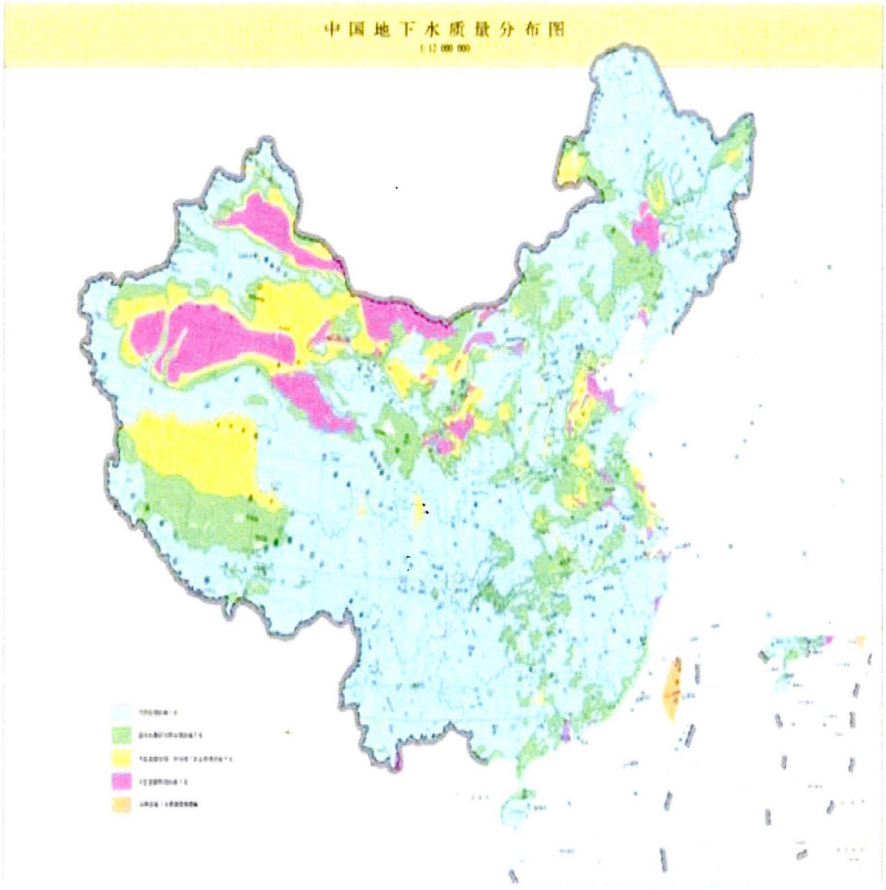

Fig.1.1 Fluoride affected areas in China (red colored) (http://image.baidu.com/)

Chapter 2 Removal of Fluoride by Adsorption onto Kanuma Mud

2.1. Introduction

In recent years, high fluoride levels in drinking water has become one of the most critical health hazards and more and more people have been drawn attention to this problem. Fluoride is a naturally occurring element in minerals, geochemical deposits and natural water systems and enters food chains through either drinking water or eating plants and cereals (Sushree et al., 2006). Fluoride in drinking water may be benificial or may have detrimental effects on health depending on concentration of fluoride present in it (Meenakshi et al., 2008). Generally, fluoride is added to drinking water in small quantities to prevent dental caries but its excess presence will be responsible for teeth mottling and bone fluorosis. There are various reports and studies established both the risks of high fluoride dosing and benefits of mineral exposure (Hichour et al., 2000). According to the World Health Organization (WHO) guidelines, the fluoride concentration in drinking water should not exceed 1.5mg/L (WHO, 2004). However, this guideline value of fluoride is not universal. Actually, there are still many countries existing high fluoride in drinking water or underground water, especially in India and Chinese northwestern regions.

There are a number of defluoridation methods which have been suggested for using in the removal of fluoride in other literatures. Recently, innovative techniques such as electrochemical (Shen et al., 2003), electrocoagulation-flotation (Hu et al., 2005), ion exchange (Meenakshi and Viswanathan, 2007), membrane filtration (Ndiaye et al.,

2005), Donnan dialysis (Tor, 2006), fluidized-bed precipitation (Aldaco et al., 2005), reverse osmosis (Sourirajan and Matsurra, 1972), nanofiltration (Simons, 1993) and adsorption (Cengeloglu et al., 2002) were investigated for fluoride removal in water.

Among these methods, adsorption is considered as the best popular technique using for the treatment of underground water or drinking water. Therefore, considerable attention focused on the study of different kinds of socially acceptable, technically feasible, and economically viable robust adsorbents (Ayoob et al., 2008) such as activated alumina, red mud (Cengeloglu et al., 2002), alum, charcoal, kaolinite, bentonite, bonechar, carbonaceous materials (Ikuo et al., 2008), calcite (Yang et al., 1999), montmorillonite (Tor, 2006), bleaching earth (Mahramanlioglu et al., 2002), etc., for adsorption of fluoride ion from water (Tor et al., 2009). However the most widely used adsorbents are activated carbons and activated alumina in terms of field applicability. But, activated carbons have very high cost and its difficult regeneration is also of a major concern. Activated alumina is one of the most popular adsorbents for defluoridation of drinking water (Ghorai and Pant, 2005; Das et al., 2005). However, the slow rate of adsorption of commercially available activated alumina limits its use for treating large quantity of water (Shihabudheen et al., 2008). In order to overcome the above-mentioned shortcomings, more environmental friendly and effective adsorbents, which can be more economically, applicable, availably and effectively, needed to be developed and used in practice.

In the present study, a novel adsorbent Kanuma mud has been investigated in batch studies. The nature and morphology of the adsorbent were examined with SEM, XRD

and EDS analysis. Various adsorption isotherm and kinetic models were used to describe the adsorption process. Attempts have also been made to explain the equilibrium and mechanism of adsorption (Shihabudheen et al., 2008; Sairam et al., 2008).

2.2. Materials and methods

2.2.1. Chemicals and reagents

All chemicals which were used in the experiment, including sodium fluoride, lanthanum nitrate, ALC, sodium chloride, sodium hydroxide, glacial acetic acid, hydrochloric acid, sodium acetate, sodium carbonate, sodium bicarbonate, sodium nitrate, sodium sulfate, acetone, were of analytical grade and obtained from Kanto Chemical Co., Inc. (Japan).

2.2.2. Preparation of Kanuma mud

The raw material was in the form of small, spherical, brown, cohesionless mud. The Kanuma mud was neutral originally. Initially, samples of the Kanuma mud were sieved to obtain<100 μm size (100%-150 B.S.S. mesh) and then the samples were washed several times with distilled water and dried at 105 °C for 24 h. Finally, samples were cooled to room temperature and transferred to an airtight glass bottles for storage.

2.2.3. Sorbent characterization

The mineralogy of supported metal-oxide was characterized by powder XRD

techniques (Rigaku, RINT2200, Japan).Surface morphology and spot elemental analysis of Kanuma mud was carried out by using SEM (JEOL, ESEM-6700F, Japan) and EDS (JEOL, JSM-6700F, Japan), respectively.

2.2.4. Batch sorption experiments

Stock solution (100 mg/L) was prepared by dissolving 0.221 g anhydrous sodium fluoride to 1L of deionized water. This will be diluted to obtain required concentration for further use. In the present case, all batch studies were carried out in 250 mL Tarson conical flask with a working volume of 100 mL. After adding a known weight of the adsorbent, the flask was shaken (100 rpm) on a horizontal rotary shaker (Tai Tec, Thermo Minder Mini-80, Japan). When the equilibrium time was reached (60 min), the liquid samples would be filtered through 0.45 μm filter paper and analyzed for residual fluoride by using fluoride reagent spectrophotometer (Hach, DR/4000U, Japan) at 620 nm wavelength according to SPADNS (APHA, Standards Method for the Examination of Water and Waste Water, 1998). The pH of the fluoride solution in the experiment was adjusted by using 0.1 M NaOH and HCl solutions. The effect of contact time on fluoride removal was investigated by adding 10 g/L of Kanuma mud into 100 mL fluoride solution of various fluoride concentrations (5, 10, 15, 20, 30 and 50 mg/L). The liquid samples were drawn from every flask after a regular time intervals to analyze for residual fluoride concentrations. Similarly, in order to investigate the effect of pH the initial values of the fluoride solutions were adjusted to 2-12 with 0.1 M HCl or o.1M NaOH using a pH meter (TES-1380, Custom, CO,

Japan). To observe effect of adsorbent dosage, different amounts (2-20 g/L) of adsorbent dosage were tested in 100 mL fluoride solutions in which the concentration of fluoride was 5 mg/L. To determine the effect of temperature the experiments were carried out at five different temperatures, i.e. 293 K, 303 K, 313 K, 323 K and 333 K.

2.2.5. Regeneration experiments

In order to test the regenerative ability of the adsorbent, studies were carried out with distilled water as the eluent with different pH (2-12) adjusted with 0.1 M NaOH or HCl. For this, the initial adsorption study was conducted using 10 g/L Kanuma mud and 5 mg/L of fluoride solution. The adsorbent was then separated by filtration and washed with distilled water to remove entrained liquid containing fluoride. After this regeneration stage, the ability of Kanuma mud to remove fluoride from aqueous solutions was again tested in an adsorption experiment, using a similar procedure to that described in Section 2.2.4.

2.3. Results and discussion

2.3.1. Characterization of Kanuma mud

The Kanuma mud was characterised by powder XRD. Fig. 2.1 shows the X-ray diffraction pattern of Kanuma mud before and after adsorption of fluoride ions. It is clear that the crystal structure of the Kanuma mud had significantly changed after the adsorption of process. This may be attributed to both physical and chemical adsorption. According to the XRD analysis (Fig. 2.1), multiple peaks were observed

and the presence of various oxides indicated heterogeneous surface sites for adsorption. This may also indicate that fluoride had caused crystalline phase transformation of the Kanuma mud (Gopal and Elango, 2006; Kagne et al., 2008). The possibility of calcium fluoride, ferric fluoride and aluminium fluoride being formed by the reaction of fluoride with soluble or exchangeable cations in Kanuma mud, at or near neutral pH, has been reported before (Rai et al., 2000). A surface complex formation model (ligand exchange model) has been proposed (Ayoob et al., 2008; Bail et al., 1988) to describe fluoride adsorption on metal oxides as:

$$MOH + H^{+} = MOH_2^{+} \quad (2.1)$$

$$MOH = MO^{-} + H^{+} \quad (2.2)$$

$$MOH + F^{-} = MF + OH^{-} \quad (2.3)$$

where M represents the metal ion (Ca, Si, Al, Fe, etc.) and MOH_2^{+}, MOH and MO^{-} are groups generated in the process of the fluoride adsorption.

The SEM and EDS patterns of the Kanuma mud before and after adsorption are shown in Fig. 2.2. As seen in Fig. 2.2a, the SEM micrographs of the Kanuma mud before fluoride adsorption shows irregularly shaped particles with surface agglomerates of small size particles adhered on larger particles, while Fig. 2.2b shows polyhedron, smooth and stretched cubic structures. This can be attributed to the precipitation of iron, calcium and aluminium fluoride (Mellah and Chegrouche, 1997). Adsorption of fluoride leads to surface modifications and structural transformation of Kanuma mud. The EDS spectrum of Kanuma mud before adsorption, given in Fig. 2.2c, shows the presence of elements in it. And there is a clear fluoride peak in the

EDS spectra of fluoride-treated Kanuma mud confirming the fluoride sorption onto Kanuma mud as shown in Fig. 2.2d. Chemical analysis of Kanuma mud was carried out by weight percentage and expressed in terms of oxides as SiO_2 (46.20%), CaO (2.00%), MgO (0.36%), Fe_2O_3 (2.20%), Al_2O_3 (28.70%) and MnO (0.04%).

2.3.2. Effect of adsorbent dose

The effect of adsorbent dose on the adsorption of fluoride is presented in Fig. 2.3a. It was observed that the percentage removal of fluoride increased from 31.4% to 100% with an increase in adsorbent dose from 2 to 20 g/L. However, after a dosage of 10 g/L, the amount removed per unit of adsorbent declined. This may be due to the over-lapping of active sites at higher dosages as well as a decrease in the effective surface area resulting in the conglomeration of exchanger particles (Fan et al., 2003). Higher doses of the adsorbent (i.e., greater than 10 g/L) will increase the amount of sludge and cost of recovery, without introducing a significant benefit in the amount of fluoride removed. This dose (10 g/L) may also be sufficient to reduce the amount of fluoride to the WHO drinking water guideline.

2.3.3. Effect of contact time

It is evident the adsorption process was very rapid and most of the fluoride ions were adsorbed in the first 20 min (fig. 2.3b). It can also be seen that equilibrium was established at about 2 h. This result is in agreement with the equilibrium times found for alum sludge and quartz, which are reported in other studies (Sujana et al., 1998; Harouiya et al., 2004). The change in the rate of removal might be due to the fact that

initially all adsorbent sites were vacant, while later the fluoride adsorbed by Kanuma mud decreased significantly, due to fewer adsorption sites and a lower fluoride concentration. The data obtained from this experiment is used below to successfully evaluate the kinetics of the adsorption process.

2.3.4. Effect of pH

Fig. 2.3c shows the influence of the initial solution pH on the fluoride removal efficiency of Kanuma mud. The adsorption of fluoride in this experiment was mainly dependent on the solution pH. Maximum adsorption of fluoride was found to be about 85% in the pH range 5.0-8.0, which is more suitable for practical application in household systems compared with red mud which can only be used at pH=4.7 (Tor et al., 2009). The removal efficiency fell sharply as the pH went below 4.0, or above 10.0. The sharp reduction in the amount of fluoride adsorbed under alkaline pH conditions is due to competition from hydroxyl ions for adsorption sites even though the oxide surface is positively charged (Raichur and Basu, 2001). Under acidic conditions the formation of weakly ionised hydrofluoric acid (Sujana et al., 1998), or the combined effect of both chemical and electrostatic interactions between the oxide surface and fluoride ion, is responsible for the adsorption reduction.

2.3.5. Effect of initial fluoride concentration

The adsorption of fluoride onto Kanuma mud at different initial fluoride concentration was studied, and the effect of initial fluoride concentration on fluoride adsorption is shown in Fig. 2.3d. With an increase in initial fluoride concentration, the

percentage removal of fluoride decreases. The initial fluoride concentration was increased from 5 to 50 mg/L and the removal efficiency reached a maximum value of 85.4% before gradually decreasing to 33.3%. The adsorption capacity of Kanuma mud was found to increase with the increase in the initial concentration of fluoride. This can be attributed to the utilisation of less accessible or energetically less active sites, or energetically less active sites, due to increased diffusivity and activity of fluoride with the increased concentration. The adsorption sites present on the interior surface of a pore may not be as easily accessible because of resistance to pore diffusion.

2.3.6. Effect of co-existing ions

Aqueous solutions contain many different anions such as chloride, sulfate, carbonate, bicarbonate, phosphate and nitrate in addition to fluoride, and the concentrations of these anions may be different in different geographical regions. These anions may compete in the adsorption process. According to the results shown in Fig. 2.4, it was observed that there is a slight increase of the adsorbent efficiency in the presence of chloride and nitrate ions. On the other hand, there is a decrease in fluoride uptake observed in the presence of monovalent (bicarbonate), divalent (sulfate and carbonate) or trivalent ions (phosphate). Chloride and nitrate ions are low-affinity ligands. Their adsorption mechanism is via formation of weaker bonds with the active sites at the outer-sphere complexation. Thus, fluoride adsorbs through formation of strong bonds with active sites at the inner-sphere complexation. The

slight increase in fluoride removal in the presence of nitrate and chloride ions could be due to an increase in the ionic strength of the solution or a weakening of lateral repulsion between adsorbed fluoride ions. Similar observations have been reported by Eskandarpour (2008). Sulfate and bicarbonate ions partially form outer-sphere complexes, or inner-sphere complexes (Onyango et al., 2004). In the present study, sulfate and bicarbonate ions decreased the fluoride adsorption slightly and this may be attributed to the high coulombic repulsive forces, which reduce the probability of fluoride interactions with the active sites. Carbonate and phosphate ions present in the reaction system had the greatest effect on fluoride adsorption. This is explained, not only in terms of the competition for the same active sites with fluoride, but also by the high affinity and capacity for carbonate and phosphate ions onto Kanuma mud. The pH of the fluoride solutions was finally 7.0, 6.5, 6.7, 8.8, 10.5 and 10.8, respectively, for Cl^-, NO_3^-, SO_4^{2-}, HCO_3^-, CO_3^{2-} and PO_4^{3-}, while the initial pH of the fluoride solution was 6.0 ± 0.2 without the addition of salt/anions. It was also confirmed from the batch study on the effect of pH that fluoride removal decreases in highly alkaline pH. However, detailed mechanistic aspects of the competitive adsorption reactions require further investigation. The results are in good agreement with similar work done by Kagne (2008) for hydrated cement. Where the fluoride removal efficiency of hydrated cement is not significantly affected by Cl^-, SO_4^{2-} and NO_3^- but is significantly affected by HCO_3^- and CO_3^{2-}.

2.3.7. Thermodynamic parameters

The free energy change (ΔG), entropy change (ΔS) and enthalpy change (ΔH) for fluoride adsorption on Kanuma mud were calculated using the following equations (Khan and Singh, 1987):

$$log\, Kc = C_{Ae}/C_e \tag{2.4}$$

$$\Delta G = -RT\, ln\, Kc \tag{2.5}$$

$$\Delta G = \Delta H - T\Delta S \tag{2.6}$$

where C_{Ae} and C_e represent the concentration (mg/L) of fluoride on adsorbent and in solutions, respectively. Values of ΔH, ΔG and ΔS are represented in Table 2.1. The positive value of entropy (ΔS=54.557 J/mol K) indicates increase in randomness at the solid-solution interface and hence a good affinity of fluoride with Kanuma mud. Furthermore, negative free energy change (ΔG) dictates the feasibility and spontaneous process of adsorption. Positive value of enthalpy (ΔH=11.782 kJ/mol) denotes that the process of fluoride adsorption was endothermic. Similarly, these results for fluoride adsorption on quick lime and laterite have also been reported (Islam and Patel, 2007; Mitali et al., 2006).

2.3.8. Adsorption isotherms

The ability of Kanuma mud to adsorb fluoride from aqueous solutions is evaluated from the shape of the adsorption isotherm plot. In the present study, isotherm data were applied to four adsorption models and the results of their linear regressions were used to find the model with the best fit. Values of resulting parameters and regression

coefficients (R^2) are listed in Table 2.3. The correlation coefficient values for the Freundlich isotherm ranged from 0.973 to 0.987, which are higher than the values obtained from the Langmuir, *R-D* and Temkin isotherm models. The Freundlich isotherm with minimum adsorption capacity is 0.7376 mg/g for the Kanuma mud, which is higher than for bone charcoal with 7.88×10^{-5} mg/g (Bhargava and Killedar, 1992) but lower than activated alumina with 2.4 mg/g (Rubel, 1983). The experimental data fit very well to this isotherm model, and indicates that fluoride adsorption occurs on heterogeneous surfaces, which is similar to the conclusion obtained from alum sludge (Sujana et al., 1998).

2.3.9. Adsorption kinetics

According to the kinetic data obtained from the experiments, various models have been used to throw light on the mechanisms of adsorption and potential rate controlling steps. In this experiment, the pseudo-first-order, pseudo-second-order, and intra-particle diffusion models were used to test the mechanism of fluoride adsorption on Kanuma mud. The pseudo-first-order rate equation is given as (Lagergren and Svenska, 1898):

$$log(q_e - q_t) = log\, q_e - k_1 t/2.303 \qquad (2.7)$$

where q_e and q_t are the amounts of fluoride adsorbed (mg/g) at equilibrium and at time t (min), respectively, and k_1(L/min) is the adsorption rate constant of first-order adsorption. A straight line of $log(q_e - q_t)$ versus t suggests the applicability of this kinetic model. q_e and k_1 were determined from the intercept and slope of the plot

which were shown in Table 2.4. From the data, q_e(calculated) and q_e(experimental) values are not in agreement with each other. Therefore, that indicates the adsorption of fluoride on Kanuma mud was not a first-order reaction. In addition, the experimental data was also applied to the pseudo-second-order kinetic model equation (Ho and Mckay, 1999):

$$t/q_t = 1/(k_2 q_e^2) + t/q_e \quad (2.8)$$

where k_2 is the rate constant of pseudo-second-order chemisorptions (g/ (mg min)). The plot t/q_t versus t giving a straight line which is shown in Fig. 2.5, and the constant calculated from the slop and intercept of the plots are given in Table 2.3. Fig. 2.5 shows that R^2 values are higher than those obtained from the first-order kinetics. In addition, theoretical and experimental q_e values are in agreement. Therefore, it is possible to prove that the adsorption process using Kanuma mud followed the second-order kinetic model.

The intra-particle diffusion equation can be described as:

$$q_t = k_i t^{0.5} \quad (2.9)$$

where k_i is the intra-particle diffusion rate constant (mg/g min).

The data shown in Fig. 2.6 have an initial curved portion, followed by a linear portion. The curved portion of the plot is due to the diffusion of fluoride through the solution to the external surface of Kanuma mud, or boundary layer diffusion. The linear portion suggests a gradual adsorption stage, where intra-particle diffusion of fluoride on the Kanuma mud surface takes place. However, the extrapolated linear regions at different initial concentrations did not pass through the origin and that

suggests that the intra-particle diffusion was not the rate-controlling step (Gupta et al., 2007).

2.3.10. Regeneration experiments

To develop a cost-effective and user-friendly process, the adsorbent should be regenerated for reuse in further fluoride adsorption cycles. Desorption studies were carried out using 10 g/L fluoride-adsorbed Kanumu mud with varying pH by adding 0.1 M HCl or NaOH. It was found that there was hardly any fluoride leached when the pH was below 6. But desorption of fluoride increased as the pH increased from 6 to 12 and reached a maximum of 88% at pH 12. The adsorption capacity of regenerated Kanumu mud reduced from 85% to 79% on the first cycle with the capacity decreasing with repetition, but it remained above 68% after three cycles. This reduction in adsorption efficiency may be attributed to the gradual dissolution of aluminium and iron from the Kanuma mud surface during the multiple regeneration process.

2.4. Conclusions

The present study shows that it is possible to utilize Kanuma mud as an adsorbent for removing fluoride from aqueous solution. The percent decrease in fluoride concentration was evaluated at optimized experimental conditions. It was found that the fluoride removal efficiency was favored at lower fluoride concentrations, increased agitation time and increased dose of Kanuma mud. The optimum pH for fluoride removal was in the pH range of 5.0-8.0. Some anions such as carbonate,

phosphate and bicarbonate showed a negative effect on fluoride adsorption by Kanuma mud. The equilibrium data fits well to a Freundlich isotherm model. The process is thermodynamically favorable, spontaneous and endothermic in nature. The kinetic data followed pseudo-second-order kinetics, and intra-particle diffusion plays a major role in the adsorption process. The use of Kanuma mud as an adsorbent for fluoride removal is potentially cost-effective and hence can be considered as an alternative method for fluoride removal.

(a)

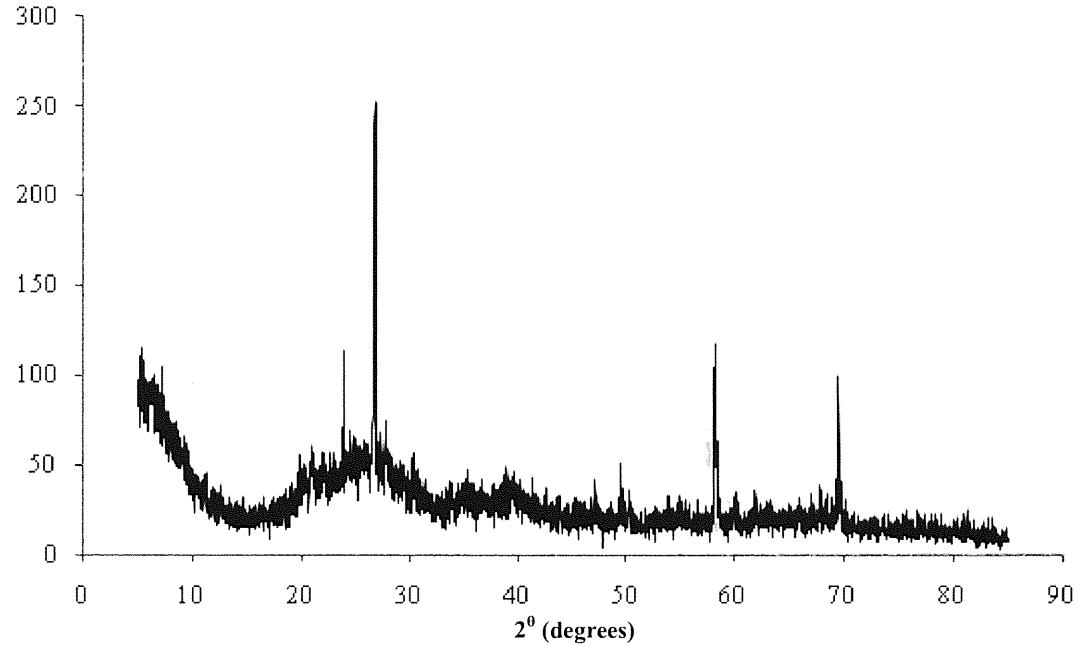

(b)

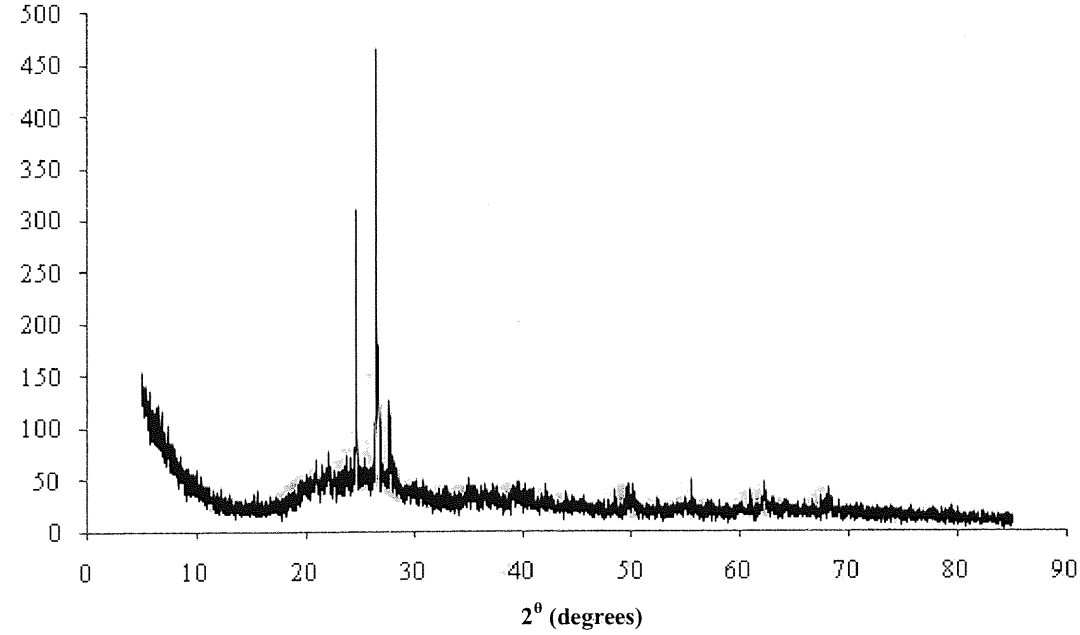

Fig.2.1 (a) XRD of Kanuma mud before adsorption, (b) XRD of Kanuma mud after adsorption

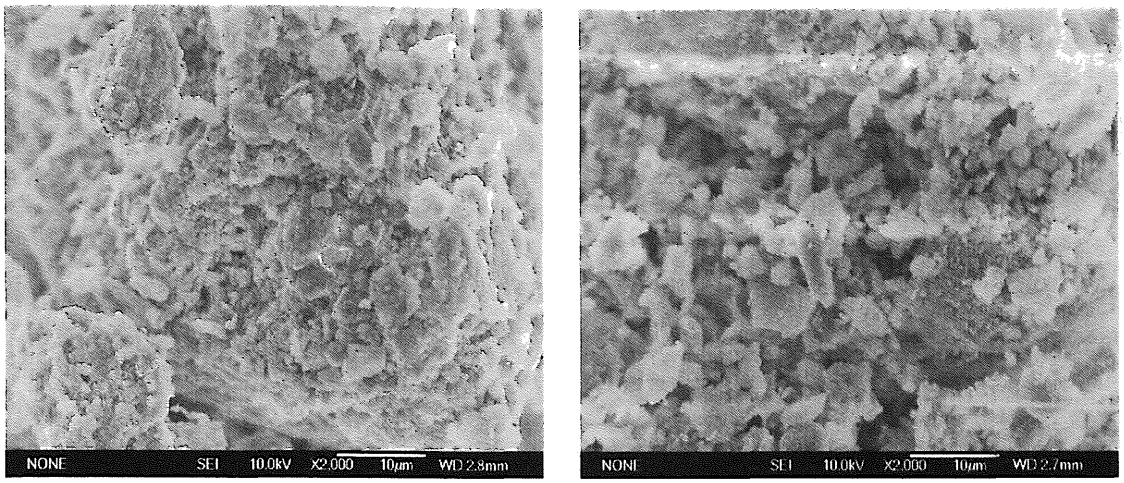

(a) (b)

(c)

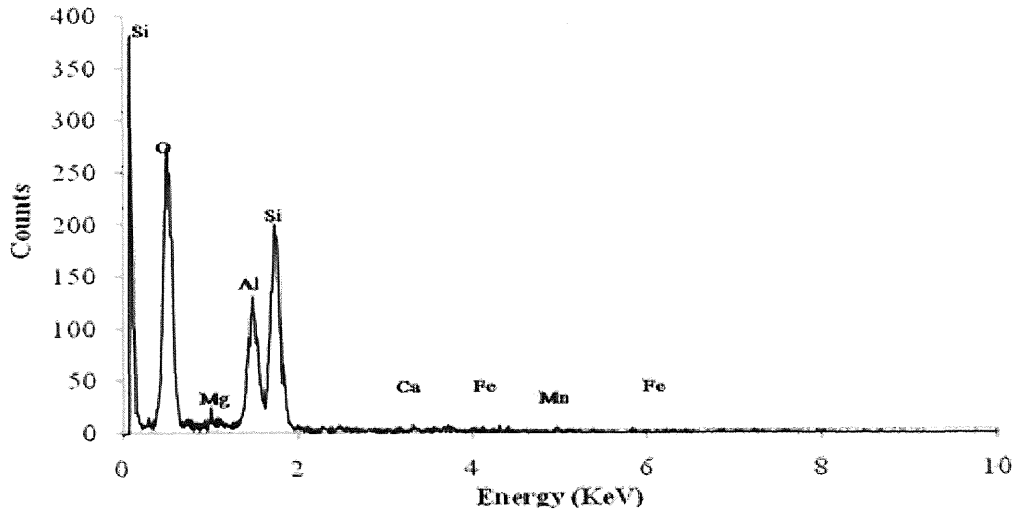

(d)

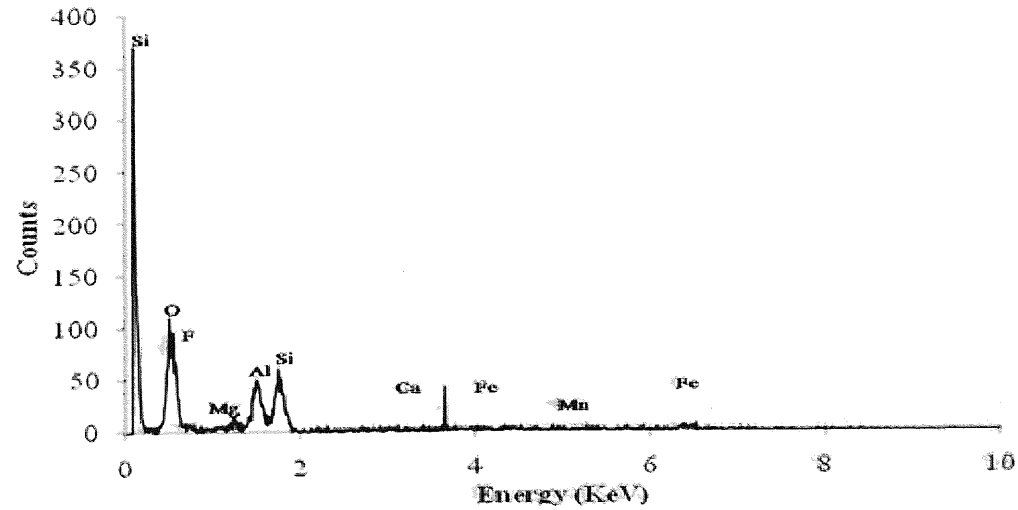

Fig.2.2 SEM micrographs of (a) Kanuma mud before adsorption and (b) Kanuma mud after adsorption, EDAX spectra of (c) Kanuma mud before adsorption and (d) Kanuma mud after adsorption

(a)

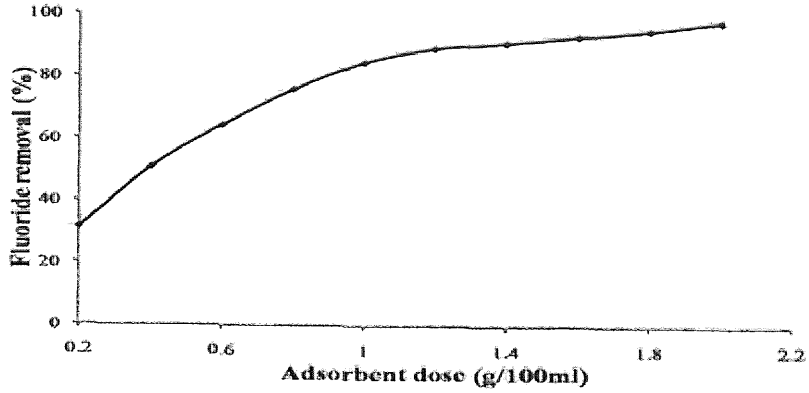

(b)

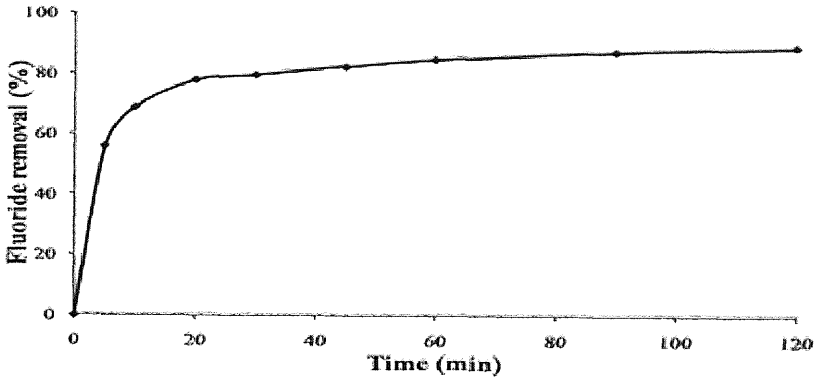

(c)

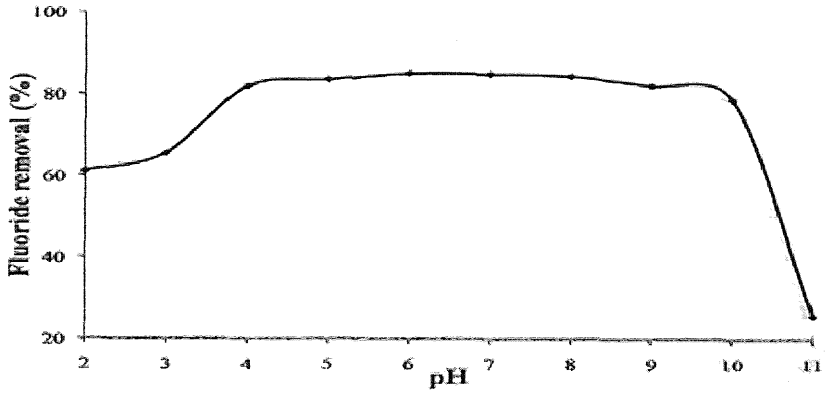

(d)

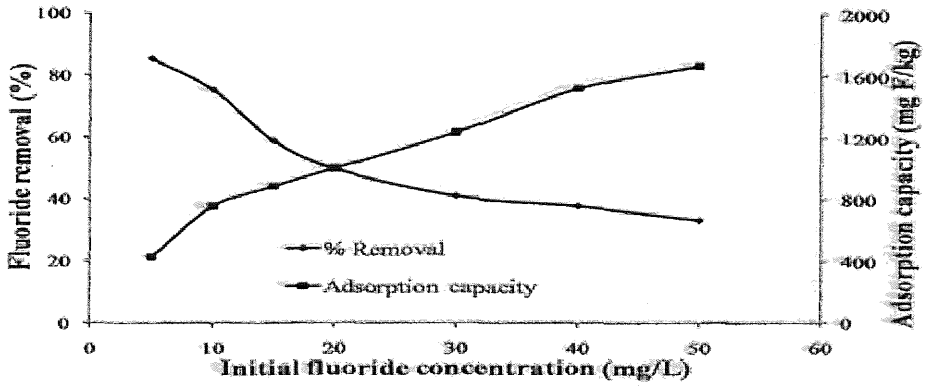

Fig.2.3 (a) Influence of adsorbent dose on fluoride removal, (b) Influence of contact time on fluoride removal, (c) Influence of pH on fluoride removal, (d) Influence of initial fluoride concentration

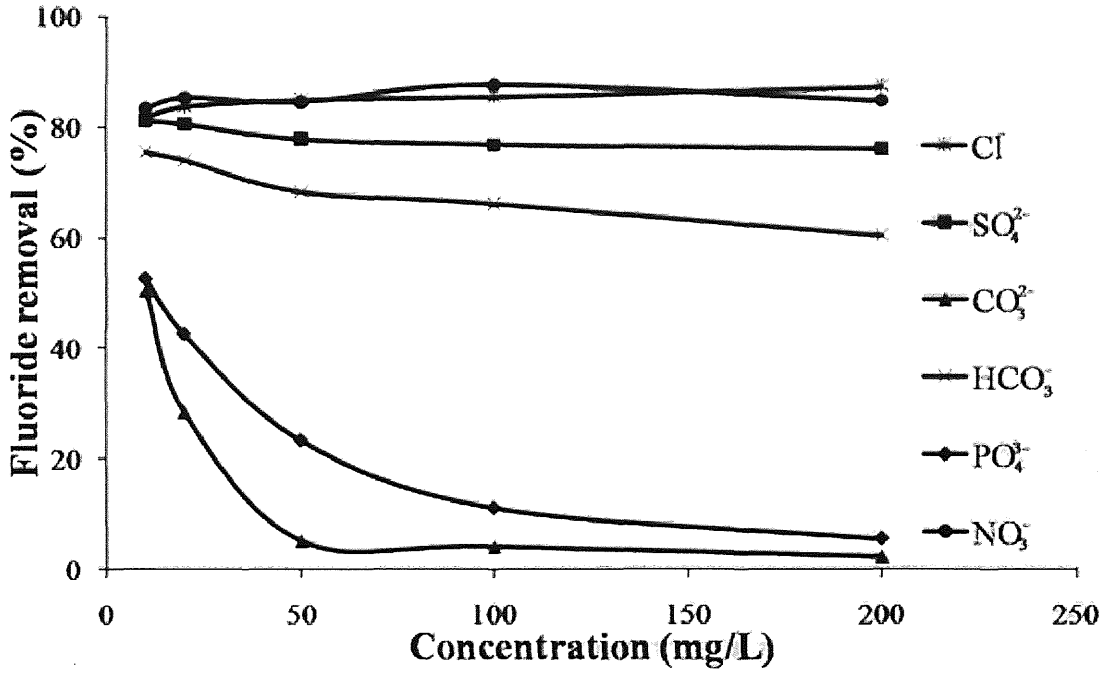

Fig.2.4 Fluoride removal efficiency at different anion concentrations (initial fluoride concentration: 5 mg/L; initial pH: 6.0; contact time: 60 min; shaking speed: 100 rpm; adsorbent dose: 10 g/L; temperature 293.16 K)

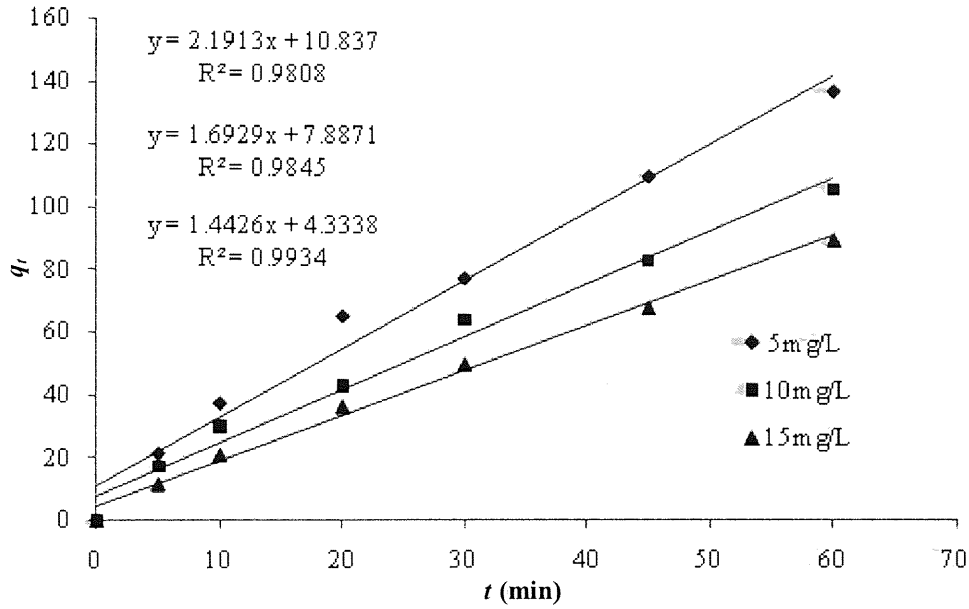

Fig.2.5 Second-order kinetic modeling of fluoride adsorption on Kanuma mud

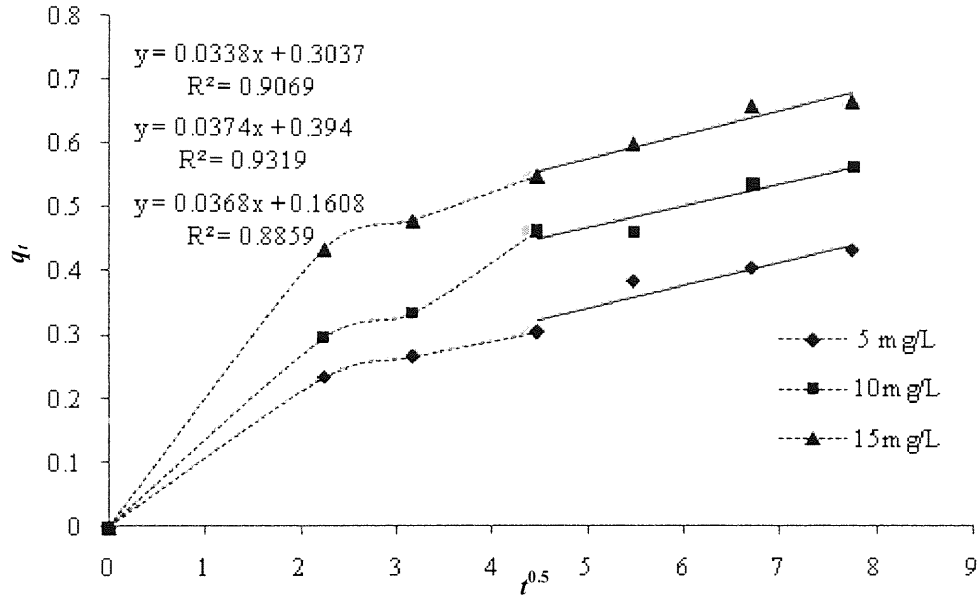

Fig.2.6 Intra-particle diffusion modeling of fluoride adsorption on Kanuma mud

Table 2.1

Thermodynamic parameters for the adsorption of fluoride on Kanuma mud using synthetic fluoride solution of 5 mg/L

Temperature (K)	ΔG (kJ/mol)	ΔS (J/mol K)	ΔH (kJ/mol)	R^2
293.16	-4.305			
303.16	-4.725			
313.16	-5.185	54.557	11.782	0.981
323.16	-5.726			
333.16	-6.533			

Table 2.2
Summary of equilibrium isotherms

Isotherm	Equation
Langmuir	$q_e = q_m \frac{BC_e}{1 + BC_e}$
Freundlich	$q_e = K_F C_e^{1/n}$
Dubinin and Radushkevich (*R-D*)	$q_e = q_m \exp(-\beta\varepsilon^2),\ E = \frac{1}{\sqrt{-2\beta}}$
Tempkin	$q_e = B_1 \ln(K_T C_e)$

(B, K_F, B_1, K_T: Langmuir, Freundlich and Tempkin constants; $1/n$: heterogeneity coefficient; q_m: maximum adsorption capacity; q_e: uptake at equilibrium; C_e: equilibrium concentration; ε: Polanyi potential; β: activity coefficient related to mean sorption energy; E: mean sorption energy.)

Table 2.3

Langmuir, Freundlich, Dubinin and Radushkevich (*R-D*) and Tempkin isotherm constants for the adsorption of fluoride on Kanuma mud at different temperatures

Temperature (K)	Langmuir isotherm		
	q_m (mg/g)	B (L/mg)	R^2
293.16	1.311	0.6436	0.9490
303.16	1.294	0.7197	0.9035
313.16	1.291	0.8252	0.8950
323.16	1.371	0.8677	0.8728
333.16	1.422	1.0520	0.8936
Temperature (K)	Freundlich isotherm		
	K_F $(mg/g)/(mg/L)^{1/n}$	1/n	R^2
293.16	0.7376	0.3312	0.9801
303.16	0.7367	0.3438	0.9732
313.16	0.7439	0.3433	0.9830
323.16	0.7589	0.3667	0.9870
333.16	0.7931	0.3497	0.9870
Temperature (K)	Dubnine- Radushkevich isotherm		
	q_m (g/g)	E (kJ/mol)	R^2
293.16	5.514	12.13	0.9776
303.16	5.209	12.31	0.9679
313.16	5.200	12.91	0.9660
323.16	4.385	12.91	0.9800
333.16	4.444	13.87	0.9706
Temperature (K)	Tempkin isotherm		
	K_T (L/mg)	B_1	R^2
293.16	22026.47	0.00002	0.9422
303.16	22026.47	0.00002	0.9252
313.16	22026.47	0.00002	0.9079
323.16	22026.47	0.00002	0.9347
333.16	22026.47	0.00002	0.9068

(Initial fluoride concentration: 5 mg/L, initial pH: 6.0±0.2 and shaking speed: 100 rpm)

Table 2.4

Comparison between adsorption rate constant, q_e estimated and coefficient of correlation associated to the Lagergren pseudo-first- and second-order adsorption and intra-particle diffusion rate constant

C (mg/L)	q_e (exp)(mg/g)	First-order kinetic model			Second-order kinetic model			Intra-particle diffusion model	
		k_1 (1/min)	q_e(cal) (mg/g)	R^2	k_2[g/(mg min)]	q_e(cal) (mg/g)	R^2	k_i(mg/g min)	R^2
5.0	0.437	0.058	0.339	0.96	0.444	0.456	0.98	0.034	0.91
10.0	0.566	0.061	0.444	0.95	0.363	0.591	0.99	0.037	0.93
15.0	0.670	0.089	0.550	0.94	0.480	0.693	0.99	0.037	0.89

(Initial pH: 6.0±0.2; shaking speed: 100 rpm; temperature: 293.16 K)

Chapter 3 Investigation on the Column Fluoride Adsorption by Kanuma Mud

3.1. Introduction

As described in chapter 2, the present study sought to investigate Kanuma mud as an alternate fluoride adsorbent. With our knowledge from the literature survey, the removal of fluoride from water by using Kanuma mud under continuous flow conditions has not been reported. Therefore, the objective of this study is to: (i) perform batch studies to examine fluoride adsorption using Kanuma mud (effect of initial fluoride concentration and pH, adsorption isotherm and kinetics), and (ii) perform column studies to investigate the fluoride uptake characteristics of the Kanuma mud under different flow rates.

3.2. Materials and methods

3.2.1. Preparation of the Kanuma mud

The raw Kanuma mud, provided by the Makino Store, Kiyosu, Japan, was in the form of small, spherical, brown and cohesionless mud. The Kanuma mud was neutral originally. Initially, Kanuma mud was crushed and sieved to obtain fractions of particles smaller than 150 μm. The samples were then washed several times with distilled water and dried at 105 °C for 24 h. Finally, samples were cooled to room temperature and transferred to an airtight glass bottles for further experiments.

3.2.2. Batch adsorption experiments

Stock solution (100 mg/L) was prepared by dissolving 0.221 g anhydrous sodium fluoride to 1 L of deionized water. This will be diluted to obtain required concentration for further use. All batch studies were carried out in 250 mL Tarson conical flask with a working volume of 100 mL. After adding a known weight of the adsorbent, the flask was shaken (100 rpm) on a horizontal rotary shaker (Tai Tec, Thermo Minder Mini-80, Japan). The pH of the fluoride solution in the experiment was adjusted by using 0.1 M NaOH and HCl solutions. When the equilibrium time was reached, the liquid samples would be filtered through 0.45 μm filter paper and analyzed for residual fluoride. The experimental parameters studied are contact time (0-180 min), initial fluoride concentration (5-50 mg/L), temperature (20-40 °C) and pH (2.0-11.0).

3.2.3. Column adsorption experiments

Continuous flow adsorption experiments were conducted in Polyethylene column of 5.0 cm inside diameter. At the top of the column, influent fluoride solution (20, 30 and 50 mg/L) was pumped through the packed column (5, 10 and 15 cm), at flow rates of 3, 5 and 7 mL/min, using a peristaltic pump (Cassette-Tube pump SMP-23AS, Japan). Samples were collected, from the exit of the column at regular time intervals and analyzed from residual fluoride concentrations. The pH was measured using a pH meter (TES-1380, Custom, Japan). The loaded Kanuma mud was regenerated using 0.1 M NaOH at flow rate of 7 mL/min. After elution, distilled water was passed

through column to wash the bed until the pH of the wash effluent stabilized near 7.0.

3.3. Results and discussion

3.3.1. Effect of pH in batch experiments

Solution pH plays a vital role in fluoride adsorption. The state of chemically active sites is changed by the variation in solution pH. In order to determine the optimum value, pH of solution was varied from 2.0 to 11.0. As depicted in Fig. 3.1, the maximum adsorption of fluoride occurred in the pH range of 5.0-7.0. This is more suitable for practical application compared with red mud which can only be used at pH=4.7 (Cengeloglu et al., 2002). The fluoride removal was not favor at a pH below 5.0. This can be attributed to the distribution of F^- and HF which are controlled by pH of the aqueous solution. When the pH of the solution exceeded 7.0, F^- adsorption also decreased. This may be explained by considering the pH_{zpc} for the Kanuma mud (pH_{zpc}=6.4). At pH > pH_{zpc}, the surface charge is negative. The metal oxides present in Kanuma mud form aqua complexes with water and develop a charged surface through amphoteric dissociation. Therefore, F^- will be adsorbed to a lesser extent due to the repulsive forces between F^- ions and negative charge of the Kanuma mud surface.

3.3.2. Effect of contact time and adsorption kinetics in batch experiments

As shown in Fig. 3.2, the fluoride adsorption process took place in two stages. The first rapid stage in which, 70-80% adsorption was achieved in 20 min and a slower

second stage, with equilibrium attained in 2 h. The first stage was due to, the initial accumulation of fluoride at the surface, as large surface area of Kanuma mud was available. With the gradual occupation of surface binding sites, the adsorption process was slowed down. The second slower stage was due to the penetration of fluoride ions to the inner active sites of the adsorbent. This is in accordance with the observations of other similar studies (Qaiser et al., 2009; Sangi et al., 2008). The experimental data were analyzed using a pseudo-second-order Lagergren equation:

$$t/q_t = 1/(K_{ad}q_e^2) + t/q_e \quad (3.1)$$

where q_t and q_e are the amount of adsorbed fluoride (mg/g) at time t and at equilibrium time, respectively. K_{ad} is the second-order rate constant for adsorption. A linear relationship with a correlation coefficient of 0.9994 was found between t/q_t and t that indicates the pseudo-second-order nature of fluoride adsorption on the Kanuma mud.

3.3.3. Adsorption isotherm models in batch experiments

Adsorption equilibrium is established when the concentration of sorbate in bulk solution is in dynamic balance with that on the liquid-solid interface. Therefore, the Langmuir and Freundlich models were utilized to describe the equilibrium data. The Langmuir model is based on the hypothesis that uptake occurs on a homogenous surface by monolayer sorption without interaction between adsorbed molecules, and is expressed as (Langmuir, 1916):

$$q_e = q_{max}bC_e/(1 + bC_e) \quad (3.2)$$

Eq. (3.2) can be written in linear form as:

$$C_e/q_e = C_e/q_{\max} + 1/q_{\max}b \quad (3.3)$$

where $q_{\max}$ represents the maximum adsorption capacity and b is a constant related to affinity and energy of binding sites.

The Freundlich model proposes a monolayer sorption with a heterogeneous energetic distribution of active sites and with interaction between adsorbed molecules. It is expressed mathematically as (Freundlich, 1906):

$$q_e = K_F C_e^{1/n} \quad (3.4)$$

Linear form of Eq. (3.4) is:

$$lnq_e = 1/n\, lnC_e + lnK_F \quad (3.5)$$

where K_F and n are the Freundlich coefficients. K_F provides an indication of the adsorption capacity and n is related to the intensity of adsorption. Fig. 3.3 shows the Langmuir and Freundlich isotherms and the experimental data. The isotherm constant and R^2 values for each model are given in Table 3.1. On the comparison of the R^2 values, it can be concluded that adsorption data can be better described by the Freundlich isotherm model. This result may be attributed that various active sites or heterogeneous mixture of several minerals on Kanuma mud has different affinities to fluoride ions (Fuhrman et al., 2004).

3.3.4. Effect of flow rate in column experiments

The adsorption columns were operated with different flow rates (3, 5 and 7 mL/min) until no further fluoride removal was observed. The breakthrough curve for a column

is determined by plotting the ratio of the C_e/C_0 (C_e and C_0 are the fluoride concentration of effluent and influent, respectively) against the time, which was shown in Fig. 3.4. The column performed well at the lowest flow rate (3 mL/min). An earlier breakthrough and exhaustion times were achieved, when the flow rate was increased from 3 to 7 mL/min. The column breakthrough time (C_e/C_0=0.05) was reduced from 39 to 9 h, with the increase in flow rate from 3 to 7 mL/min. This behavior was due to the decrease in the residence time, which restricted the contact of fluoride solution to the Kanuma mud. At higher flow rates the fluoride ions did not have enough time to diffuse into the pores of the Kanuma mud and they leave the column before equilibrium occurred.

Successful design of a column fluoride adsorption process required to describe the dynamic behavior of compound in a fixed bed. Various simple mathematical models have been developed to describe and possibly predict the dynamic behavior of the bed in column performance (Aksu and Gonen, 2004). One of these models used for the continuous flow conditions is the Thomas model (Thomas, 1944), which can be written as:

$$C_e/C_0 = 1/1 + exp\left((k_{\text{th}}/Q)(q_0 M - C_0 V_{\text{eff}})\right) \quad (3.6)$$

Eq. (3.6) can be expressed in linear form as:

$$ln[C_0/C_e - 1] = k_{\text{th}} q_0 M/Q - k_{\text{th}} C_0 t \quad (3.7)$$

where V_{eff} is the volume of effluent (L), k_{th} is the Thomas model constant (L/mg h), q_0 is the adsorption capacity (mg/g), Q is the volumetric flow rate through column (L/h), M is the mass of adsorbent in the column (g), C_0 is the initial fluoride concentration

(mg/L) and C_e is the effluent fluoride concentration (mg/L) at any time t (h). The Thomas model constants k_{th} and q_0 were determined from plot of $ln[C_0/C_e\text{-}1]$ versus t at a given flow rate. The model parameters were given in Table 3.2. The Thomas model gave a good fit of the experimental data, at all the flow rates examined, with high correlation coefficients of greater than 0.94. The rate constant (k_{th}) increased with increasing the flow rate which indicates that the mass transport resistance decreases.

3.3.5. Effect of bed height in column experiments

Accumulation of fluoride in fixed-bed column is dependent on the quantity of adsorbent inside the column. In order to study the effect of bed height on fluoride retention, Kanuma mud of three different bed heights, viz. 5, 10, 15 cm were taken. Fluoride solution of fixed concentration (20 mg/L) was passed through the fixed-bed column at a constant flow rate of 5 mL/min. As depicted by Fig. 3.5 the breakthrough time varied with bed height. Steeper breakthrough curves were achieved with decrease in bed depth. The breakthrough time decreased with decreasing bed depth from 15 to 5 cm, as binding sites were restricted at low bed depths. At low bed depth, the fluoride ions do not have enough time to diffuse into the surface of the Kanuma mud, due to which reduction in breakthrough time occurred. With the increase in bed depth, the residence time of fluoride solution inside the column was increased, allowing the fluoride ions to diffuse deeper into the Kanuma mud.

The breakthrough service time (BDST) model is based on physically measuring the

capacity of the bed at various percentage breakthrough values. The BDST model constants can be helpful to scale up the process for other flow rates and concentration without further experimental run. It is used to predict the column performance for any bed length, if that for some other depth is known. It states that the bed depth, Z and service time, t of a column bears a linear relationship. The rate of adsorption is controlled by the surface reaction between adsorbate and unused capacity of the adsorbent.

The BDST equation can be expressed as follows (Hutchins, 1973):

$$t = NZ/C_0v - 1/K_aC_0\, ln[(C_0/C_b) - 1] \quad (3.8)$$

where C_b is the breakthrough fluoride concentration (mg/L), N is the adsorption capacity of bed (mg/L), Z is depth of column bed (cm), v is the linear flow velocity of fluoride solution through the bed (mL/cm^2 h), K_a is the rate constant (L/mg h). The column service time was selected as time when the normalized concentration, C_e/C_0 reached to 0.05. The plot of service time versus bed depth, at flow rate of 5 mL/min (Fig. 3.6) was linear. The high correlation coefficient value (R^2 = 0.9465) indicated the validity of the BDST model for the present system. The value of N and K_a were evaluated from the slop (N/C_0v) and intercept ($(1/K_aC_0)ln[(C_0/C_b)$-1]) of the BDST plot. The values of BDST model parameters are presented in Table 3.2. The value of K_a characterizes the rate of the transfer from the fluid phase to the solid phase. If K_a is large, even a short bed will avoid breakthrough, but as K_a decreases a progressively longer bed is required to avoid breakthrough.

3.3.6. Effect of initial fluoride concentration in column experiments

The adsorption breakthrough curves obtained by changing initial fluoride concentration from 20 to 50 mg/L at 5 mL/min flow rate and 10 cm bed depth are given in Fig. 3.7. As expected, a decrease fluoride concentration gave a later breakthrough curve and the treated volume was greatest at the lowest transport due to a decreased diffusion coefficient or decreased mass transfer coefficient (Uddin et al., 2009). Breakthrough time (C_e/C_0=0.05) occurred after 23 h at 20 mg/L initial fluoride concentration while as breakthrough time appeared after 13 h at 50 mg/L initial fluoride concentration. The breakthrough time decreased with increasing fluoride concentration as the binding sites became more quickly saturated in the column.

3.3.7. Regeneration experiments

The regeneration of Kanuma mud is vital, if the Kanuma mud is to be utilized for treatment of water solution. The adsorbed Kanuma mud was regenerated by 0.1 M NaOH solution. About 85% of fluoride was recovered. The regenerated Kanuma mud was reused for further cycles of adsorption in batch study. After three cycles of adsorption-desorption, 32% loss in efficiency of Kanuma mud was observed. The column desorption of fluoride was achieved by passing 0.1 M NaOH solution at flow rate of 7 mL/min. A negligible loss in bed height and mass of Kanuma mud as observed after three adsorption-desorption cycles. The elution efficiencies were observed greater than 89% after three cycles.

3.4. Conclusions

In this study, Kanuma mud is used and its fluoride adsorption capacity is evaluated according to the batch and fixed-bed column adsorption experiments. Batch experiments indicate that the time to attain equilibrium was 2 h and adsorption was followed the pseudo-second-order kinetic model. Maximum adsorption for fluoride removal was achieved at pH range of 5.0-7.0. The adsorption of fluoride on Kanuma mud in batch systems can be described by the Freundlich isotherm, and the adsorption capacity was 3.067 mg/g. The fixed-bed column breakthrough curves were analyzed at different flow rates, bed depth and initial fluoride concentration. Thomas and BDST model can be used for predicting of breakthrough curves for fluoride removal by a fixed bed of Kanuma mud for different flow rates and bed depths. The adsorbed Kanuma mud can be regenerated three cycles after each cycle of adsorption. Kanuma mud as an adsorbent for fluoride removal is potentially cost-effective and hence can be considered as an alternative method for fluoride removal.

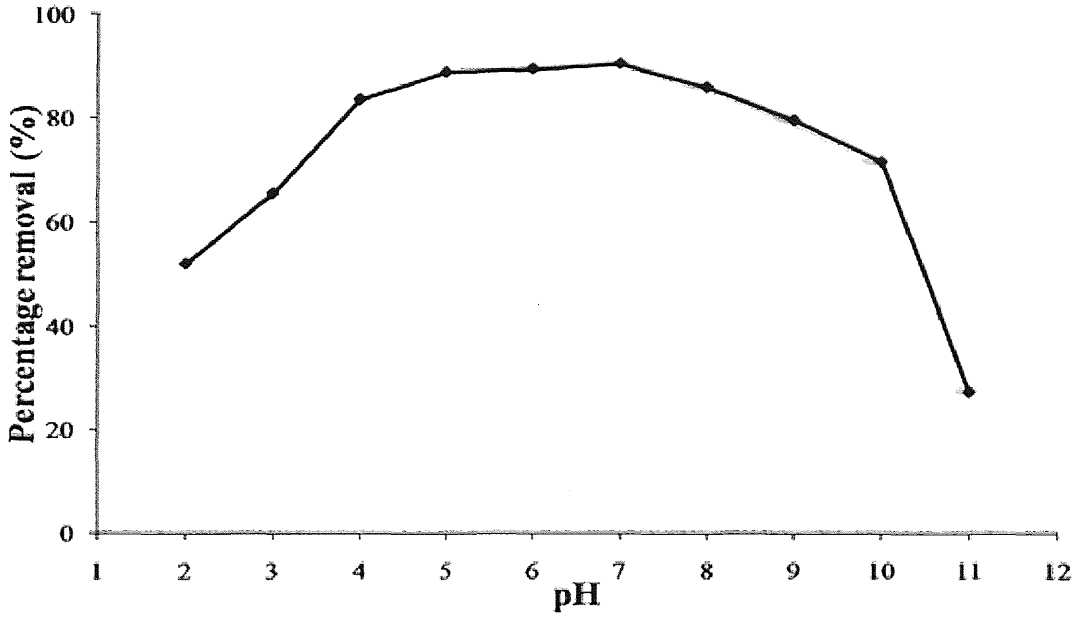

Fig.3.1 Effect of pH on fluoride adsorption by Kanuma mud (initial fluoride concentration 10 mg/L, equilibrium contact time 2 h, adsorbent dosage 20 g/L, shaken speed 100 rpm and temperature 30 ± 1°C)

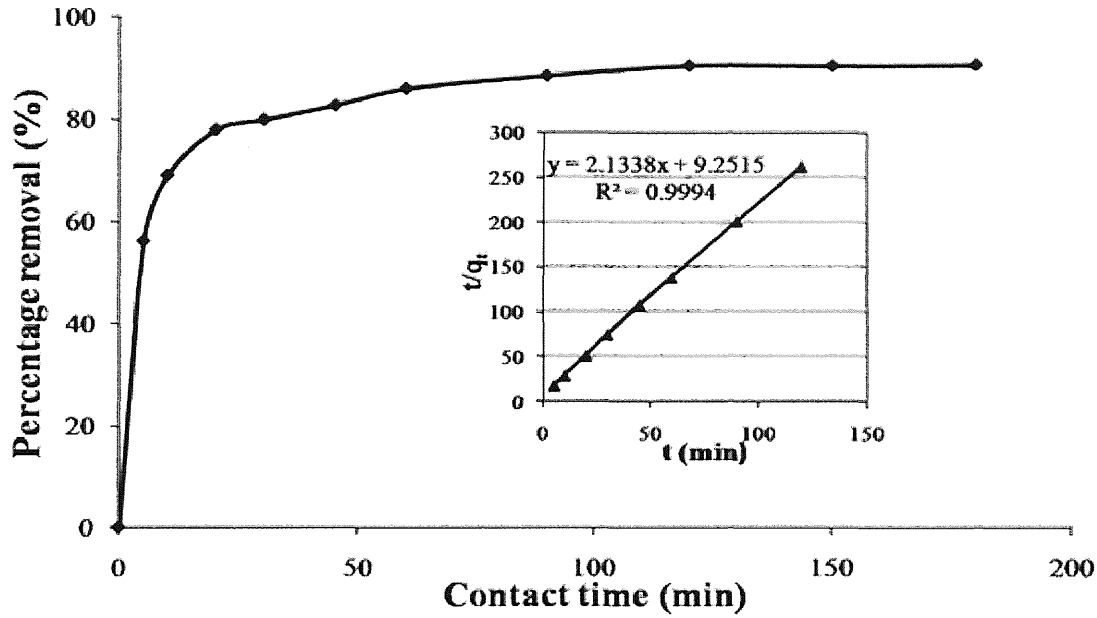

Fig.3.2 Effect of contact time on Kanuma mud for fluoride adsorption (adsorption kinetics) (initial fluoride concentration 10 mg/L, initial pH 6.9 ± 0.1, equilibrium contact time 2 h, adsorbent dosage 20 g/L, shaken speed 100 rpm and temperature 30 ± 1°C)

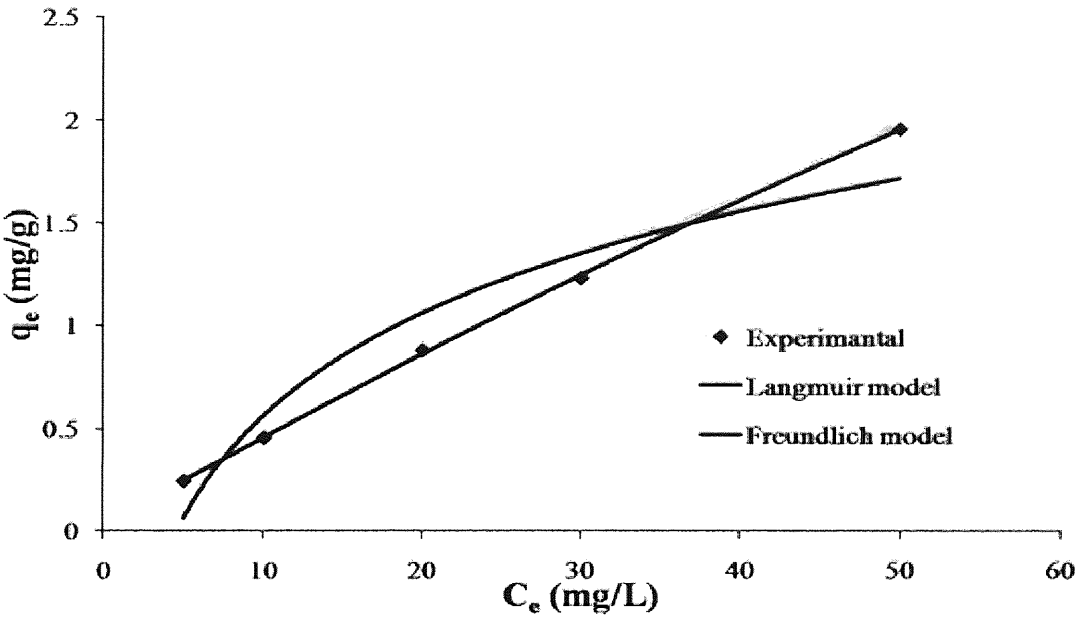

Fig.3.3 Langmuir and Freundlich isotherms plot for fluoride adsorption on Kanuma mud (initial pH 6.9 ± 0.1, equilibrium contact time 2 h, adsorbent dosage 20 g/L, shaken speed 100 rpm and temperature 30 ± 1°C)

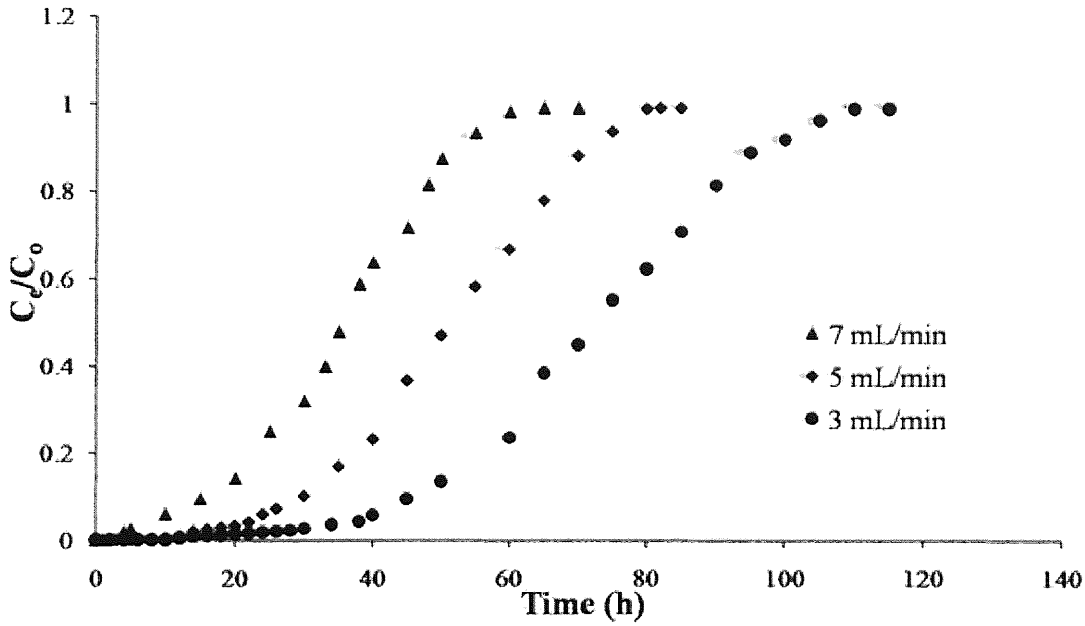

Fig.3.4 Breakthrough curves expressed as C_e/C_0 versus time at different flow rate (initial fluoride concentration 20 mg/L, initial pH 6.9 $\pm$ 0.1, bed depth 10 cm and temperature 30 $\pm$ 1°C)

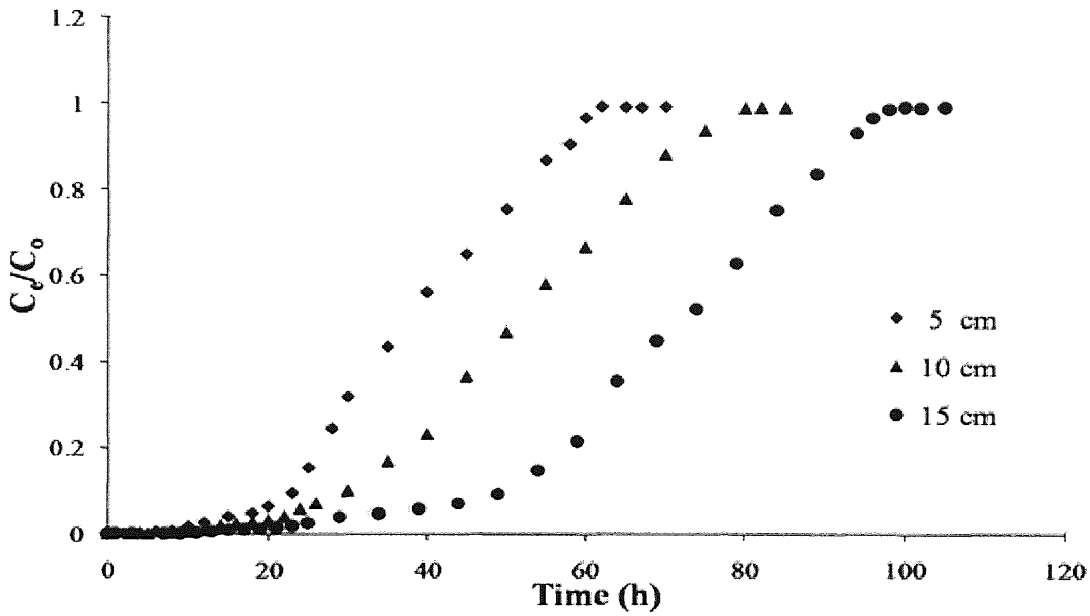

Fig.3.5 Breakthrough curves expressed as C_e/C_0 versus time at different bed depth (initial fluoride concentration 20 mg/L, initial pH 6.9 $\pm$ 0.1, flow rate 5 mL/min and temperature 30 $\pm$ 1°C)

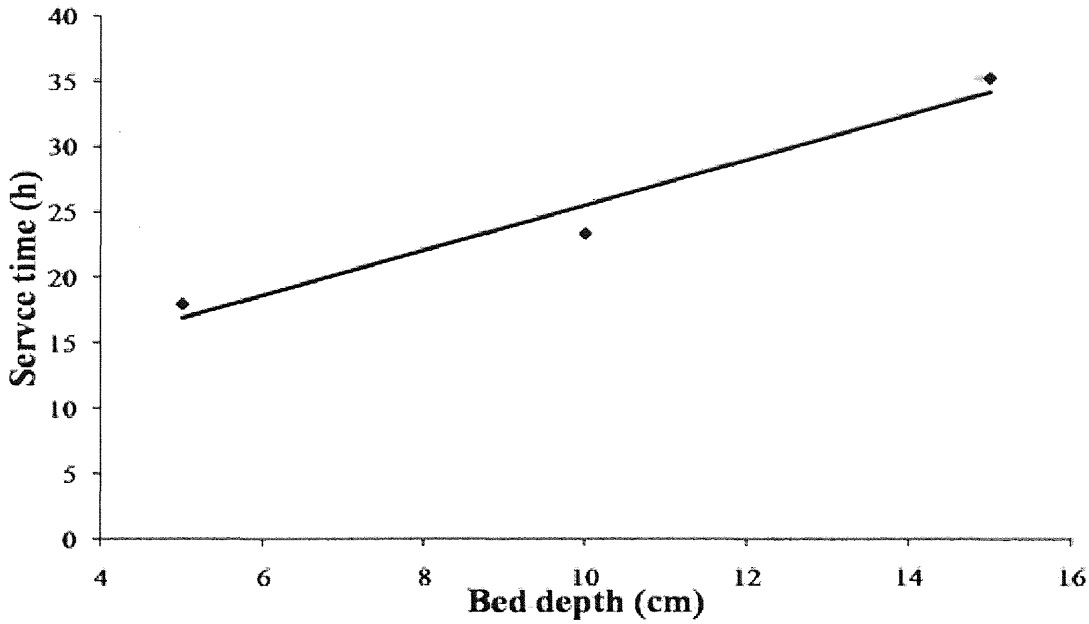

Fig.3.6 Plot of BDST equation for fluoride adsorption on Kanuma mud

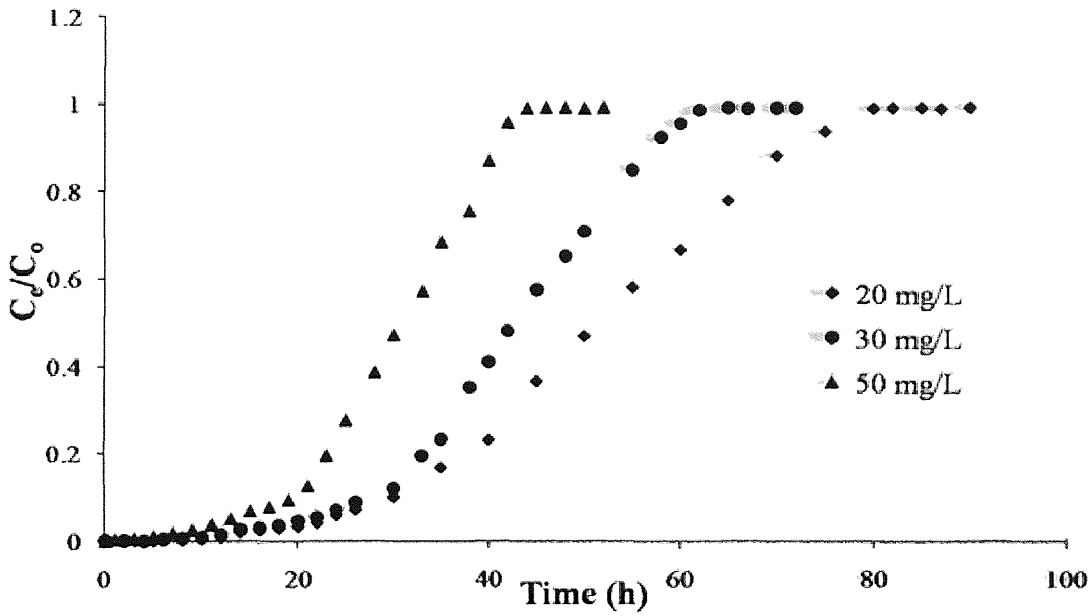

Fig.3.7 Breakthrough curves expressed as C_e/C_0 versus time at different fluoride concentration (initial pH 6.9 $\pm$ 0.1, flow rate 5 mL/min, bed depth 10 cm and temperature 30 $\pm$ 1°C)

Table 3.1
Langmuir and Freundlich isotherm parameters for the adsorption of fluoride by Kanuma mud

Langmuir isotherm		Freundlich isotherm	
q_{max} (mg/g)	0.562	n	0.486
b (L/mg)	0.843	K_F (mg/g)	3.067
R^2	0.899	R^2	0.981

Table 3.2
The Thomas model and BDST model parameters for the adsorption of fluoride by Kanuma mud

The Thomas model parameters			
Flow rate (mL/min)	q_0 (mg/g)	k_{th} (L/mg h)	R^2
3	0.512	0.00448	0.9833
5	0.585	0.00641	0.9486
7	0.572	0.00659	0.9732

The BDST model parameters		
N (mg/L)	K_a (L/mg h)	R^2
1632	0.0176	0.9465

Chapter 4 An Excellent Fluoride Sorption Behavior of Ceramic Adsorbent

4.1. Introduction

As described in Chapter 2, this study has developed a novel ceramic adsorbent for removal fluoride from aqueous solution in order to overcome these obstacles. This ceramic adsorbent is the solid phase of a spherical shape, with high fluoride removal efficiency and sufficient mechanical strength to retain its physical integrity after long-time adsorption. Ceramic adsorbents were prepared by cost-effective mixture materials consisting of Kanuma mud, which is widespread in Japan, with zeolite, starch, and $FeSO_4 \cdot 7H_2O$. The major objective of this study was to develop and investigate the ceramic material as a feasible fluoride adsorbent. Kinetic, equilibrium and effects of solution pH studies of fluoride removal by the optimized ceramic were discussed in batch experiments.

4.2. Materials and methods

4.2.1. Preparation of ceramic adsorbent

Kanuma mud, a common, inexpensive deposit of volcanic ash, was provided by Makino Store, Kiyosu, Japan. Kanuma mud was sieved to obtain less than 100 μm and then dried at 105 °C for 2 h to use for developing the ceramic adsorbent. Zeolite (the grain size was less than 75 μm) was supplied by the Azuwan Cement Factory, Japan. Starch and $FeSO_4 \cdot 7H_2O$ were supplied by the Wako Pure Chemical Industries,

Ltd, Japan. 4 g of Kanuma mud, 3 g of zeolite, 2 g of starch and 1 g of $FeSO_4 \cdot 7H_2O$ were mixed to homogeneity. Ultra pure water (resistivity18.2 MΩ cm at 25 °C) was then added into the mixture to make a paste and the granulation procedure was carried out manually. The obtained granules were then dried at 110 °C for 48 h and calcined at 600 °C for 1 h in a muffle furnace. Finally, the developed ceramic material was allowed to cool to room temperature in the furnace and then used for adsorption experiment.

4.2.2. Characterization of ceramic adsorbent

The developed optimized ceramic adsorbent was analyzed in order to determine its physicochemical properties. The specific surface area and pore-size distributions were determined with a Brunauer-Emmett-Teller (BET) method by gas adsorption (Coulter SA3100, US). The morphological images were acquired by scanning electron microscope (SEM) (JSM-6700F, JEOL, Japan). The spot element analysis of the ceramic adsorbent was carried out using the energy dispersive X-ray spectroscopy (EDS) detector (SEM-EDS, JEOL, Japan). Fluoride analysis was performed by a UV-visible spectrophotometer (Hitachi, DR/4000U, Japan). The determination of leached iron and aluminum was carried out by an inductively coupled plasma atomic emission spectrometer (ICP-AES, ICP-7500, Shimadzu, Japan).

4.2.3. Batch sorption studies

The adsorption of fluoride on ceramic adsorbent was studied at room temperature (30 °C) by batch experiments. The adsorbent used for this study was sieved to obtain

uniform particle size of 2-3 mm. About 2 g ceramic adsorbent was added into 100 mL of 10 mg/ L sodium fluoride solution with a desired pH value. The mixture was shaken in a shaker at a speed of 100 rpm (Tai Tec, Thermo Minder Mini-80, Japan). The effect of contact time (0-48 h) was examined at pH 6.9±0.1 with initial fluoride concentration of 10 mg/L. The adsorption isotherm was studied by varying the initial fluoride concentration from 5 to 50 mg/L at pH 6.9±0.1. The effect of pH was investigated by adjusting solution pH from 2 to 12 using 0.1 M HCl and 0.1 M NaOH under an initial fluoride concentration of 10 mg/L. The effects of competing anions (chloride, nitrate, carbonate, sulfate and phosphate) on fluoride adsorption were investigated by performing fluoride adsorption under a fixed fluoride concentration (10 mg/L), and initial competing anion concentrations of 20-200 mg/L at pH 6.9±0.1 over 48 h.

4.2.4. Sorption-desorption cycle

In order to test the regenerative ability of the ceramic adsorbent, a single sorption-desorption cycle was tested. Initially, the sorption study was conducted using 20 g/L of ceramic adsorbent and 10 mg/L of fluoride concentration (see Section 4.2.3). Then desorption of fluoride loaded on ceramic adsorbent was carried out with 0.1 M HCl and 0.1 M NaOH as the eluent. After the regeneration, the ability of ceramic adsorbent to remove fluoride from solution was again tested in an sorption experiment, using a similar procedure to that described in Section 4.2.3.

4.3. Results and discussion

4.3.1. Characterization of ceramic adsorbent

The surface morphology of the ceramic adsorbent was examined by SEM (Fig. 4.1a), clearly revealing a flocced and porous surface texture, which indicates the adsorbents were highly porous, with a high adsorption capacity. After extensive flow-through exposure (for 48 h) during fluoride adsorption, the surface changed to be smooth, polyhedron and stretched cubic structures (Fig. 4.1b). Fluoride adsorption may not only occur at the surface of the adsorbent but also inside of the pores. The EDS (Table 4.1) results showed that the iron content of ceramic adsorbent accounted for 12.24%, comparing with Kanuma mud, the proportion increased 5.5 times due to the addition of $FeSO_4 \cdot 7H_2O$. EDS (Fig. 4.1c) detection indicated that the adsorbent consisted mainly of Fe, O and F, implying that the F was bound with iron oxide. The specific surface area of ceramic adsorbent was found to be 80.94 sq m/g, and the pore volume was 0.1176 ml/g. The pore-size distributions (Fig. 4.1d) revealed that the observed pore sizes mostly varied between 6 and 80 nm (69.47%). The result also indicated that a large percentage of the pores (17.86%) were under 6 nm. According to IUPAC classification, this ceramic adsorbent is a typical mesoporous material.

4.3.2. Sorption isotherms

The experimental data was validated by using Fruendlich and Langmuir isotherm models. The linear forms of Freundlich and Langmuir isotherm equation are as:

$$logq_e = logK_f + 1/nlogC_e \quad (4.1)$$

$$1/q_e = 1/q_m + 1/Bq_m(1/C_e) \quad (4.2)$$

where q_e is the amount of fluoride ion adsorbed per unit mass of the adsorbent and C_e is the amount of fluoride ion in liquid phase at equilibrium. K_f, n, q_m and B are Freundlich and Langmuir constants, respectively. These equation are applied to correlate the amount of the fluoride adsorbed per unit amount of the adsorbent and can be calculated from slope and intercept. Fig. 4.2a shows a plot of $\log q_e$ versus $\log C_e$. The constants $1/n$ and $\log K_f$ were calculated from the slope and intercept. From the linear graph the correlation coefficient R^2 value and minimum sorption capacity were found 0.95 and 0.53 mg/g respectively. The experimental data fit well to the Freundlich isotherm model. The condition for the validity of a Freundlich type adsorption model is sorption on heterogeneous surfaces (Sujana et al., 1998). In Fig. 4.2b plot of $1/q_e$ versus $1/C_e$ yields straight line which demonstrates that sorption data followed by Langmuir sorption model well. The value of q_m is 2.16 mg/g and the Langmuir constant B is 0.3946. The essential characteristic of the Langmuir isotherm can be denoted by the dimensionless constant called equilibrium parameter, R_L, defined by:

$$R_L = 1/1 + BC_0 \quad (4.3)$$

where B is the Langmuir constant and C_0 is the initial adsorbate concentration (mg/L), R_L value indicate the type of isotherm to be irreversible (R_L=0), favourable (0<R_L<1), linear (R_L=1) and unfavourable (R_L>1) (Worku et al., 2007; Arami e al., 2005). The value of R_L 0.202 indicates favourable sorption of fluoride onto the ceramic adsorbent.

4.3.3. Effect of solution pH

The results presented in Fig. 4.3 indicate that the percentage fluoride removal greatly depends on the solution pH. The optimal pH for fluoride uptake appeared to be pH 7, with a removal percentage of 94.23%. The experimental data agree with the results obtained by Solangi (2010). The removal ability fluctuated slightly over the pH range of 4-11, which means that this ceramic adsorbent can adapt to a wide range of pH for fluoride adsorption from water and is suitable for practical applications. The equilibrium pH (pH_{final}) values were measured after 48 h sorption. It is clear that pH_{final} increases smoothly with increasing initial pH (Fig. 4.3). However, it was observed that ceramic adsorbent had a significant capacity to buffer highly acidic and alkaline solutions. The pH of zero point charge (pH_{zpc}) of ceramic adsorbent was 5.8 ± 0.2, estimated by using batch equilibrium techniques described by Chutia et al. (2009). The sharp decrease in the amount of fluoride adsorbed under alkaline pH conditions is probably due to competition for adsorption sites between fluoride and hydroxyl ions even though the oxide surface is positively charge (Raichur and Basu, 2001). On the other hand, under acidic conditions, the decrease may be attributed to the formation of weakly ionized hydrofluoric acid (Sujana et al., 1998) or the combined effects of chemical and electrostatic interactions between the oxide surface and fluoride ions.

4.3.4. Kinetic modeling

According to the kinetic data obtained from the experiment, pseudo-first-order and

pseudo-second-order mechanisms have been used to elucidate the mechanisms of adsorption and potential rate controlling steps (Solangi et al., 2010; Chutia et al., 2009).

$$log(q_e - q_t) = log\, q_e - k_1 t/2.303 \quad (4.4)$$

$$t/q_t = 1/(k_2 q_e^2) + t/q_e \quad (4.5)$$

where q_t and q_e are the amount of adsorbed fluoride (mg/g) at time t and at equilibrium time, respectively. k_1 and k_2 are first-order and second-order rate constants for adsorption. Kinetic constants obtained from the pseudo-first-order and pseudo-second-order models are given in Table 4.2. The value of correlation coefficient (R^2=0.9996) for the pseudo-second-order sorption model is higher than that (R^2=0.9463) obtained from the pseudo-first-order kinetic. Additionally, theoretical and experimental $q_{e,exp}$ (0.4721 mg/g) value is in a good accordance with the calculated equilibrium adsorption capacity $q_{e,cal}$ (0.5020 mg/g). The well-fitting to pseudo-second-order kinetic model for the sorption of fluoride by ceramic adsorbent suggests a chemisorptions process involving ion exchange (Ho, 2006).

4.3.5. Effect of competing anions

The fluoride-contaminated water may contain several other anions which may compete with the sorption of fluoride. The adsorption studies were carried out in the presence of 20-200 mg/L salt solutions of chloride, nitrate, sulfate, carbonate and phosphate independently at an initial fluoride concentration of 10 mg/L. The effects of these co-existing ions on fluoride removal are shown in Fig. 4.4. It was observed that

fluoride removal slightly increased in the presence of chloride and nitrate ions, which could be due to an increase in the ionic strength of the solution or a weakening of lateral repulsion between adsorbed fluoride ions. Similar observations have been reported by Eskandarpour (2008). It was also observed that fluoride removal slightly decreased from 94.4% to 87.8% in the presence of sulfate, and obviously decreased to 58.1% and 44.3% in the presence of carbonate and phosphate ions. Fluoride sorption slightly decreased by sulfate ion may be attributed to the high coulombic repulsive forces, which reduce the probability of fluoride interactions with the active sites (Onyango et al., 2004). Carbonate and phosphate ions had the greatest effect on fluoride sorption may be explained not only in terms of the competition for the same active sites with fluoride, but also by the high affinity and capacity for carbonate and phosphate ions on ceramic adsorbent. The results are in good agreement with similar work done by Kagne (2008) for hydrated cement, where the fluoride removal efficiency is not significantly affected by chloride, nitrate and sulfate but is significantly affected by carbonate and phosphate.

4.3.6. Possible mechanism

The mechanism of fluoride sorption on iron oxide surfaces can be given as (Stumm, 1992):

$$\equiv Fe - OH + F^- \leftrightarrow \equiv Fe - F + OH^- \quad (4.6)$$

$$Fe(OH)^{2+}(aq) + F^- \leftrightarrow FeF^{2+} + OH^- \quad (4.7)$$

Hiemstra et al. (2000) investigated the adsorption of fluoride on goethite and

confirmed by IR analysis that the process mainly occurred through coordination to surface FeOH groups. They formulated the formation of $FeF^{-1/2}$ as:

$$FeOH^{-1/2} + H^{+}(aq) + F^{-}(aq) \leftrightarrow FeF^{-1/2} + H_2O \quad (4.8)$$

It is expected that similar process occur on the present study by using ceramic adsorbent. It has been reported that fluoride interacts with singly coordinated FeOH surface groups and the mechanism of fluoride adsorption on iron oxide surfaces can be described as an exchange reaction against OH^- of surface groups. The OH/F exchange further suggests that the fluoride ion can be considered as fully located in the surface (Hiemstra and Riemsdijk, 2000; Kumr et al., 2009).

4.3.7. Comparison of fluoride sorption with other adsorbents

A comparison has been made between ceramic adsorbent and previously reported adsorbents for fluoride removal. As can be seen from Table 4.3, ceramic-supported iron oxide as adsorbent is better than many other adsorbents in terms of defluoridation capacity. The high fluoride adsorption capacity obtained in this work is mainly due to the dispersion of Fe in the ceramic adsorbent. This element has a strong affinity with fluoride ions. Therefore synthesized ceramic adsorbent that is easy to implement is effective adsorbent for removing fluoride from aqueous solution.

4.3.8. Sorption-desorption cycle

Water purification by adsorption technology is economical if the adsorbent is regenerable. Moreover, reuse of adsorbent helps reduce environmental impacts of disposing used adsorbents. Initially, fluoride removal on ceramic adsorbent was

calculated to be 94.4% (see Fig. 4.5). Then, desorption of fluoride from the adsorbent and regeneration of the ceramic adsorbent were done with 0.1 M HCl and NaOH as eluent. The results (Fig. 4.5) showed that a reduction in sorption efficiency occurred after the regeneration. At the end of the forth cycle, the fluoride sorption efficiency was observed to be 80.2% and 34.7% by using 0.1 M HCl and NaOH as eluent, respectively. That may indicate the eluent with 0.1 M HCl was more suitable to be used to regenerate the ceramic adsorbent. However, after the forth sorption cycle, about 14.2% reduction in efficiency was observed by using the eluent with 0.1 M HCl. This reduction in sorption efficiency may be attributed to the gradual dissolution of iron from the ceramic adsorbent surface during vigorous washing of the sorbent.

4.4. Conclusions

In this study, a novel sorbent, ferrous-amended ceramic adsorbent has been prepared and examined for its potential in removing fluoride from aqueous environment. Its granular structure, high surface area and effective capacity of fluoride removal make the adsorbent a highly potential media to be used in purification of fluoride from water. The adsorption capacity of ceramic adsorbent for fluoride was 2.16 mg/g at 30 °C. The sorption process was fitted well with both the Langmuir and Freundlich isotherm models. Kinetic study results indicate that the adsorption process followed a pseudo-second-order kinetic model. The optimum fluoride removal was observed at pH ranges of 4.0-11.0 indicating that the ceramic adsorbent has promising potential utility in practical application. The fluoride

adsorption was reduced in the presence of carbonate, phosphate and sulfate and increased slightly in the presence of chloride and nitrate ions. The ceramic adsorbent also can be regenerated several times with 0.1 M HCl as eluent. Therefore, the new ceramic adsorbent is a promising material for fluoride removal from water environment.

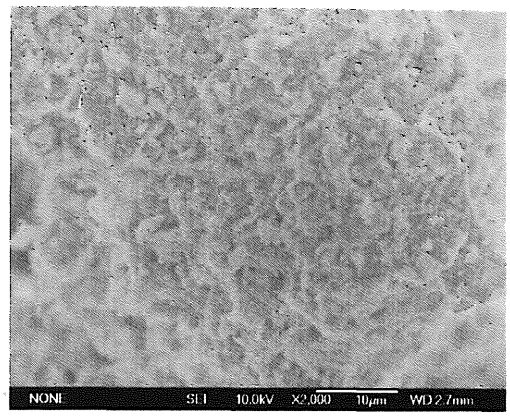

(a)

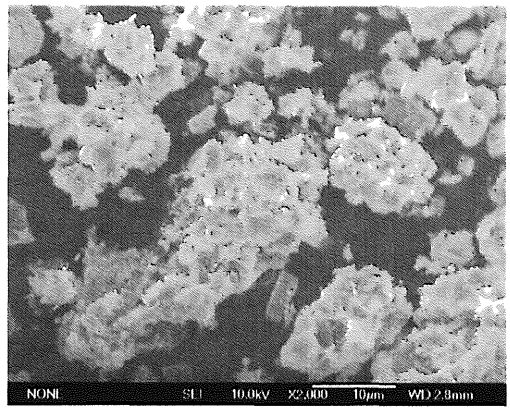

(b)

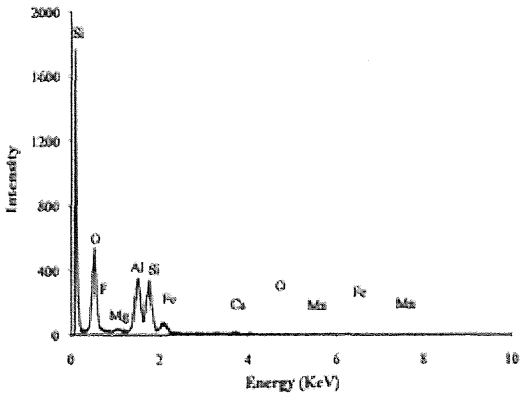

(c)

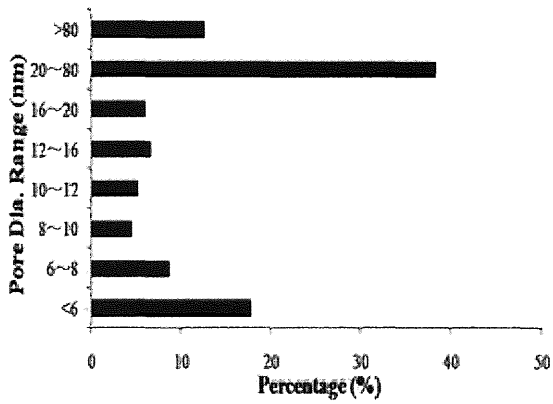

(d)

Fig.4.1 SEM images of (a) ceramic adsorbent and (b) fluoride-adsorbed ceramic adsorbent, EDS spectra of (c) fluoride-adsorbed ceramic adsorbent composite, BJH (Barrett-Joyner-Halenda) pore-size distribution of (d) ceramic adsorbent

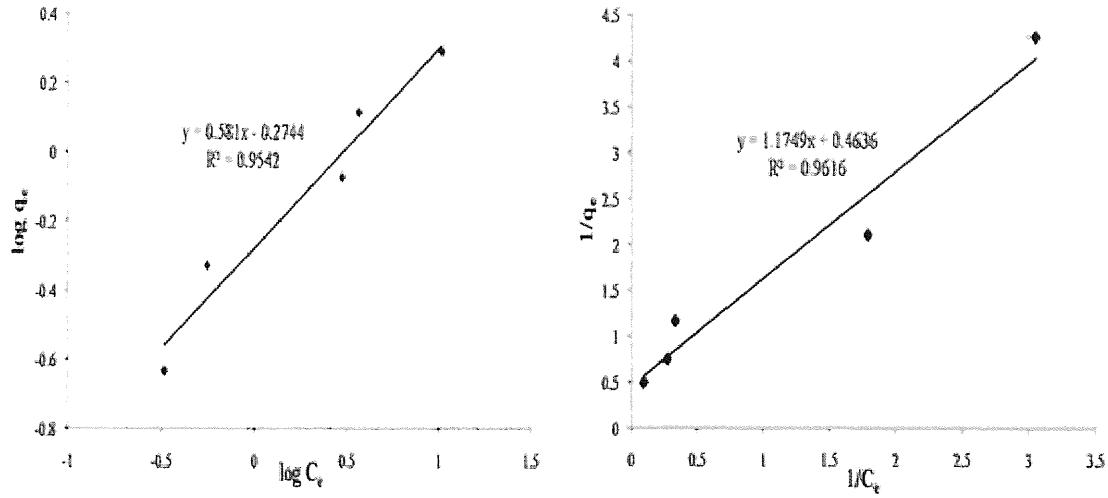

(a) (b)

Fig.4.2 Isotherm modeling of fluoride adsorption on the ceramic adsorbent (a) Freundlich isotherm; (b) Langmuir isotherm (initial fluoride concentration 10 mg/L, equilibrium contact time 48 h, initial pH 6.9±0.1, and temperature 30 °C)

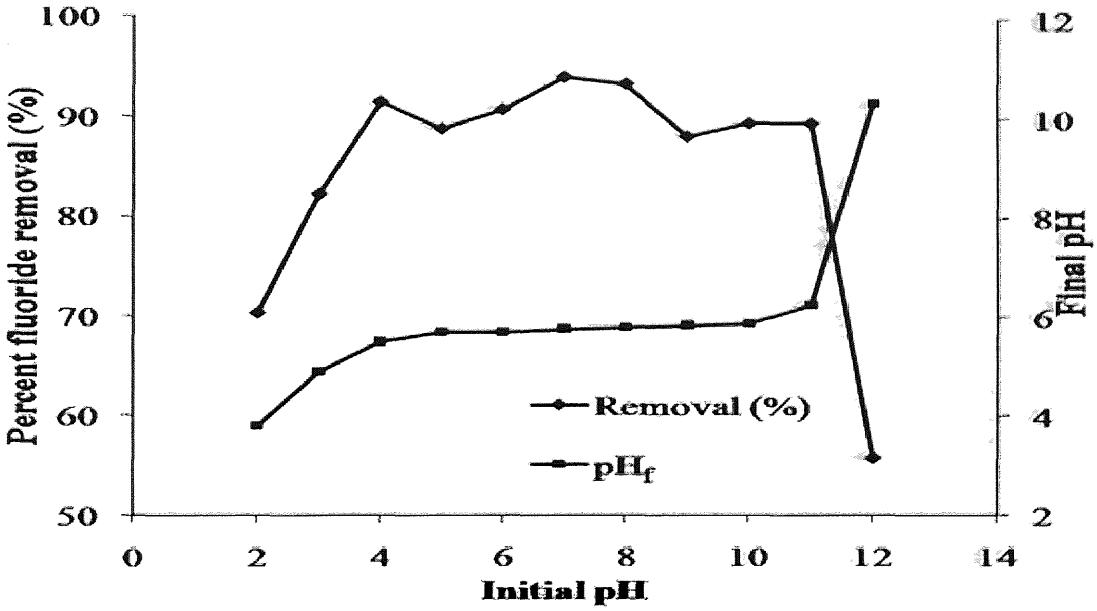

Fig.4.3 Effect of initial pH on fluoride removal and the equilibrium pH (pH_{final}) by the ceramic adsorbent (initial fluoride concentration 10 mg/L, equilibrium contact time 48 h, adsorbent dosage 20 g/L, and temperature 30 °C)

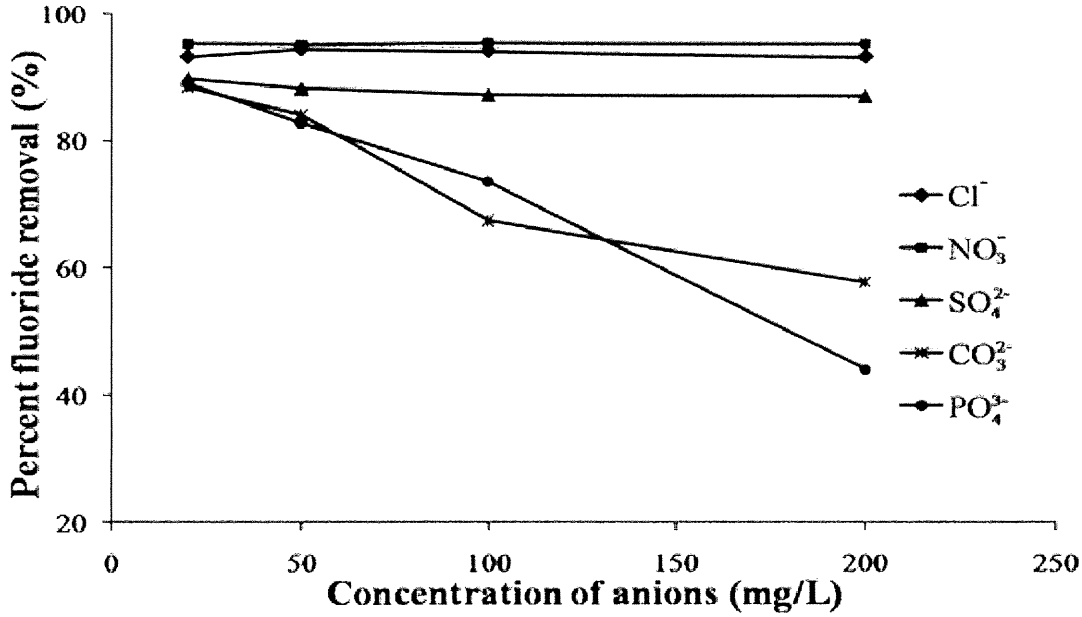

Fig.4.4 Effect of different concentrations of competing anions on fluoride adsorption by the ceramic adsorbent (initial fluoride concentration 10 mg/L, equilibrium contact time 48 h, adsorbent dosage 20 g/L, and temperature 30 °C)

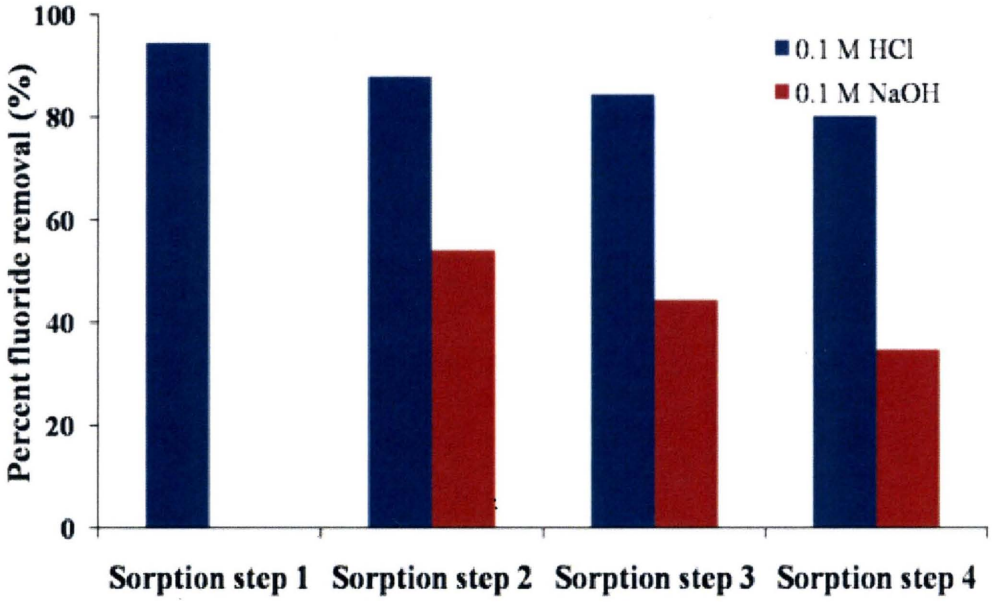

Fig.4.5 Fluoride sorption-desorption cycle (initial fluoride concentration 10 mg/L, equilibrium contact time 48 h, adsorbent dosage 20 g/L, and temperature 30 °C)

Table 4.1

Chemical analysis of Kanuma mud and ceramic adsorbent by SEM-EDS test

Composition (wt.%)	SiO_2	Al_2O_3	Fe_2O_3	MgO	CaO	MnO	pH_{zpc}
Kanuma mud[a]	56.20	38.70	2.20	0.36	2.00	0.54	6.1[b]
Ceramic adsorbent	44.91	37.28	12.24	1.27	1.93	2.37	5.8±0.2

[a] The effect on LOI (600 °C) has been neglected.

[b] Information supplied by the manufacturer.

Table 4.2
Kinetics constant for adsorption of fluoride onto ceramic adsorbent

C (mg/L)	Experiment $q_{e,exp}$ (mg/g)	Pseudo-first-order			Pseudo-second-order		
		k_1 (1/min)	$q_{e,cal}$ (mg/g)	R^2	k_2 [g/(mg min)]	$q_{e,cal}$ (mg/g)	R^2
10.00	0.4721	0.0930	0.2389	0.9463	0.6464	0.5020	0.9996

Table 4.3
Comparison between various adsorbents used for fluoride removal

Name of sorbent	Adsorption capacity (mg/g)	Reference
AlFe650/C	13.64	Eric et al. (2010)
Carbon slurry	4.86	Gupta et al. (2007)
Zn-Al layered double hydroxides	4.14	Mandal et al. (2008)
Magnesia-amended activated alumina	4.04	Shihabudheen et al. (2008)
Activated alumina	2.41	Ghorai et al. (2005)
Ceramic adsorbent	2.16	In current study
Activated carbon (Al-C300)	1.10	Ramos et al. (1999)
Calcite	0.39	Min et al. (1999)
Red mud	6.28×10^{-3}	Cengeloglu et al. (2002)
Charcoal	7.88×10^{-5}	Bhargava et al. (1992)

Chapter 5 Studies on Fluoride Adsorption of Iron-impregnated Granular Ceramics

5.1. Introduction

As described in chapter 3, iron-impregnated mesoporous granular ceramics were reported to exhibit high fluoride adsorption capacities (Chen et al., 2010). In this work, two representative samples of different iron-impregnated granular ceramics were synthesized and tested for removal of fluoride in aqueous solution. It is necessary to figure out the adsorption performances over different composition granular ceramic samples to draw a correct relationship between adsorption capacity and textural parameters of iron, since these two iron-impregnated granular ceramics prepared using different kinds of iron salt have been claimed. Adsorption kinetics and isotherms were conducted and modeled to investigate the adsorption behavior. Mechanisms involved in fluoride removal were explored by combining materials characterization and adsorption performance in batch studies.

5.2. Materials and methods

5.2.1. Synthesis of iron-impregnated granular ceramics

Kanuma mud (sieved less than 100 μm), a common, inexpensive deposit of volcanic ash, was purchased by Makino Store, Kiyosu, Japan. The chemical composition was analyzed by energy dispersive X-ray spectrometry (EDS). The result was shown in Table 1 and it shows that Kanuma mud is primarily a mixture of Si, Al

and Fe oxides. Zeolite (granule size: 50-75 μm) was supplied by the Azuwan Cement Factoty, Japan. Starch (granule size: 1-5 μm), Fe_2O_3 and $FeSO_4 \cdot 7H_2O$ were supplied by the Wako Pure Chemical Industries, Ltd, Japan. The iron-impregnated granular ceramics were made of the prepared powders (Kanuma mud, zeolite, starch and Fe_2O_3/ $FeSO_4 \cdot 7H_2O$) with the mass ratio of 4:3:2:1. Ultra pure water (resistivity18.2 MΩ cm at 25 °C) was then added into the mixture to make a paste and the granulation procedure was carried out manually at room temperature. The obtained granules were then dried at 110 °C for 48 h and calcined at 600 °C for 1 h in a muffle furnace. Finally, the developed ceramic materials were allowed to cool to room temperature in the furnace and then used for adsorption experiment.

5.2.2. Fluoride adsorption experiments

A 100 mg/L fluoride stock solution was prepared by dissolving 0.221 g of NaF in 1000 mL of ultra pure water. The test solution was prepared by diluting the stock solution to certain concentrations with ultra pure water. The pH value for test solution was adjusted by 0.1 M HCl and 0.1 M NaOH. Adsorption experiments were performed by agitating 20 g/L of iron-impregnated granular ceramics with 100 mL of fluoride solution of desired concentrations at constant temperature (about 30 °C) in different polypropylene conical flasks in a shaking machine (Tai Tec, Thermo Minder Mini-80, Japan) operated at 100 rpm. Experimental variables considered were: (a) contact time between granular ceramics and fluoride solution, 0-48 h; (b) initial fluoride concentration, 5-50 mg/L; (c) pH of test solution, 2-12; (d) possible

mechanisms for both of the different iron-impregnated granular ceramics. Fluoride analysis was performed by a UV-visible spectrophotometer (Hitachi, DR/4000U, Japan). The specific surface area was determined with a Brunauer-Emmett-Teller (BET) method by gas adsorption (Coulter SA3100, US). The morphological images and the spot element analysis of the granular ceramics were acquired by scanning electron microscope (SEM) and the energy dispersive X-ray spectroscopy (EDS) detector (SEM-EDS-6700F, JEOL, Japan).

5.3. Results and discussion

5.3.1. Chemical composition and characterization

The samples of $FeSO_4 \cdot 7H_2O$ impregnated granular ceramic (GC ($FeSO_4 \cdot 7H_2O$)) and Fe_2O_3 impregnated granular ceramic (GC (Fe_2O_3)) were brown and red-brown colored particles, respectively (Fig. 5.1(e) and (f)). The EDS (Table 5.1) showed the atom proportion of Al to Fe at the surface was about 3:1 and 1:1.6. EDS (Fig. 5.1c) detection indicated that the GC ($FeSO_4 \cdot 7H_2O$) consisted mainly of Al, Fe, and F, implying that the F was bound with aluminum and iron oxide, while the chemical composition outside the pores was mostly silicon dioxide with no F. EDS (Fig. 5.1d) detection did not show any F peak in GC (Fe_2O_3) which indicated weak adsorption ability for this adsorbent. The surface morphology of GC ($FeSO_4 \cdot 7H_2O$) and GC (Fe_2O_3) were shown in Fig.5.1. Compared with GC (Fe_2O_3), GC ($FeSO_4 \cdot 7H_2O$) had a significantly rougher surface with a lot of pores and flocs (Fig. 5.1a). The scalability of the needle-like surface of GC (Fe_2O_3) appeared to be less porosity which would

make F ions difficult to attach to the adsorbent. Textural properties obtained from nitrogen adsorption/desorption isotherms were summarized in Table 5.1. BET surface area of GC ($FeSO_4 \cdot 7H_2O$) and GC (Fe_2O_3) were 80.94 m^2/g and 50.01 m^2/g. The point of zero charge (pH_{pzc}) of the GC ($FeSO_4 \cdot 7H_2O$) and GC (Fe_2O_3) was about 5.8 and 6.9, estimated by using batch equilibrium techniques described by Chutia et al. (2009).

5.3.2. Effect of solution pH

Anions can be adsorbed on adsorbents through specific and/or nonspecific adsorption. The specific adsorption, involves ligand exchange reactions where the anions displace OH^- and/or H_2O from the surface (Ruthven, 1984). The nonspecific adsorption involves the coulombic forces, and mainly depends on the pH_{pzc} of the adsorbent (Rude and Aller, 1993). The effect of pH on removing fluoride from aqueous solution by GC ($FeSO_4 \cdot 7H_2O$) and GC (Fe_2O_3) was examined at pH ranging from 2 to 12 and the results are shown in Fig. 5.2. It is evident from the figure that for GC ($FeSO_4 \cdot 7H_2O$) sample, the maxima occurs at pH range of 4-11, with a maximum removal percentage of 94.23%, whereas for GC (Fe_2O_3) sample, the maxima is in the pH of 4, with a removal percentage of 60.48%. As both of these two adsorbents are combination of hydrous metal oxides like Al and Fe, therefore, the pH-dependent interaction of fluoride on these oxide species can be represented schematically as follows:

$$\equiv (Al/Fe)OH + H^+ \leftrightarrow \equiv (Al/Fe)OH_2^+ \qquad (5.1)$$

$$\equiv (Al/Fe)OH_2^+ + F^- \leftrightarrow \equiv (Al/Fe)F + H_2O \quad (5.2)$$

The overall reaction can be written as

$$\equiv (Al/Fe)OH + H^+ + F^- \leftrightarrow \equiv (Al/Fe)F + H_2O \quad (5.3)$$

where $\equiv$ is the functional group in the compound. The minimum adsorption in acidic range (pH<4) for this two adsorbents can be attributed to the formation of weak hydrofluoric acid. The decrease of adsorption in the alkaline pH range (pH>11) may be due to the competition of the hydroxyl ions with the fluoride for surface sites on adsorbent or electrostatic repulsion of fluoride ion to the negatively charged surface. In the pH range from 4 to 11, the fluoride removal ability fluctuated, which may be due to both specific and nonspecific adsorption on these surfaces (Sujana et al., 2009).

5.3.3. Equilibrium isotherms

Adsorption equilibrium is established when the concentration of adsorbate in bulk solution is in dynamic balance with that on the liquid-solid interface. Adsorption isotherms are the equilibrium relationships between the concentrations of adsorbed fluoride and fluoride in solution at a given temperature (Tor et al., 2009). In the current study, the Langmuir and Freundlich models were used to describe the equilibrium data by GC ($FeSO_4 \cdot 7H_2O$) and GC (Fe_2O_3). The Langmuir model is based on the hypothesis that uptake occurs on a homogenous surface by monolayer adsorption without interaction between adsorbed molecules, and is expressed as (Langmuir, 1916):

$$q_e = q_{max} b C_e / (1 + b C_e) \quad (5.4)$$

where q_{max} represents the maximum adsorption capacity and b is a constant related to affinity and energy of binding sites.

The Freundlich model proposes a monolayer sorption with a heterogeneous energetic distribution of active sites and with interaction between adsorbed molecules. It is expressed mathematically as (Freundlich, 1906):

$$q_e = K_F C_e^{1/n} \tag{5.5}$$

where K_F and n are the Freundlich coefficients. K_F provides an indication of the adsorption capacity and n is related to the intensity of adsorption. Fig. 5.3 demonstrates the plot of C_e versus q_e on the adsorption of fluoride by GC ($FeSO_4 \cdot 7H_2O$) and GC (Fe_2O_3). The equilibrium data of Fig. 5.3 have been analyzed by non-linear regression method using the isotherm Eq. (5.4) and (5.5). Table 5.2 presents the estimated model parameters. It was found that the adsorption data of fluoride on both of the two samples was fitted well to both Langmuir and Freundlich isotherm models. The magnitude of the Langmuir constant b has small values (0.018 and 0.395 L/mg), which indicates a low heat of adsorption. The Freundlich constant n values (1.862 and 1.193) indicate the high bond strength between adsorbate and adsorbent and it also indicates the adsorbent surface to be of heterogeneous (Dogan et al., 2004). The Langmuir adsorption capacities of these two granular adsorbents (2.16 and 1.70 mg/g) are higher than the reported values for fluoride by using calcite (0.39 mg/g) and activated carbon (Al-C300) (1.10 mg/g) (Yang et al., 1999; Ramos et al., 1999).

5.3.4. Kinetic studies

The time data generated was used to determine the rate constants. The adsorption rate constants of fluoride on GC ($FeSO_4 \cdot 7H_2O$) and GC (Fe_2O_3) were determined to understand the adsorption phenomena in terms of the adherence of fluoride on the active sites of the adsorbent as well as its intra-particle diffusion within the pores of the adsorbent (Ramos et al., 2005). The pseudo-first-order and pseudo-second-order equations have been used to throw light on the mechanisms of adsorption and potential rate controlling steps (Lagergren and Svenska, 1898; Ho and Mckay, 1999).

$$log(q_e - q_t) = log\, q_e - k_1 t/2.303 \quad (5.6)$$

$$t/q_t = 1/(k_2 q_e^2) + t/q_e \quad (5.7)$$

where q_t and q_e are the amount of adsorbed fluoride (mg/g) at time t and at equilibrium time, respectively. k_1 and k_2 are first-order and second-order rate constants for adsorption. The kinetic parameters estimated are shown in Table 5.3. It was found that the values of correlation coefficient described the pseudo-second-order equation very well (0.9996 and 0.9858), and that was better than the pseudo-first-order equation (0.9463 and 0.8084) for both of these two adsorbents. The modeled q_e values obtained from the pseudo-second-order kinetic equation were found very close to the experimental q_e. Thus, it had been concluded that the fluoride adsorption reaction with GC ($FeSO_4 \cdot 7H_2O$) and GC (Fe_2O_3) takes place obeying the pseudo-second-order kinetics under the conditions of experiment. The adsorption rate constant k_2 values were found to be 0.6464 and 0.4452 g/mg min for GC ($FeSO_4 \cdot 7H_2O$) and GC (Fe_2O_3) respectively.

Besides adsorption at the outer surface of the adsorbent, the fluoride ions may also diffuse into the interior of the porous adsorbent (Mahramanlioglu et al., 2002). Intra-particle diffusion model based on the theory proposed by Weber and Morris was tested to identify the diffusion mechanism (Weber and Morris, 1963). The intra-particle diffusion equation can be written as:

$$q_t = k_i t^{0.5} \tag{5.8}$$

where q_t is the amount adsorbed (mg/g) at a given time t (h), k_i (mg/g $h^{0.5}$) is the intra-particle diffusion rate constant. Fig. 5.4 shows the plot of the amount of fluoride adsorbed versus the square root of time. It is observed that the intra-particle diffusion modeling of fluoride adsorption on GC ($FeSO_4 \cdot 7H_2O$) and GC (Fe_2O_3) both are not linear form over the whole time range and the graphs of this figure reflect a three-step nature, with a initial linear portion followed by an intermediate linear portion and a plateau (Chen et al., 2010). The fluoride adsorption process by GC ($FeSO_4 \cdot 7H_2O$) and GC (Fe_2O_3) is very similar to each other, which can be obviously divided into 3 steps. The first step is the external surface adsorption (during the first 6 h). The second step is the intra-particle diffusion process, which is attained and continued to 18 h. The last step is the equilibrium adsorption process, and it begins after 18 h. The fluoride ions are rapidly adsorbed on the external surface of the adsorbents and slowly transported via intra-particle diffusion into the particles, then are finally retained in the inter pores of the GC ($FeSO_4 \cdot 7H_2O$) and GC (Fe_2O_3). In addition, the intra-particle diffusion rate constants k_i were calculated from the slopes of the plots from the second step of Fig. 5.4 and are found to be 5.71 and 2.49×10^{-2} mg/g $h^{0.5}$ for GC ($FeSO_4 \cdot 7H_2O$) and GC

(Fe_2O_3), respectively.

5.3.5. Effect of temperature

The effect of temperature on fluoride removal was studied in the solution temperature range from 303 to 323 K. It reveals that fluoride removal increased with the increase in temperature for both of the GC ($FeSO_4 \cdot 7H_2O$) and GC (Fe_2O_3) adsorbents (Fig. 5.5). This may be happening because the rise in temperature increases the binding tendency of the fluoride ions onto the interface and thereby strengthens the extent of adsorption. And it also shows that the fluoride adsorption process is endothermic in nature and confirms the combination of physical and chemical adsorption of fluoride on the GC ($FeSO_4 \cdot 7H_2O$) and GC (Fe_2O_3) surfaces.

In order to study the feasibility of the adsorption process, the change in free energy (ΔG), enthalpy (ΔH) and entropy (ΔS) of adsorption were calculated from the following equations (Khan and Singh, 1987):

$$K_c = C_{Ae}/C_e \tag{5.9}$$

$$\Delta G = -RT \ln K_c \tag{5.10}$$

$$\Delta G = \Delta H - T\Delta S \tag{5.11}$$

where C_{Ae} and C_e represent the concentration (mg/L) of fluoride on adsorbent and in solution, respectively. Values of ΔH, ΔG and ΔS are represented in Table 5.4. The positive value of entropy (ΔS) indicates increase in randomness of the ongoing process and hence a good affinity of fluoride with GC ($FeSO_4 \cdot 7H_2O$) and GC (Fe_2O_3) surfaces. Negative value of ΔG values reveals that the adsorption of fluoride on both

of these two samples is favorable and spontaneous under standard conditions. The endothermic nature of the process was once again confirmed by the positive value of enthalpy (ΔH). These results for fluoride adsorption on quick lime and laterite have also been reported (Islam and Patel, 2007; Sarkar et al., 2006).

5.4. Conclusions

In the present study, iron-impregnated novel granular ceramic adsorbents with high specific surface areas were synthesized by simple granulation procedure at room temperature. This study has demonstrated that both GC ($FeSO_4 \cdot 7H_2O$) and GC (Fe_2O_3) adsorbents can be used for fluoride removal from aqueous solution, while GC ($FeSO_4 \cdot 7H_2O$) is more effective for fluoride removal than GC (Fe_2O_3). Maximum adsorption of fluoride on GC ($FeSO_4 \cdot 7H_2O$) and GC (Fe_2O_3) at pH 7.0 and 4.0 were 94.23% and 60.48%, respectively. The equilibrium data of samples fitted well to both Langmuir and Freundlich isotherms. Both of these two granular adsorbents followed second-order kinetics and were governed by intra-particle diffusion model. With the increase in temperature from 303 to 323 K, fluoride removal on these two adsorbents increased indicating combination of physical and chemical adsorption process. The calculated thermodynamic parameters showed that both of the adsorption processes were thermodynamically favorable, spontaneous and endothermic in nature. Moreover, the particle size of these granular ceramics was around 3~5 mm, which would not block the sewer and could be easily separated from water.

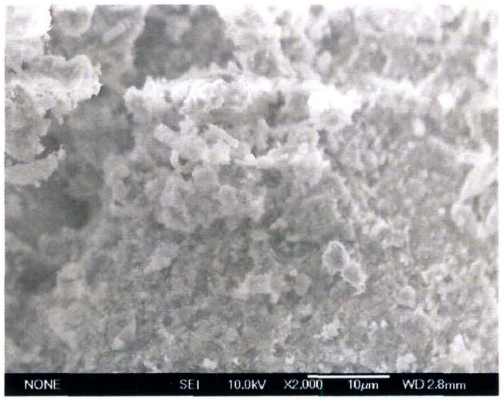

(a)

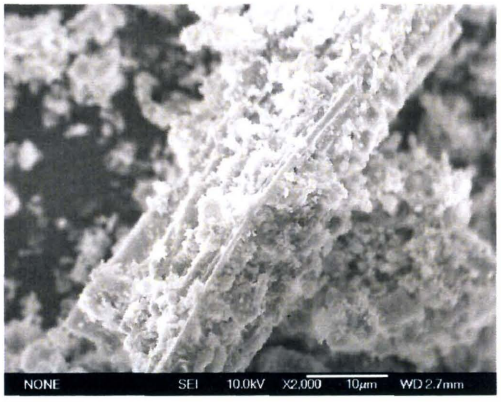

(b)

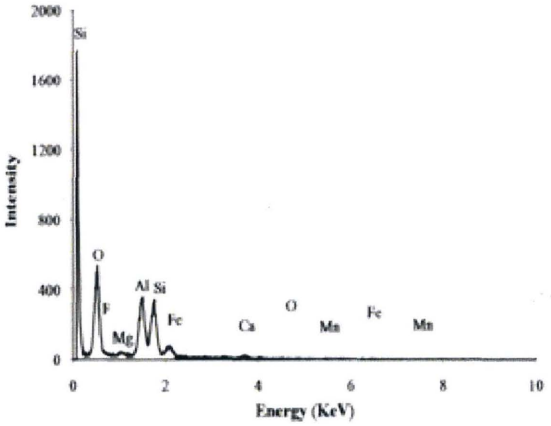

(c)

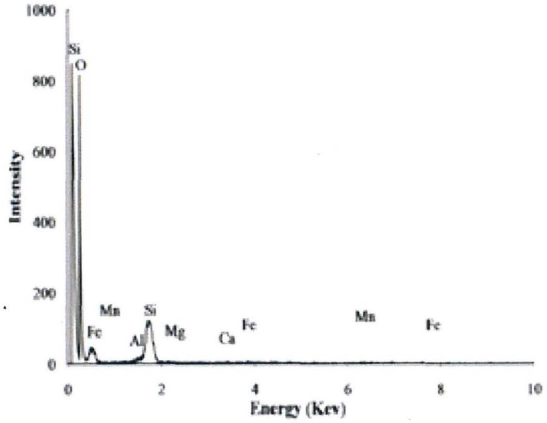

(d)

(e)

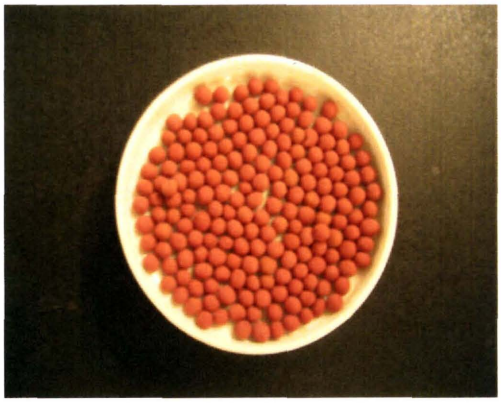

(f)

Fig.5.1 SEM images of pristine (a) GC ($FeSO_4 \cdot 7H_2O$) 2000× and (b) GC (Fe_2O_3) 2000×; EDS spectra of fluoride-adsorbed (c) GC ($FeSO_4 \cdot 7H_2O$) and (d) GC (Fe_2O_3); Photos of pristine (e) GC ($FeSO_4 \cdot 7H_2O$) and (f) GC (Fe_2O_3)

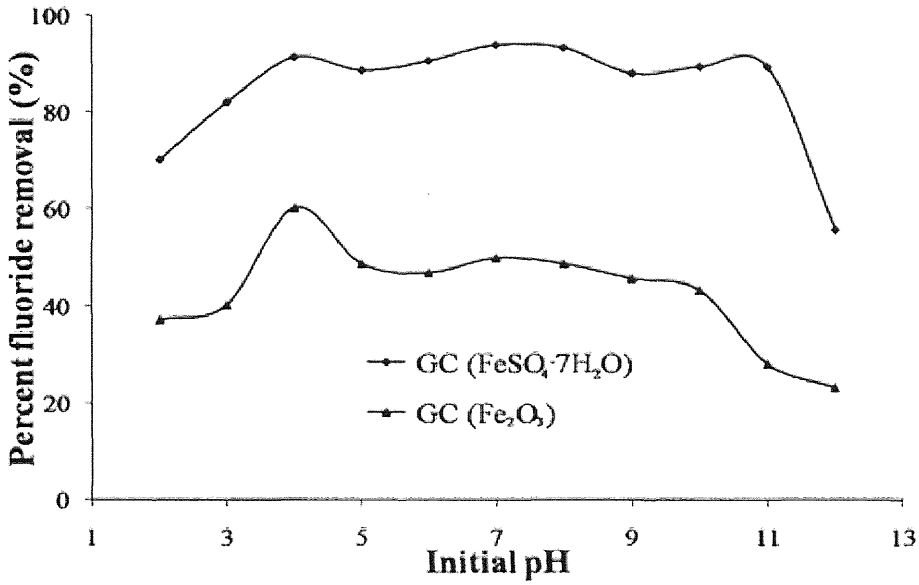

Fig.5.2 Effect of solution pH on fluoride removal by GC ($FeSO_4 \cdot 7H_2O$) and GC (Fe_2O_3) (initial fluoride concentration 10 mg/L, equilibrium contact time 48 h, adsorbent dosage 20 g/L, shaken speed 100 rpm, initial pH 6.9±0.1, and temperature 30 °C)

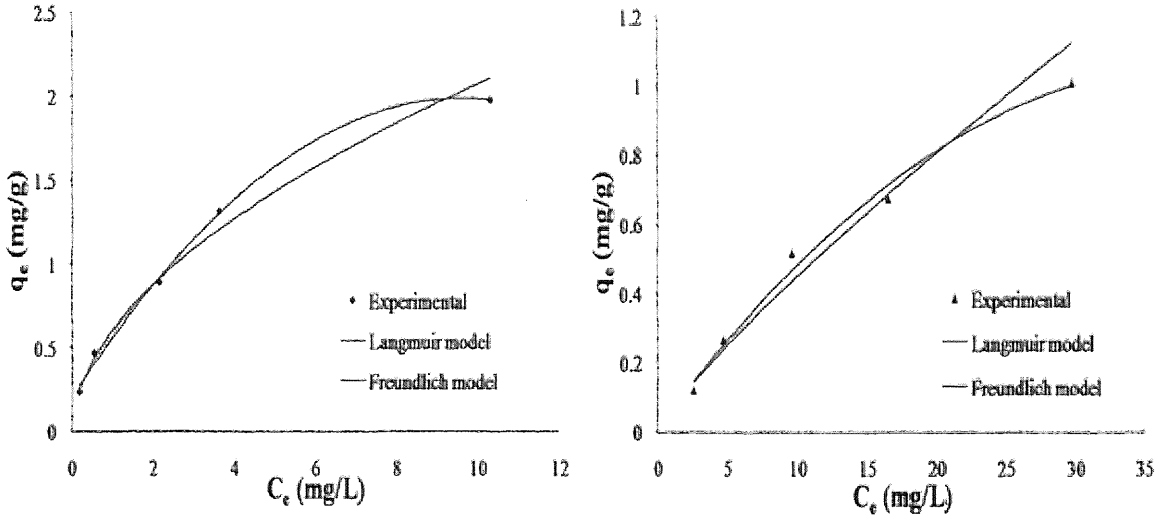

(a) (b)

Fig.5.3 The plot of C_e versus q_e on adsorption of fluoride by (a) GC ($FeSO_4 \cdot 7H_2O$) and (b) GC (Fe_2O_3) (initial pH 6.9 $\pm$ 0.1, equilibrium contact time 48 h, adsorbent dosage 20 g/L, shaken speed 100 rpm and temperature 30 °C)

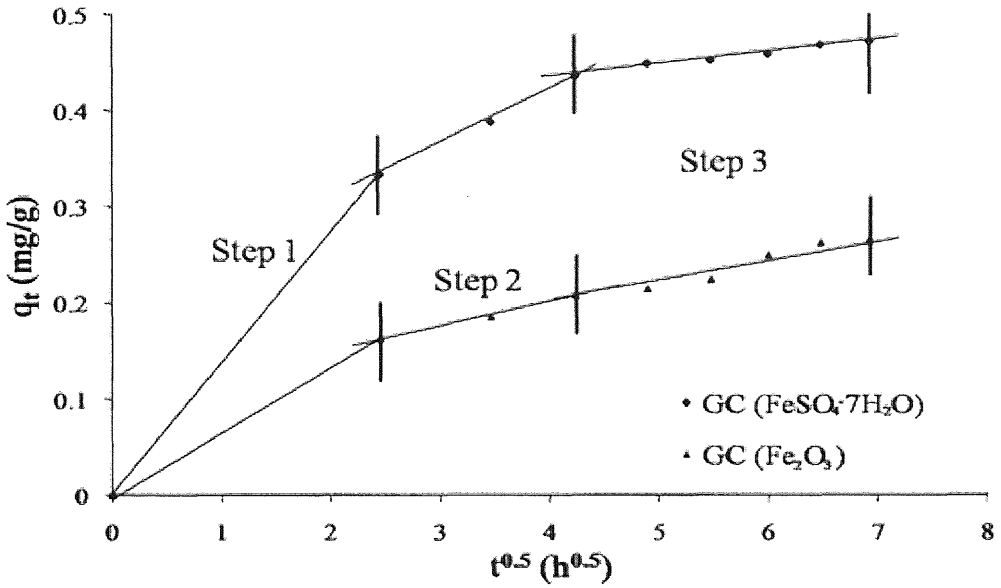

Fig.5.4 Intra-particle diffusion modeling of fluoride adsorption on GC ($FeSO_4 \cdot 7H_2O$) and GC (Fe_2O_3) (initial pH 6.9 $\pm$ 0.1, initial fluoride concentration 10 mg/L, equilibrium contact time 48 h, adsorbent dosage 20 g/L, shaken speed 100 rpm and temperature 30 °C)

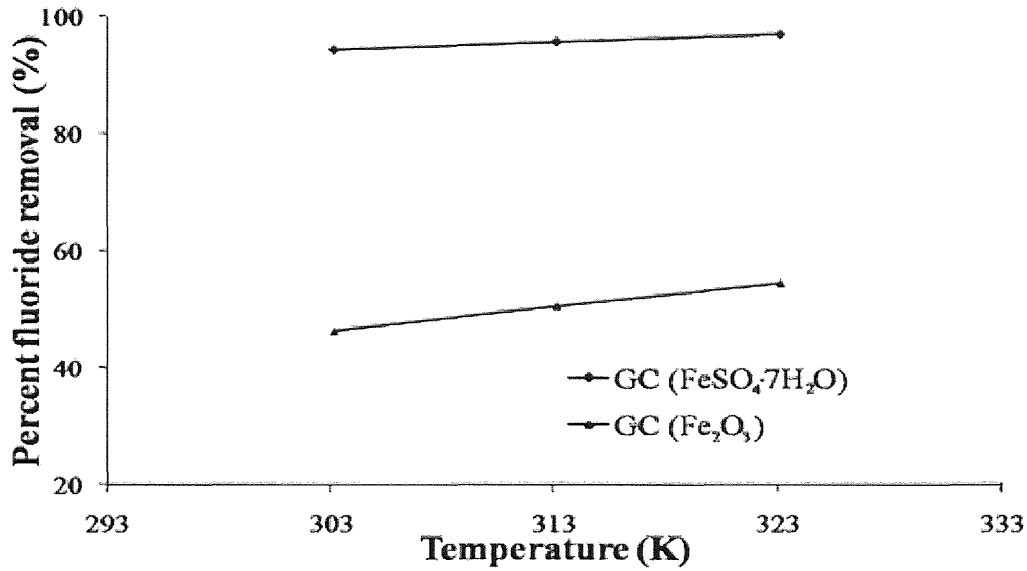

Fig.5.5 Effect of temperature on fluoride removal by GC ($FeSO_4 \cdot 7H_2O$) and GC (Fe_2O_3) (initial pH 6.9±0.1, initial fluoride concentration 10 mg/L, equilibrium contact time 48 h, adsorbent dosage 20 g/L and shaken speed 100 rpm)

Table 5.1
Chemical analysis and surface area characterization of Kanuma mud and iron-impregnated granular ceramics

Chemical analysis of Kanuma mud and iron-impregnated granular ceramics by SEM-EDS test

Composition (wt.%)	SiO_2	Al_2O_3	Fe_2O_3	MgO	CaO	MnO	pH_{pzc}
Kanuma mud[a]	56.20	38.70	2.20	0.36	2.00	0.54	6.4[b]
GC ($FeSO_4 \cdot 7H_2O$)	44.91	37.28	12.24	1.27	1.93	2.37	5.8±0.1
GC (Fe_2O_3)	55.82	14.96	24.45	0.81	1.84	2.12	6.9±0.1

Surface area and pore volume analysis by BET test

	BET surface area (m^2/g)	Langmuir surface area (m^2/g)	T-plot surface area (m^2/g)	Pore volume (cm^3/g)
GC($FeSO_4 \cdot 7H_2O$)	80.94	51.75	68.80	0.1176
GC (Fe_2O_3)	50.01	45.19	55.47	0.1008

[a] The effect on LOI (600 °C) has been neglected.

[b] Information supplied by the manufacturer.

Table 5.2
Langmuir and Freundlich isotherm parameters for the adsorption of fluoride on GC ($FeSO_4 \cdot 7H_2O$) and GC (Fe_2O_3)

Ceramic adsorbent	Langmuir isotherm			Freundlich isotherm		
	q_{max} (mg/g)	b (L/mg)	R^2	K_f (mg/g)	n	R^2
GC ($FeSO_4 \cdot 7H_2O$)	2.157	0.395	0.962	0.604	1.862	0.993
GC (Fe_2O_3)	1.699	0.018	0.961	0.065	1.193	0.971

(Initial pH 6.9±0.1, initial fluoride concentration 5-50 mg/L, adsorbent dosage 20 g/L and temperature 30 °C)

Table 5.3
Kinetic constants for adsorption of fluoride on GC ($FeSO_4 \cdot 7H_2O$) and GC (Fe_2O_3)

Ceramic adsorbent	Experiment	Pseudo-first-order			Pseudo-second-order		
	$q_{e,exp}$ (mg/g)	k_1 (1/min)	$q_{e,cal}$ (mg/g)	R^2	k_2 [g/(mg min)]	$q_{e,cal}$ (mg/g)	R^2
GC ($FeSO_4 \cdot 7H_2O$)	0.4721	0.0930	0.2392	0.9463	0.6464	0.5020	0.9996
GC (Fe_2O_3)	0.2665	0.0829	0.2493	0.8084	0.4452	0.3011	0.9858

(Initial pH 6.9±0.1, initial fluoride concentration 10 mg/L, shaken speed 100 rpm, adsorbent dosage 20 g/L and temperature 30 °C)

Table 5.4

Thermodynamic parameters for the fluoride removal on GC ($FeSO_4 \cdot 7H_2O$) and GC (Fe_2O_3)

Ceramic adsorbent	ΔG (kJ/mol)	ΔS (J/mol K)	ΔH (kJ/mol)
GC ($FeSO_4 \cdot 7H_2O$)	-7.13	114.86	27.72
GC (Fe_2O_3)	-0.49	43.03	13.41

(Initial pH 6.9±0.1, initial fluoride concentration 10 mg/L, shaken speed 100 rpm and adsorbent dosage 20 g/L)

Chapter 6 Preparation of Granular Ceramic Containing Dispersed Al and Fe Oxides

6.1. Introduction

As described in chapter 5, in the present study, we successfully developed a new adsorbent by impregnation of porous granular ceramics with aluminum and iron salts for fluoride removal. Batch studies were conducted into using this novel adsorbent with optimization of various experimental conditions, including contact time, adsorbent dose, initial pH and co-existing ions in solutions. The nature and morphology of the adsorbents were therefore discussed on the basis of SEM, XRD, EDS, and BET studies. The Langmuir and Freundlich isotherm models were used to explain the mechanism of fluoride removal by this novel adsorbent. Various kinetic models were also used to describe the adsorption process.

6.2. Materials and methods

6.2.1. Material preparation

Knar clay (particle size was less than 75 μm) was purchased in the Isehisa Store (Japan), zeolite (particle size was less than 100 μm) was supplied by the Azuwan Cement Factory (Japan), wheat starch was supplied by the Wako Pure Chemical Industries, Ltd (Japan). Knar clay, zeolite and starch with mass ratio 1:1:1 was prepared to be porous granular ceramic by simple co-precipitation method by ultra pure water (resistivity18.2 MΩ cm at 25 °C). Detailed procedure is given in previous

publication (Chen et al., 2010). Then the prepared porous granular ceramics were impregnated with a boiling mixture of 1M $AlCl_3$ and 1M $FeCl_3$ aqueous solution for 2 h. After the heating, the samples remained immersed in the aqueous solution for 2 h. The impregnated granules were removed from the solution, then dried in the open air for 2 h and afterwards dried in an oven at 105 °C for 24 h. The obtained granules were calcined at 600 °C for 1 h in a muffle furnace. Finally, the samples was cooled to room temperature and sieved to 2~3 mm for further studies.

6.2.2. Adsorption experiments

Stock solution (100 mg/L) was prepared by dissolving 0.221 g anhydrous sodium fluoride to 1 L of ultra pure water. This will be diluted to obtain required concentration for further use. The experimental procedure for adsorption isotherms and kinetics, adsorption at different adsorbent dose, initial pH and interference of other ions has been described in batch studies.

6.3. Results and discussion

6.3.1. Characterization of adsorbent

The prepared Al/Fe dispersed in porous granular ceramic adsorbent is reddish brown colored and 2-3 mm in diameter (shown in Fig. 6.1b). As can be seen from Fig. 6.1a, the adsorbents have the expected large number of porous structure in the cross section which indicates the adsorbent has a high adsorption capacity. This microcosmic pore texture was attributed to the sintering of certain inorganic and

organic substances (such as starch) during the calcination process. The EDS spectrum of Fig. 6.1e shows the presence of Fe, Al, Si, O and Cl in the surface of adsorbent, which can be attributed to the impregnation with $AlCl_3$ and $FeCl_3$ solutions. It is difficult to establish the chemical composition of the inorganic compounds which were formed in granular ceramics, because of the possible existence of some amorphous compounds and the complexity of the knar clay. However, it appears that there would be mainly iron and aluminum oxides on the surface of ceramics. The XRD patterns of the ceramic adsorbents that contain iron and aluminum oxides are shown in Fig. 6.1c and Fig. 6.1d. It was observed from Fig. 6.1c that diffraction peaks attributed to crystalline iron oxide, aluminum oxide, hematite and maghemite. The peaks of Fe and Al in Fig. 6.1c were due to the granular ceramics coated by $AlCl_3$ and $FeCl_3$ solutions. The XRD study reveals that the amorphous structure of adsorbent showed significant changes after the fluoride adsorbed in Fig. 6.1d. The diffraction peaks are attributed to crystalline iron and aluminum fluoride hydroxide hydrate and iron zinc oxide fluoride. This suggests that the uptake of fluoride ions is partly by chemical adsorption. The specific surface area of ceramic adsorbent was found to be 50.69 sq m/g, and the pore volume was 0.1108 ml/g. The pore-size distributions (Fig. 6.1f) revealed that the observed pore sizes mostly varied between 6 and 80 nm (73.23%). As the radius of fluorine (1.33Å) is much smaller than this value, this pore size range is conducive to the penetration of fluorine into the inner layer of the adsorbents.

6.3.2. Effect of adsorbent dose

The effect of adsorbent dose on the fluoride removal was studied at pH 6.9 ± 0.1, room temperature and 10 mg/L of fluoride. The results obtained are shown as percent adsorption and loading capacity in Fig. 6.2a. The increase in fluoride removal with increase of adsorbent dose is the consequence of a greater amount of available binding sites for fluoride. The distribution coefficient (K_D) for fluoride on adsorbent was calculated by (Murray and Stumm, 1988):

$$K_D = [F^-]_{ads}/[F^-]_{diss}(1/C_p) \quad (6.1)$$

where C_p is the solid concentration in kg/L and K_D has the units of L/kg. A distribution coefficient reflects the binding ability of the surface for an element. The K_D value of a system mainly depends on pH and the type of surface. It was found that the K_D values increased with increase of adsorbent dose (Fig. 6.2b), which is very similar to the results investigated by M.G Sujana etc (2010). It is clearly revealed that the binding ability of the surface, as reflected in the K_D values, decreased with the adsorbent dose increased. If the surface is homogeneous the K_D value should not change with adsorbent dose at constant pH, so the increase of K_D values indicated the heterogeneous in nature of adsorbent surface (Sujana and Anand, 2010; Moore, 1971).

6.3.3. Effect of solution pH

The initial pH of solution is one of the important parameters that obviously affect the extent of fluoride adsorption. As shown in Fig. 6.3a, the amount of adsorbed fluoride enhances significantly with increasing pH and it attains a maximum at pH 6,

thereafter it declines. The maximum fluoride removal was found to be 89.3%, with a fluoride adsorption capacity of 0.4464 mg/g. Fig. 6.3b demonstrates the variation of equilibrium pH (pH_f) from the initial pH (pH_i) during experiments. Horizontal portion at pH_f ranged in 6.5-6.6 should be the pH_{zpc} of prepared adsorbent. Therefore, the surface characteristic of the mixed oxide is (i) positive at $pH_f < 6.5$, (ii) neutral at $pH_f = 6.5$-6.6, and (iii) negative at $pH_f > 6.6$.

The mechanism involved in the fluoride adsorption process using Al/Fe dispersed in porous granular ceramics can be described by the following equations, where M is Al^{3+} and Fe^{3+} bound to porous granular ceramics.

$$MCl_{(s)} + H_2O \rightarrow MOH_{(s)} + H^+_{(aq)} + Cl^-_{(aq)} \quad (6.2)$$

$$MOH_{(s)} + H_3O^+_{(aq)} + F^- \rightarrow MOH_2^+ \cdots F^-_{(s)} + H_2O \quad (6.3)$$

$$MOH + F^- + H_3O^+ \rightarrow M^+ \cdots F^-_{(s)} + 2H_2O \quad (6.4)$$

It was evident from our results that the granular ceramics exhibited significantly fluoride removal in the acidic pH range (the fluoride removal is 86.7% at pH 4, which is similar to the maximal value 89.3% at pH 6). This may be due to the fact that for $pH_i < pH_{zpc}$, the positive adsorbent surface adsorbed fluoride with electrostatic force of attraction (Eq. 6.3) or by exchange of hydroxyl ion on the solid surface (Eq. 6.4). The minimal fluoride removal at pH < 4 may be attributed to the formation of HF, which would reduce the coulombic attraction between fluoride and the adsorbent surface (Sujana et al., 1998). The decrease in the amount of fluoride adsorbed at pH > 6 is probably due to competition for adsorption sites between fluoride and hydroxyl ions even though the oxide surface is positively charge (Raichur and Basu, 2001). The

mechanism as suggested are found to be similar to that had been reported for fluoride adsorption by iron (III)-aluminum (III)-chromium (III) ternary mixed oxide (Biswas et al., 2010), concrete materials (Oguz, 2005) and activated cerium (IV) oxide SiMCM-41 adsorbent (Xu et al., 2001).

6.3.4. Effect of co-existing anions

The fluoride-contaminated water may contain several other anions which may compete with fluoride ions in the adsorption process. The present study assessed fluoride adsorption behavior in the presence of 200 mg/L chloride, nitrate, sulfate, carbonate, and phosphate ions, with initial fluoride concentration of 10 mg/L. As can be seen from Fig. 6.4, it was observed that carbonate and phosphate showed extremely negative effect, nitrate showed slightly positive effect while chloride and sulfate really did not affect the fluoride removal. This may be due to the change in pH as well as competing effect of these co-existing ions for the active sites of the adsorbent. The pH of the fluoride solutions were 6.15, 6.45, 6.57, 10.34 and 10.78, respectively, for Cl^-, NO_3^-, SO_4^{2-}, CO_3^{2-} and PO_4^{3-} while the pH of the fluoride was 6.9 without addition of anions. It was also confirmed from the experiment on the effect of pH (Section 6.3.3) that the fluoride removal decreases in highly alkaline pH as also explained. Similar observations have been reported by Eskandarpour and Kagne etc (2008).

6.3.5. Adsorption isotherms

The distribution of fluoride ion between the liquid and solid phase is a measure of

the position of equilibrium in the adsorption process which can be expressed by the Freundlich and Langmuir isotherm models.

Freundlich equation is derived to model the multilayer adsorption and for the adsorption on heterogeneous surfaces. The linearized form of Freundlich model is formulated as (Freundlich, 1906)

$$logq_e = logk_F + 1/n\, logC_e \tag{6.5}$$

where C_e is equilibrium concentration, q_e is equilibrium adsorption capacity, K_F and $1/n$ are Freundlich constants, related to minimum adsorption capacity and adsorption intensity, respectively. The values of K_F and $1/n$ were obtained from the slope and intercept of the linear Freundlich plot of $\log q_e$ versus $\log C_e$, and the results were shown in Table 6.1. It was found that the value of adsorption intensity ($1/n = 0.468$) is less than unity, which indicates favorable in the fluoride adsorption process (Mahramlioglu et al., 2002).

Langmuir adsorption isotherm models the monolayer coverage of the adsorption surfaces and assumes that adsorption take places on a structurally homogeneous surface of the adsorbent. The linear form of the Langmuir model can be presented as (Langmuir, 1916):

$$1/q_e = 1/q_{max}bC_e + 1/q_{max} \tag{6.6}$$

where C_e is the concentration of fluoride at equilibrium, q_e is the adsorption capacity at equilibrium, q_{max} is the monolayer capacity of the adsorbent and b is the Langmuir adsorption constant. The values of Langmuir parameters, q_{max} and b were calculated from the slope and intercept of the linear plots of $1/ q_e$ versus $1/ C_e$ and were found to

be 1.788 mg/g and 0.313 L/mg respectively, with regression coefficient (R^2) of 0.995.

The essential characteristic of the Langmuir isotherm can be denoted by the dimensionless constant called equilibrium parameter, R_L, defined by:

$$R_L = 1/1 + bC_0 \quad (6.7)$$

where b is the Langmuir constant and C_0 is the initial fluoride concentration (mg/L). The value of $R_L < 1$ represents favorable adsorption and $R_L > 1$ represents unfavorable adsorption (Arami et al., 2005). The value of R_L for an initial fluoride concentration of 10 mg/L is found to be 0.242, which indicates that this system is favorable for adsorption.

6.3.6. Adsorption kinetics

The effect of contact time was studied up to 72 h at initial fluoride concentration of 10 mg/L, adsorbent dose of 20 g/L, initial solution pH of 6.9, temperature of 25 °C. The results showed that loading capacity was 0.4464 mg/g, and the equilibrium was attained within 48 h. According to the kinetic data obtained from the experiment, pseudo-first-order and pseudo-second-order mechanisms have been used to elucidate the mechanisms of adsorption and potential rate controlling steps (Solangi et al., 2010; Chutia et al., 2009).

$$log(q_e - q_t) = logq_e - k_1 t/2.303 \quad (6.8)$$

$$t/q_t = 1/k_2 q_e^2 + t/q_e \quad (6.9)$$

where q_t and q_e are the amount of adsorbed fluoride (mg/g) at time t and at equilibrium time, respectively. k_1 and k_2 are first-order and second-order rate constants

for adsorption. The adsorption rate constant k_1 was determined from the slope of the linear plot of $log\ (q_e\text{-}q_t)$ versus t (Fig. 6.5a), and k_2 was obtained by plotting t/q_t versus t (Fig. 6.5b). The adsorption kinetic constants obtained from the pseudo-first and pseudo-second order models are shown in Table 6.2. The kinetic data indicates that the fluoride adsorption on Al/Fe dispersed in porous granular ceramics obeys the pseudo-second order kinetic model (R^2=0.995) more than pseudo-first order kinetic model (R^2=0.975), which suggests a chemisorption process in this experiment.

The possible contribution of intra-particle diffusion on fluoride adsorption process was described by using Weber-Morris model. The linear form of intra-particle diffusion model is given by (Weber and Morris, 1963):

$$q_t = k_i t^{1/2} + C \tag{6.10}$$

where k_i can be calculated from the slope of the plot of q_t versus $t^{1/2}$. As shown in Fig. 6.5c, the linear portion of plot is not passing through the origin, which indicates the fluoride adsorption on Al/Fe dispersed in porous granular ceramics is a complex procedure. Both the surface adsorption as well as intra-particle diffusion contributes to the rate determining step (Sujana et al., 2010; Mahramlioglu et al., 2002).

6.3.7. Adsorbent regeneration

Regeneration of any exhausted adsorbent is a crucial factor in any sorption process for improving the process economics. In the present study, 0.1 M HCl and NaOH were used as an eluent to check its eluting potential. From the results, it was observed that 0.1 M HCl could elute nearly 85% adsorbed fluoride from porous granular

ceramics. Then the adsorption study was carried out using 20 g/L fluoride-desorbed adsorbents with initial fluoride concentration of 10 mg/L. The results showed that a considerable reduction in adsorption efficiency after the regeneration, which may be attributed to the gradual dissolution of coated layer from the surface during vigorous washing of the adsorbent. Hence, a new regeneration protocol was developed by recoating the adsorbent before adsorption. For this, after desorption process using 0.1 M HCl, the adsorbents were dipped in 1 M $AlCl_3$ and $FeCl_3$ solutions for 2-3 h. The mixture were dried and calcined at 600 °C and used for next adsorption cycle. After the adsorption experiment, it was found that adsorption efficiency of adsorbent after recoating was no reduction.

6.4. Conclusions

In this study, these low-cost adsorbents have shown a good efficiency in fluoride removal from aqueous solution and can be useful for environmental protection purposes. The loading capacity of these prepared adsorbents for fluoride was 1.79 mg/g at room temperature. The optimum fluoride removal was observed at pH ranges of 4.0-9.0 indicating that the adsorbent has promising potential utility in practical application. Carbonate and phosphate ions showed extremely negative effect, nitrate ion showed slightly positive effect while chloride and sulfate ions really did not affect the fluoride removal. The adsorption process was fitted well with both the Freundlich and Langmuir isotherm models. Kinetic study results indicate that the adsorption process followed a pseudo-second-order kinetic model.

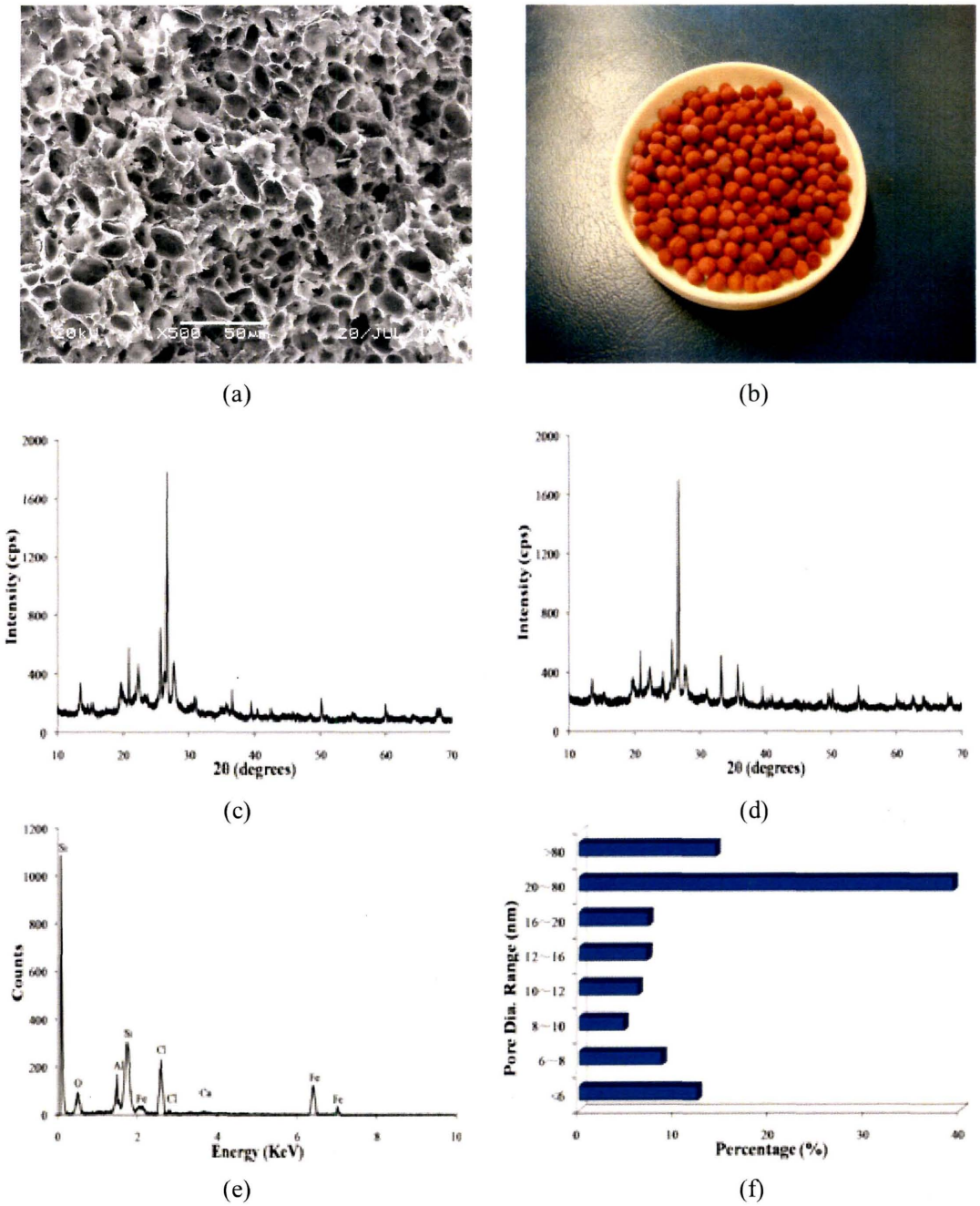

Fig.6.1 SEM images of (a) cross section of pristine granular ceramics and (b) Photo of pristine granular ceramics, Powder XRD patterns of (c) pristine granular ceramics and (d) adsorbed granular ceramics, EDS spectra of (e) pristine granular ceramics, BJH (Barrett-Joyner-Halenda) pore-size distribution of (f) pristine granular ceramics

(a)

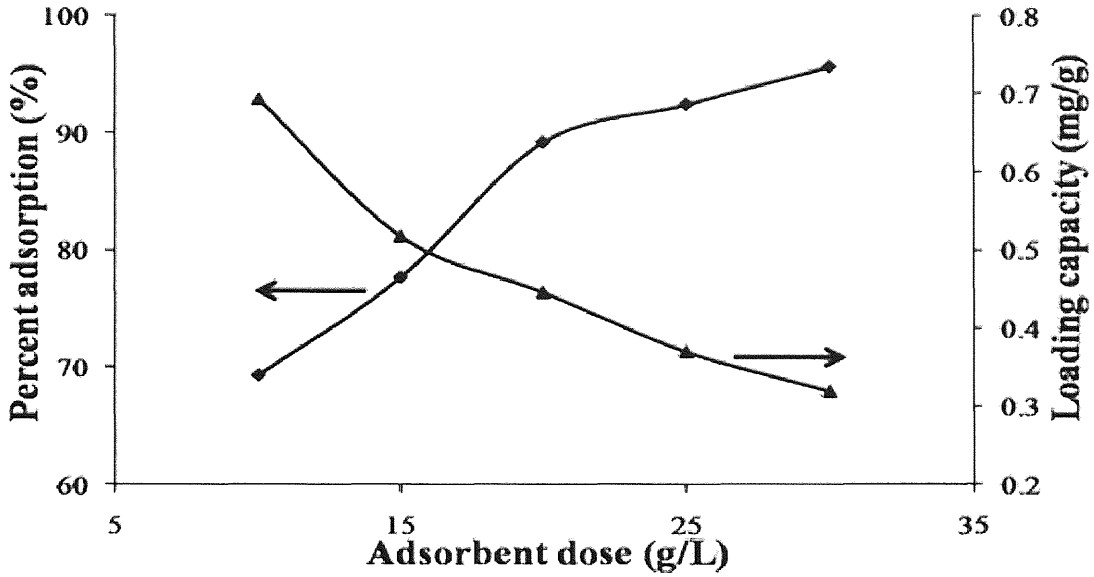

(b)

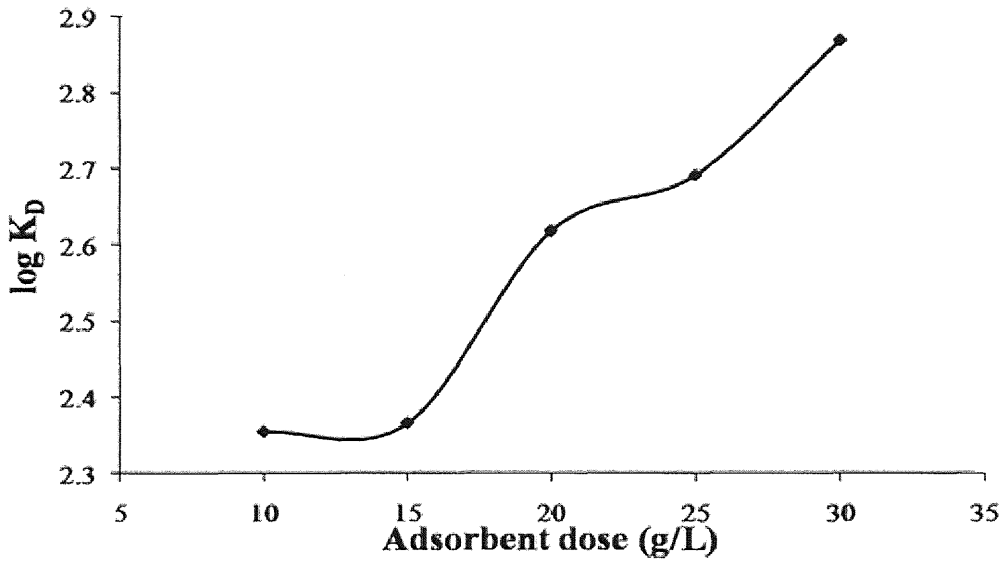

Fig.6.2 (a) Effect of prepared adsorbent dose variation on fluoride removal (Initial pH 6.9 ± 0.1, initial fluoride concentration 10 mg/L, equilibrium contact time 48 h and temperature 25 ± 1 °C). (b) The plot of log K_D value as a function of prepared adsorbent dose (data corresponding to (a))

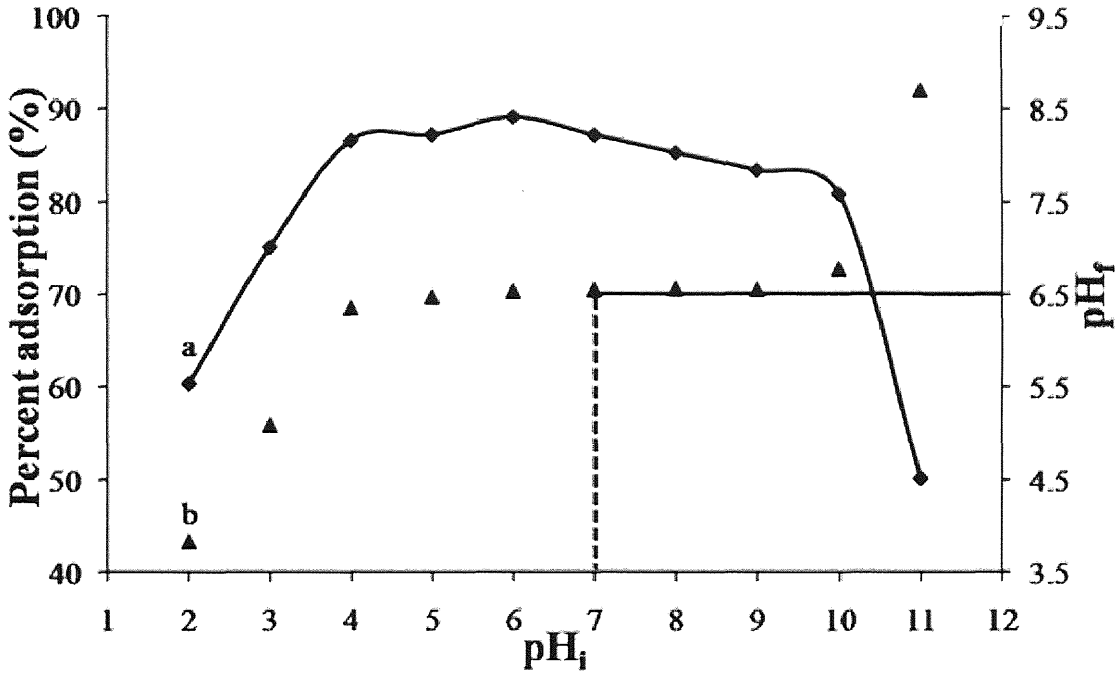

Fig.6.3 (a) Effect of initial pH (pH_i) variation on fluoride removal (Adsorbent dose 20 g/L, initial fluoride concentration 10 mg/L, equilibrium contact time 48 h and temperature 25 ± 1 °C). (b) The variation of final pH (pH_f) against initial pH (pH_i)

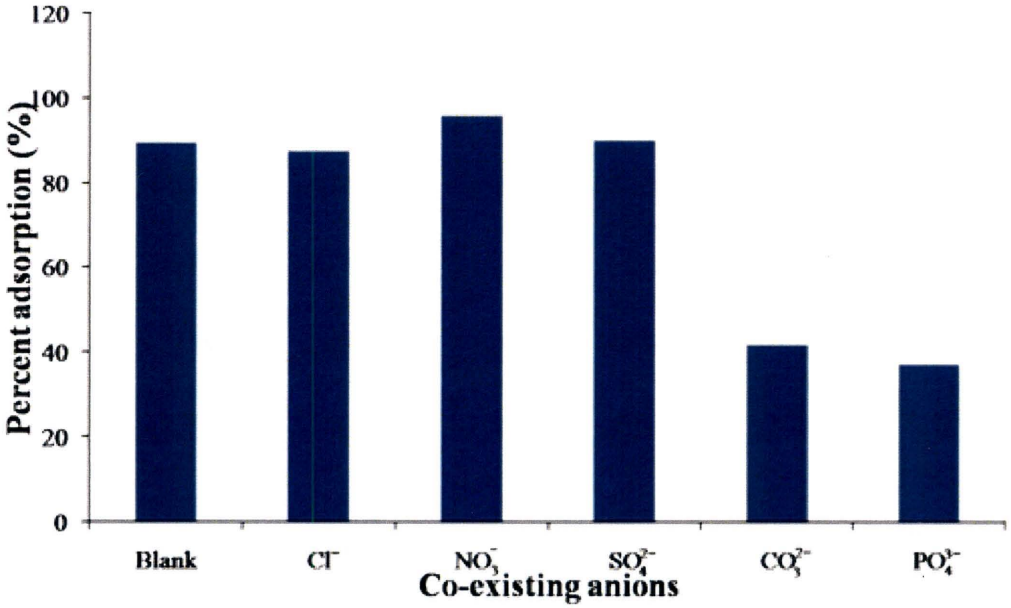

Fig.6.4 Effect of different co-existing anions for fluoride removal (Adsorbent dose 20 g/L, initial fluoride concentration 10 mg/L, equilibrium contact time 48 h and temperature 25 ± 1 °C)

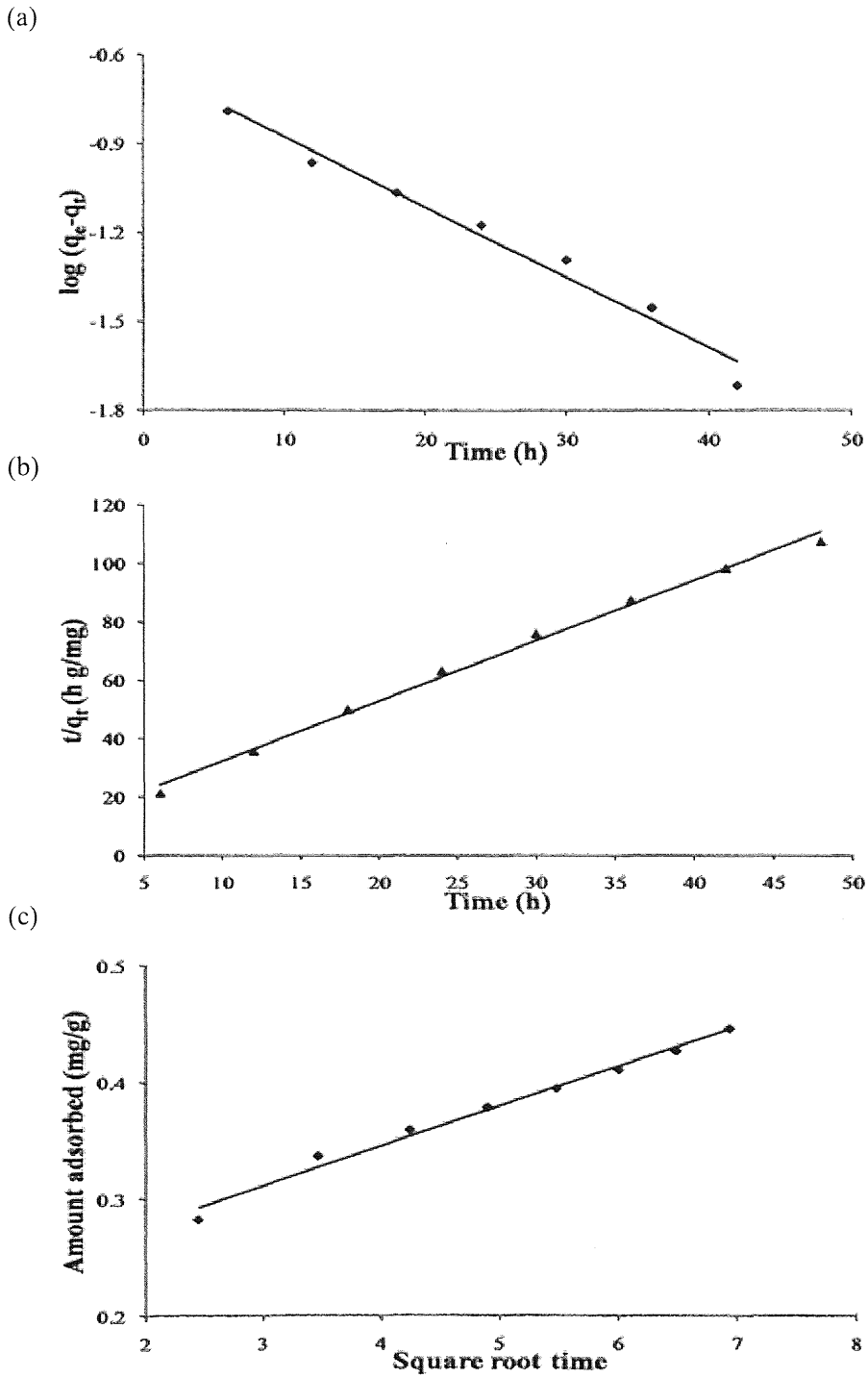

Fig.6.5 (a) Pseudo-first-order kinetic plot for fluoride removal (b) Pseudo-second-order kinetic plot for fluoride removal (c) Intra-particle diffusion plot for fluoride removal (Adsorbent dose 20 g/L, initial pH 6.9 $\pm$ 0.1, initial fluoride concentration 10 mg/L, equilibrium contact time 48 h and temperature 25 $\pm$ 1 °C)

Table 6.1
Langmuir and Freundlich isotherm parameters for the adsorption of fluoride on Al/Fe dispersed in porous granular ceramics

Langmuir isotherm		Freundlich isotherm	
q_{max} (mg/g)	1.788	$1/n$	0.468
b (L/mg)	0.313	K_F (mg/g)	0.386
R^2	0.995	R^2	0.976

Table 6.2
Kinetics parameters for adsorption of fluoride onto Al/Fe dispersed in porous granular ceramics

Initial F^- conc. (mg/L)	Pseudo-first order			Pseudo-second order			Intra-particle diffusion	
	k_1 (min^{-1})	q_e (mg g^{-1})	R^2	k_2 (g(mg^{-1} min^{-1}))	q_e (mg g^{-1})	R^2	k_i (mg g^{-1} $min^{1/2}$)	R^2
10.00	0.055	0.231	0.975	0.371	0.483	0.995	0.034	0.987

Chapter 7 Fluoride Removal by Synthetic Fe/Al Impregnated Granular Ceramics

7.1. Introduction

As described in chapter 6, in the present study, granular ceramic supported metals are prepared by impregnating granular ceramic with the corresponding iron and aluminum salt solutions followed by heat treatment. Then, a batch study was conducted into using this novel adsorbent with optimization of various experimental conditions, including initial pH, contact time, adsorbent dose and interfering ions. The experimental data were described with various isotherms and kinetic models generally adapted in the literatures to identify the adsorption mechanism.

7.2. Materials and methods

7.2.1. Preparation of adsorbent

King Kong clay (particle size was less than 75 μm), a common and inexpensive pottery clay, was provided by the Isehisa Store (Japan). Zeolite (particle size was less than 100 μm) was supplied by the Azuwan Cement Factory (Japan). Starch was purchased in the Wako Pure Chemical Industries, Ltd (Japan). King Kong clay, zeolite and starch were mixed with mass ratio 1:1:1 and prepared to be granular ceramic (particle size was 2~3 mm) according to the procedure which was given in previous literature (Chen et al., 2010). Then the prepared granular ceramic samples were immersed in a boiling mixture (100 °C) of 1.5 M $FeCl_3$ and $AlCl_3$ salt solution for 120

min. Afterwards, the impregnated granular ceramics were transferred to an oven at 105 °C for 24 h. Finally, the obtained samples were calcined at 600 °C in a muffle furnace for 1 h and then were used for further studies (Fig. 7.1).

7.2.2. Batch adsorption experiments

100 mL of the desired fluoride solution was taken into a 250 mL of conical flask and stated weight of the adsorbent was added. Then the mixture was shaken (100 rpm) on a horizontal rotary shaker (Tai Tec, Thermo Minder Mini-80, Japan). All the batch adsorption experiments were conducted at room temperature (25 ± 1 °C). Similar procedure was performed to study the effect of initial pH, adsorbent dose, initial fluoride concentration, contact time and interfering ions. The adsorption capacity was calculated using the following mass balance equation:

$$q_e = V\,(C_0 - C_e)/W \tag{7.1}$$

where q_e is the adsorption capacity (mg/g); C_0 and C_e are the initial and equilibrium fluoride concentrations (mg/L); V is the volume of aqueous solution (L) and W is the mass of adsorbent used (g).

7.2.3. Method of analysis

The synthetic iron (III)-aluminum (III) impregnated granular ceramic adsorbent was analyzed in order to determine its physicochemical properties. The morphology of adsorbent was acquired by scanning electron microscope (SEM) (JEOL, JSM-6700F, Japan). The spot element analysis of adsorbent was carried out by the energy dispersive X-ray spectroscopy detector (EDS) (JEOL, SEM-EDS, Japan). The

mineralogy of supported metal oxide was characterized by X-ray powder diffraction (XRD) (Rigaku, RINT2200, Japan). The specific surface area and pore size distributions were determined with a Brunauer-Emmett-Teller (BET) method by gas adsorption (Coulter, SA3100, Japan).

7.3. Results and discussion

7.3.1. Characterization of prepared adsorbent

As can be seen from Fig. 7.2A and B, the pristine granular ceramics and iron (III)-aluminum (III) impregnated granular ceramics were white and carmine colored spherical particles (2~3 mm in diameter), respectively. The SEM image of the pristine granular ceramics showed the expected nano-porous structure (Fig. 7.2C). A large number of microporous structures in the cross section which were formed by the sintering of inorganic and organic substances (starch) during the calcinations process. An irregular repartition of particles was observed in Fig. 7.2D. These particles were attributed to the formation of an inorganic layer dispersed by iron and aluminum salts on the granular ceramics during the impregnation process. It can be significantly observed from Fig. 7.2C and D, the inorganic particles clog up the pores of pristine granular ceramics.

The EDS spectrum of Fig. 7.3A showed the presence of Fe, Al, Ca, Mg, Si, O and Cl in the synthetic adsorbents. These results confirmed the presence of inorganic elements performed by impregnation process by iron and aluminum salts. It also can be seen that the Fe content is greater than the one of Al, which may be speculated that

Fe had a higher affinity to the granular ceramics than Al. It was difficult to establish the chemical composition of the inorganic compounds, because of the possible existence of some amorphous compounds and the complexity of the King Kong clay. However, it obviously appeared that there would be mainly iron and aluminum elements in the surface of granular ceramics from EDS results. The BET specific surface area of the synthetic adsorbents was 40.22 m^2/g and the total pore volume was 0.078 cm^3/g. The pore-size distributions showed the typical surface of the adsorbents was highly porous, with pore diameters ranging from 20 to 80 nm (Fig. 7.3B). As the radius of F (1.33 Å) is much smaller than this value, this pore size range is conductive to the penetration of F into the inner layer of the synthetic adsorbents (Chen et al., 2010).

The powder X-ray diffraction patterns of the granular ceramics that contain Fe and Al oxides are shown in Fig. 7.4. It was observed from Fig. 7.4a that diffraction peaks attributed to crystalline iron oxide, ferrimordenite, aluminum oxide, hematite and magnetite, which were due to the impregnation process by $FeCl_3$ and $AlCl_3$ salts. From Fig. 7.4b, it can be observed that the amorphous structure was significantly changed after fluoride adsorption. The diffraction peaks are attributed to crystalline iron and aluminum fluoride hydroxide hydrate and iron zinc oxide fluoride, which suggested that the uptake of fluoride ions is partly by chemical adsorption (Biswas et al., 2009).

7.3.2. Effect of solution pH

Fig. 7.5a shows the influence of initial solution pH (pH_i) on fluoride removal by iron (III)-aluminum (III) impregnated granular ceramics. The results showed that the fluoride removal efficiency increased sharply with increasing pH_i from 2.0 to 4.0, and remained nearly constant up to pH_i 9.0 and that declined against with increasing pH_i from 9.0 to 11.0. Fig. 7.5b demonstrated the variation of equilibrium pH (pH_f) from the initial pH (pH_i) during experiments. Horizontal portion at pH 6.2 $\pm$ 0.1 should be the pH_{zpc} of synthetic adsorbent. The maximum removal efficiency found at pH_i 6.0 is presumably due to the electrostatic attraction (Eq. 7.2) of fluoride by the surface positive charge or ligand/anion-exchange reaction (Eq. 7.3) of fluoride with surface hydroxyl group of the solid adsorbent (pH_{zpc} 6.2 $\pm$ 0.1) (Biswas et al., 2009). The increase in fluoride removal efficiency with increasing pH_i from 2.0 to 4.0 may be attributed to the formation of HF, which would reduce the coulombic attraction between fluoride and the adsorbent surface (Sujana et al., 1998). The fluoride removal efficiency remained nearly unaltered at pH_i 4.0-9.0, which is presumably due to the neutral or near neutral surface of the solid and may be described by the ligand/anion-exchange type reaction (Eq. 7.4). The low fluoride removal efficiency obtained at $pH_i > 9.0$ is due to the adsorption of fluoride competing with hydroxyl ion at secondary adsorption sphere (Eq. 7.5) where the Na^+ (available in solution) is at the first adsorption sphere of the solid adsorbent (Biswas et al., 2009; Raichur and Basu, 2001).

$$Fe/Al - OH + H_3O^+ + F^- \rightarrow Fe/Al - OH_2^+ \cdots F^- + H_2O \quad (7.2)$$

$$Fe/Al - OH + H_3O^+ + F^- \rightarrow (Fe/Al)^+ \cdots F^- + 2H_2O \quad (7.3)$$

$$Fe/Al - OH + F^- \rightarrow (Fe/Al)^+ \cdots F^- + OH^- \quad (7.4)$$

$$Fe/Al - OH + Na^+ + F^- + OH^- \rightarrow (Fe/Al)O^- \cdots Na^+ \cdots F^- + H_2O \quad (7.5)$$

7.3.3. Effect of adsorbent dose

Fig. 7.6 shows the effect of adsorbent dose on the fluoride removal at pH 6.9 ± 0.1. It can be found that the fluoride removal efficiency increased from 81.59% to 99.55% when the adsorbent dose increased from 10 to 30 g/L. Furthermore, the adsorption capacity (q_e, mg/g) value decreased for a fixed fluoride concentration (10 mg/L) with the increase of adsorbent dose. These results fit quite well with the increase of solid dose for a fixed solute load, and surface sites heterogeneity of the adsorbent. According to surface site heterogeneity model, the surface is composed of sites with a spectrum of binding energies. At the high adsorbent dose, the availability of higher energy sites decreases with a larger fraction of lower energy sites occupied, resulting in a low q_e value. But, at lower adsorbent dose, all types of sites are entirely exposed and the adsorption on the surface is saturated faster showing a higher q_e value (Das et al., 2005; Daifullah et al., 2007).

7.3.4. Effect of co-existing anions

Aqueous solutions usually contain many different anions such as chloride, nitrate, sulfate, carbonate and phosphate, which may interfere with the fluoride adsorption process. The present study accessed fluoride adsorption behavior in the presence of 200 mg/L different kinds of anion concentration, with initial fluoride concentration of

10 mg/L. It can be seen from Fig. 7.7 that the presence of NO_3^- and SO_4^{2-} did not interfere much with fluoride adsorption while Cl^- had a slightly negative influence. However, there was a sharp decrease in fluoride removal efficiency from 96.98% (blank) to 32.62% and 13.31% in the presence of CO_3^{2-} and PO_4^{3-}, respectively. The negative effect may be attributed to preferential/selective adsorption of CO_3^{2-} and PO_4^{3-} anions by the iron (III)-aluminum (III) impregnated granular ceramics. Similar observations have been reported by some other researchers (Mandal and Mayadeyi, 2009; Kagne et al., 2008).

7.3.5. Adsorption isotherms

The experimental data for the equilibrium isotherm of fluoride adsorption on iron (III)-aluminum (III) impregnated granular ceramics were fitted to the Langmuir and Freundlich isotherm models that are usually used to describe equilibrium adsorption data (Langmuir, 1916; Freundlich, 1906).

$$1/q_e = (1/q^0 B C_e) + 1/q^0 \quad (7.6)$$

$$log q_e = log K_f + 1/n log C_e \quad (7.7)$$

where q_e is the amount of solute adsorbed per unit weight of material (mg/g), q^0 is the maximum adsorption capacity (mg/g), B is the Langmuir constant, K_f is the minimum sorption capacity (mg/g), $1/n$ is the adsorption intensity of the Freundlich isotherm, and C_e is the equilibrium concentration of fluoride (mg/L). The isotherm constants are shown in Table 7.1. The applicability of the isotherm equations were compared by evaluating the correlation coefficients R^2. It can be seen that both the Langmuir and

the Freundlich isotherm models could fit the adsorption process. However, the Langmuir isotherm equation gave a more satisfactory fit, which indicates the adsorption takes place on a structurally homogeneous surface of the adsorbent (Langmuir, 1916). Langmuir isotherm gives a maximum monolayer capacity of 3.38 mg/g (room temperature) for iron (III)-aluminum (III) impregnated granular ceramics, which is higher than for activated alumina at 2.41 mg/g (Ghorai and Pant, 2005). The high fluoride adsorption capacity obtained in this study is mainly due to the dispersion of Fe and Al in the granular ceramics. These both elements have a strong affinity with fluoride ions. Therefore synthesized granular ceramics that are easy to implement are effective adsorbents for removing fluoride from heterogeneous environments.

7.3.6. Adsorption kinetics

Rate of adsorption, which varies with the surface and pore properties of the adsorbent is an important factor in any adsorption process. In the present study, iron (III)-aluminum (III) impregnated granular ceramics have successfully removed fluoride within 12 h and the pseudo-equilibrium was reached in 48 h. In order to describe the kinetics of fluoride adsorption in a better manner, adsorption kinetics was analyzed using two reaction kinetic models, which included pseudo-first-order (Lagergren, 1898; Ho and Mckay, 1998) and pseudo-second-order equations (Ho and Mckay, 2000).

$$\log(q_e - q_t) = \log q_e - k_1 t/2.303 \quad (7.8)$$

$$t/q_t = 1/k_2 q_e^2 + t/q_e \quad (7.9)$$

where q_t and q_e are the amount of adsorbed fluoride (mg/g) at time t and at equilibrium time, respectively. k_1 and k_2 are first-order and second-order rate constants for adsorption. The kinetics parameters for adsorption of fluoride are shown in Table 7.2. The correlation coefficient value for the pseudo-second-order (R^2=0.996) is higher than that obtained from the pseudo-first-order (R^2=0.984). Therefore, it is possible to conclude that the adsorption process by iron (III)-aluminum (III) impregnated granular ceramics followed a second-order kinetic model. This suggests that a chemisorptions step may be rate determining in the fluoride adsorption process.

To evaluate the rate-limiting of the fluoride adsorption onto iron (III)-aluminum (III) impregnated granular ceramic, the possible contribution of intra-particle diffusion on fluoride adsorption process was explored by using Weber-Morris model (Weber and Morris, 1963).

$$q_t = k_i t^{1/2} + C \tag{7.10}$$

where k_i can be calculated from the slope of the plot of q_t versus $t^{1/2}$. As shown in Fig. 7.8A, the linear portion of plot is not passing through the origin, which indicates the fluoride adsorption on iron (III)-aluminum (III) impregnated granular ceramics is a complex procedure. Both the surface adsorption as well as intra-particle diffusion contributes to the rate determining step (Mahramanlioglu et al., 2002; Sujana and Anand, 2010).

The data were further used to investigate the slow step occurring in the present adsorption system. The applicability of Bahangam's equation was given by (Aharoni and Ungarish, 1977):

$$\text{loglog}[C_0/(C_0 - q_t m)] = \log(k_0 m/2.303V) + \alpha \log t \quad (7.11)$$

where C_0 is the initial concentration of the adsorbate in solution (mg/L), V is the volume of the solution (mL), m is the weight of adsorbent used per liter of solution (g/L), q_t is the amount of adsorbate retained at time t (mg/g), α (<1) and k_0 are constants to the present system was examined. As such loglog[C_0/(C_0-$q_t m$)] was plotted against log$t$ in Fig. 7.8B. The plot was found to be linear indicating that kinetics confirmed to Bahangam's equation and therefore the adsorption of fluoride on iron (III)-aluminum (III) impregnated granular ceramics was pore diffusion controlled (Gupta et al., 2007).

7.3.7. Comparison of fluoride adsorption with other adsorbents

A comparison has been made between iron (III)-aluminum (III) impregnated granular ceramics and previously reported adsorbents for fluoride removal. As can be seen from Table 7.3, granular ceramic-supported iron and aluminum oxides as adsorbent are better than many other adsorbents in terms of fluoride adsorption capacity. The high fluoride adsorption capacity obtained in the present study is mainly due to the dispersion of Fe and Al in the granular ceramics. These both elements have a strong affinity with fluoride ions. Therefore, the iron (III)-aluminum (III) impregnated granular ceramics that are easy to implement are effectively adsorbents for removing fluoride from aqueous solution.

7.4. Conclusions

The iron (III)-aluminum (III) impregnated granular ceramic adsorbent has been

synthesized by a simple method and the material is porous with irregular surface morphology. The pH_{zpc} was 6.2 ($\pm$ 0.1) for this adsorbent. The fluoride removal efficiency increased with increasing initial solution pH (pH_i) from 2.0 to 4.0, and remained nearly constant up to pH_i 9.0 indicating that the adsorbent has promising potential utility in practical application. The presence of nitrate and sulfate did not interfere much with fluoride adsorption while chloride had a slightly negative influence. However, carbonate and phosphate showed extremely negative effect for fluoride removal efficiency. The equilibrium data described the Langmuir isotherm well, and the monolayer adsorption capacity was 3.38 mg/g. The kinetic data described the pseudo-second-order model very well. Both the intra-particle diffusion and pore diffusion played important roles in fluoride adsorption process by this adsorbent. Therefore, the elaborated iron (III)-aluminum (III) impregnated granular ceramics have a very good potential by promising environmental materials for fluoride removal from aqueous solution.

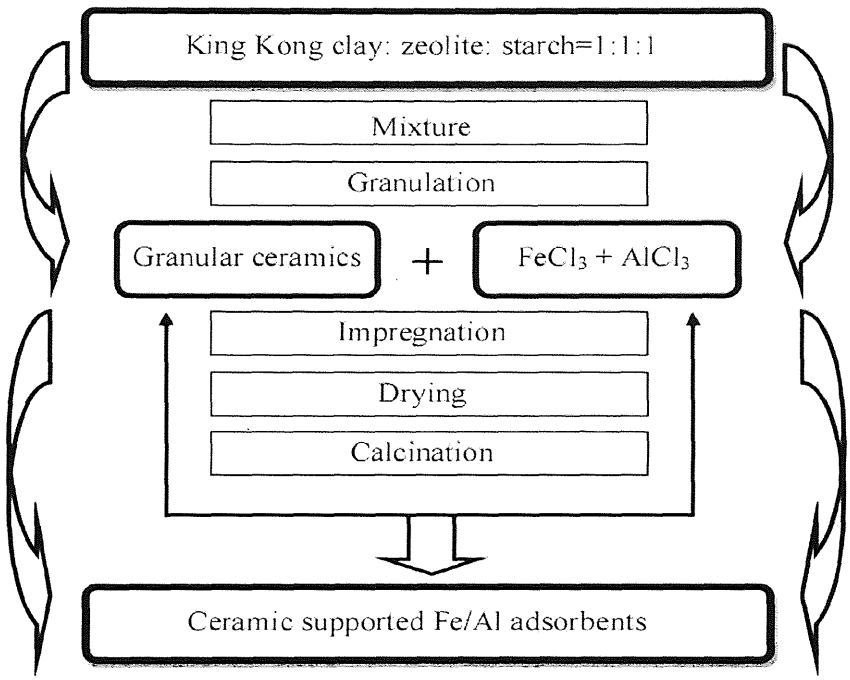

Fig.7.1 Schematic diagram for the preparation of iron (III)-aluminum (III) impregnated granular ceramics as adsorbents

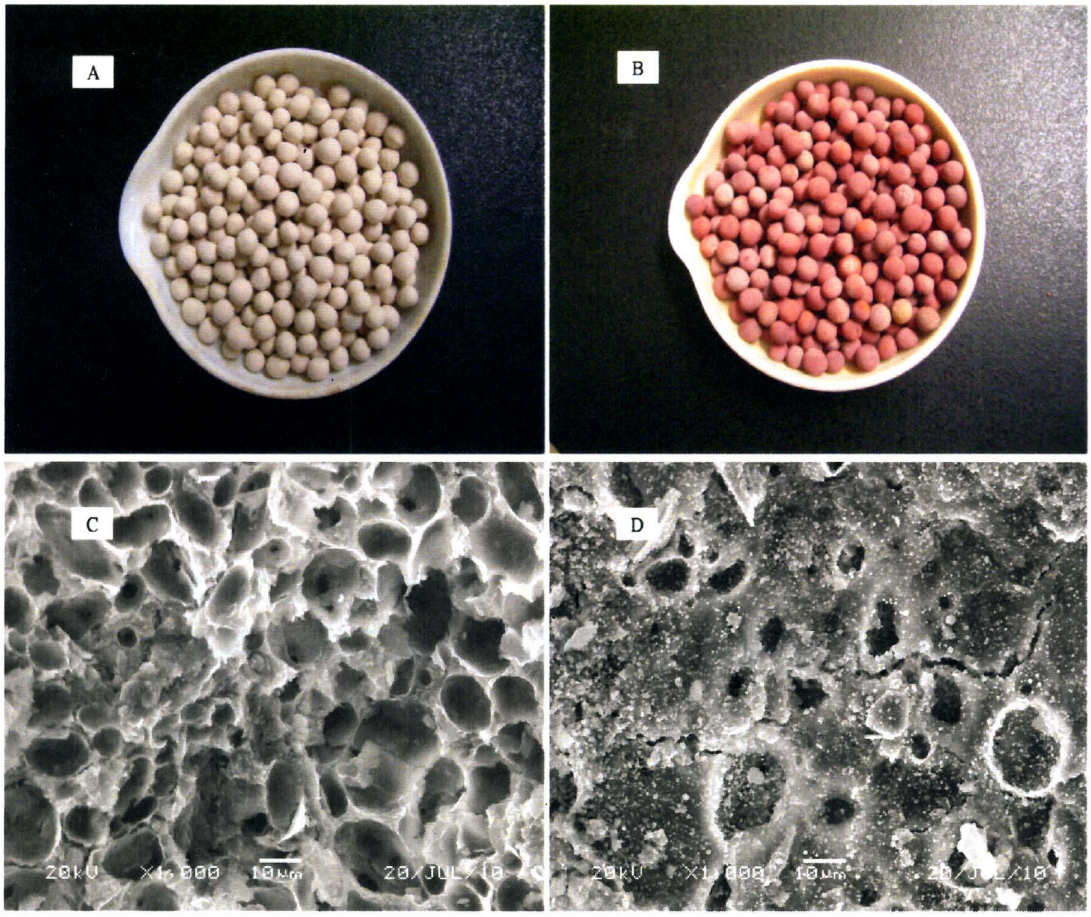

Fig.7.2 (A) Photo of pristine granular ceramics and (B) Photo of iron (III)-aluminum (III) impregnated granular ceramics, SEM images of (C) cross section of pristine granular ceramics and (D) surface section of iron (III)-aluminum (III) impregnated granular ceramics

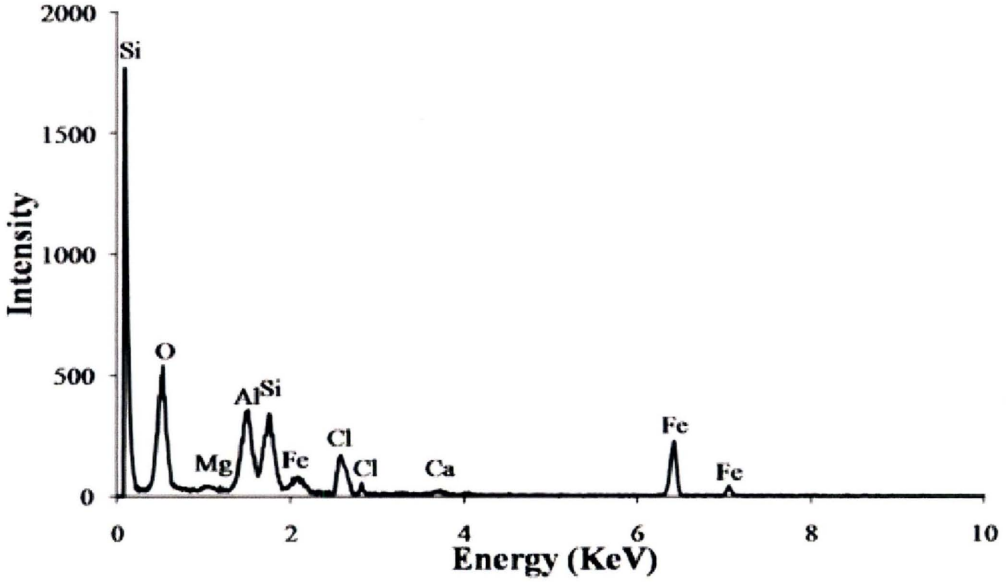

(A)

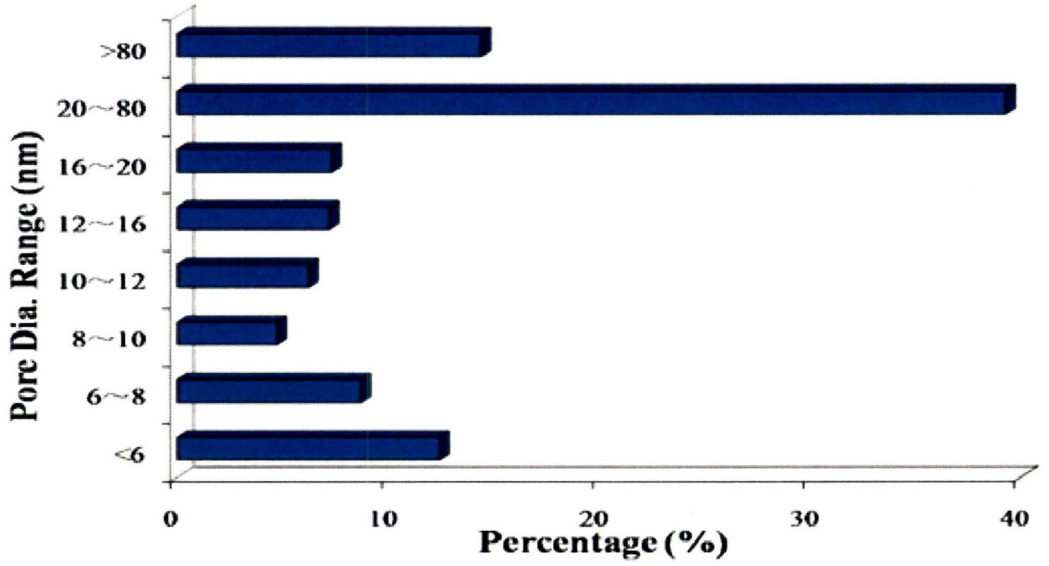

(B)

Fig.7.3 EDS spectrum of (A) iron (III)-aluminum (III) impregnated granular ceramics, BJH (Barrett-Joyner-Halenda) pore-size distribution of (B) iron (III)-aluminum (III) impregnated granular ceramics

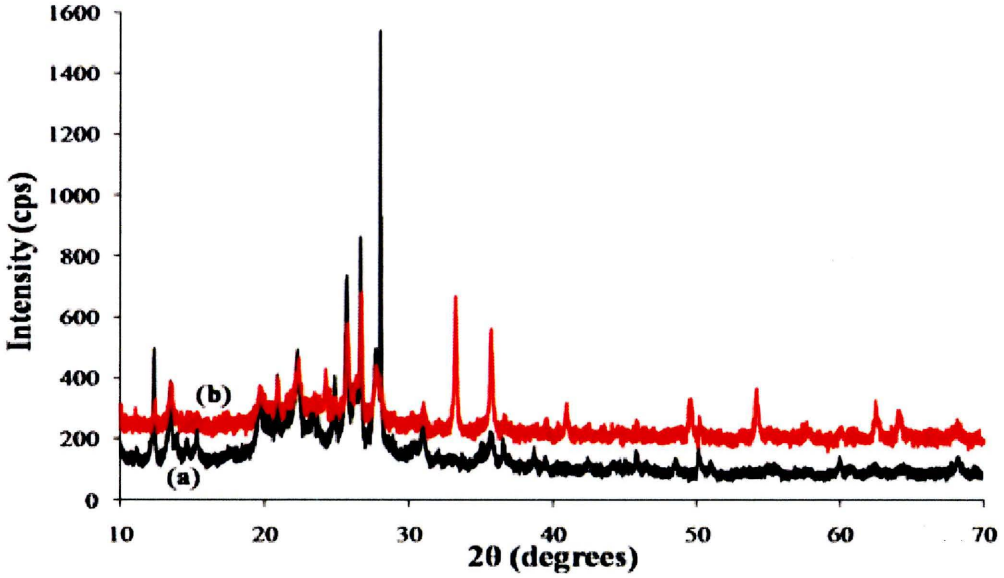

Fig.7.4 Powder XRD patterns of (a) iron (III)-aluminum (III) impregnated granular ceramics and (b) adsorbed granular ceramics

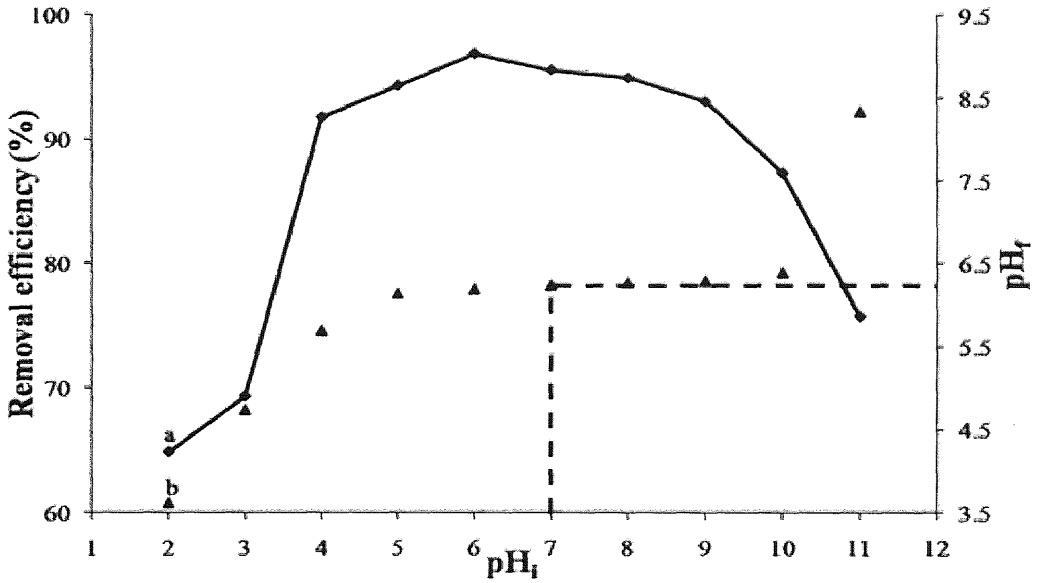

Fig.7.5 (a) The effect of initial pH (pH_i) variation on fluoride removal (Adsorbent dose 20 g/L, initial fluoride concentration 10 mg/L, equilibrium time 48 h and temperature 25 ± 1 °C), and (b) The variation of final pH (pH_f) against initial pH (pH_i)

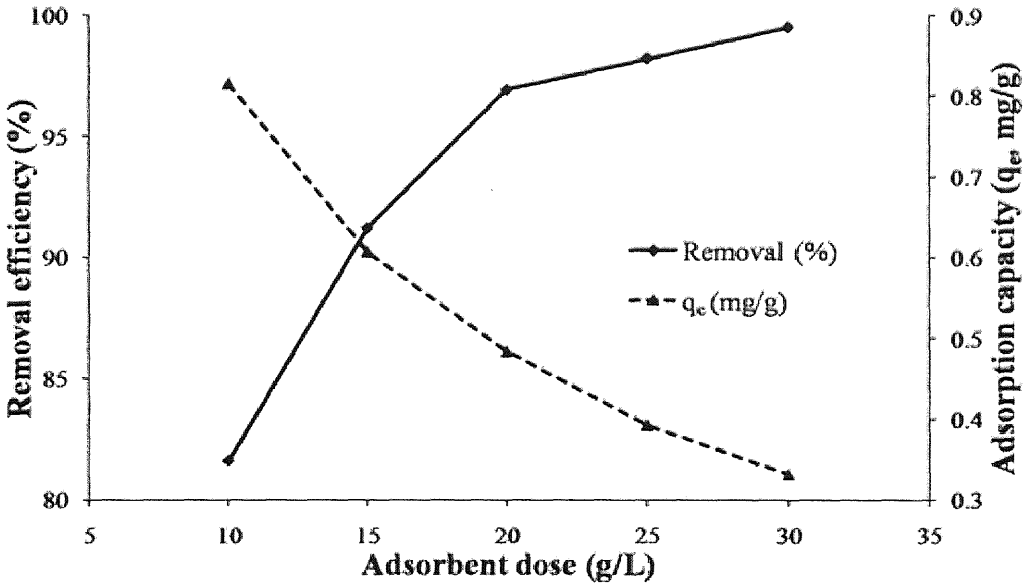

Fig.7.6 The effect of adsorbent dose on fluoride removal (Initial pH 6.9 ± 0.1, initial fluoride concentration 10 mg/L, equilibrium time 48 h and temperature 25 ± 1 °C)

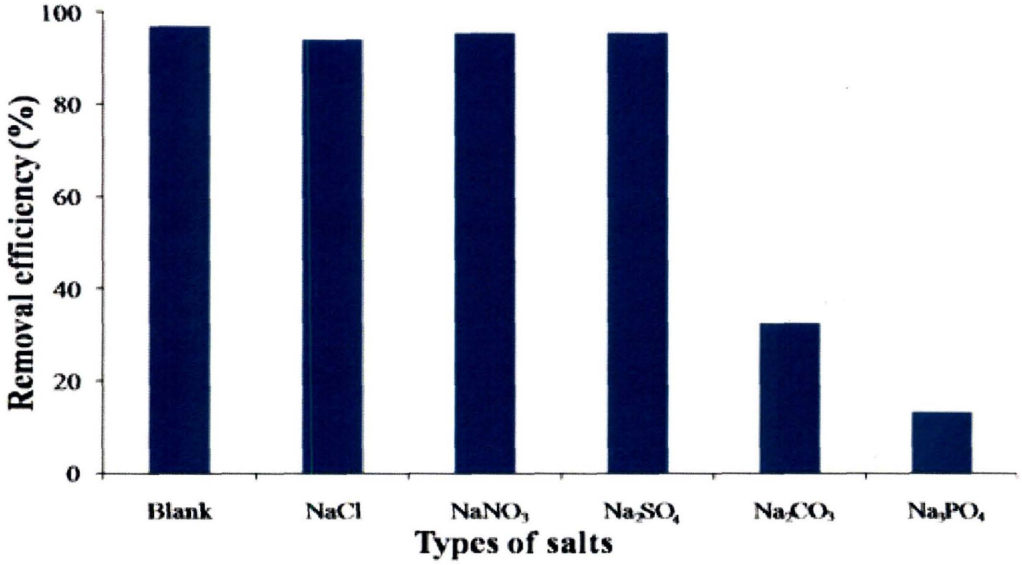

Fig.7.7 The effect of co-existing anions on fluoride removal (Adsorbent dose 20 g/L, initial fluoride concentration 10 mg/L, equilibrium time 48 h and temperature 25 ± 1 °C)

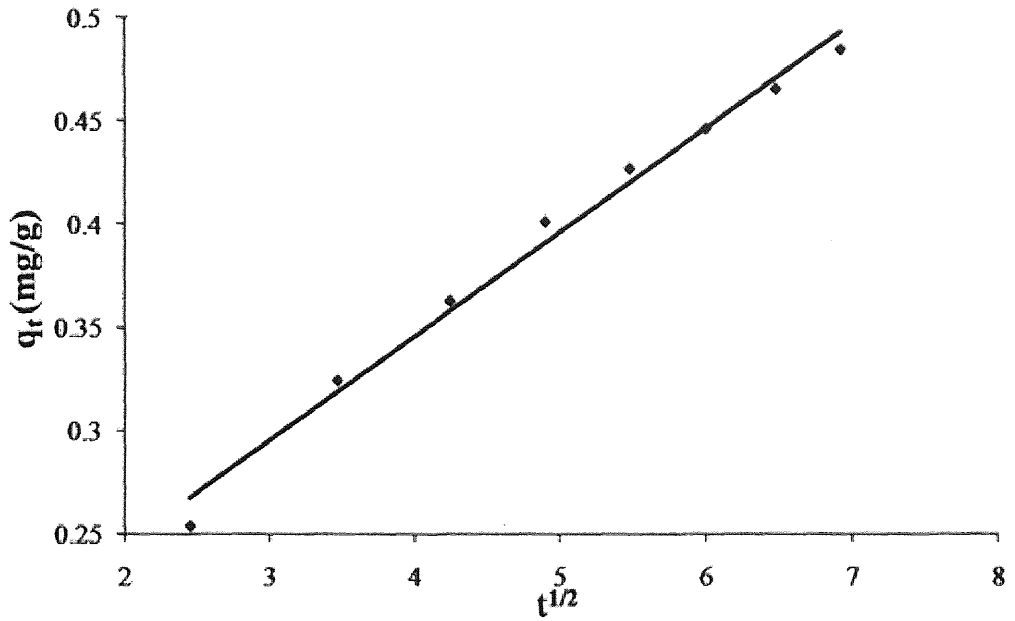

(A)

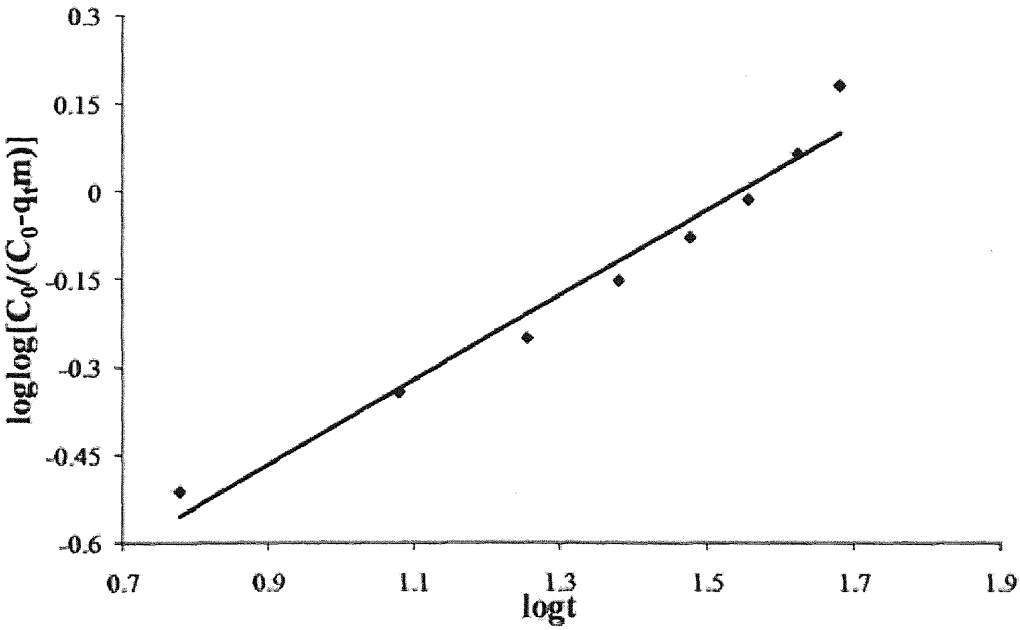

(B)

Fig.7.8 (A) Intra-particle diffusion model and (B) Bahangam's equation plot (Adsorbent dose 20 g/L, initial pH 6.9 ± 0.1, initial fluoride concentration 10 mg/L, equilibrium time 48 h and temperature 25 ± 1 °C)

Table 7.1
Langmuir and Freundlich isotherm constants for the adsorption of fluoride on iron (III)-aluminum (III) impregnated granular ceramics

Langmuir isotherm		Freundlich isotherm	
q_{max} (mg/g)	3.382	$1/n$	0.344
b (L/mg)	1.813	K_F (mg/g)	0.943
R^2	0.997	R^2	0.942

Table 7.2
Kinetics parameters for adsorption of fluoride onto iron (III)-aluminum (III) impregnated granular ceramics

Initial F^- conc. (mg/L)	Pseudo-first order			Pseudo-second order			Intra-particle diffusion	
	k_1 (min^{-1})	q_e (mg g^{-1})	R^2	k_2 (g(mg^{-1} min^{-1}))	q_e (mg g^{-1})	R^2	k_i (mg g^{-1} $min^{1/2}$)	R^2
10.00	0.069	0.417	0.984	0.202	0.562	0.996	0.051	0.988

Table 7.3
Comparison between various adsorbents used for fluoride removal

Name of sorbent	Adsorption capacity (mg/g)	Reference
AlFe650/C	13.64	Eric et al. (2010)
Iron-tin bimetal	10.05	Biswas et al. (2009)
Bleaching earth	7.75	Mahramanlioglu et al. (2002)
Carbon slurry	4.86	Gupta et al. (2007)
Iron (III)-aluminum (III) impregnated granular ceramics	3.38	Present study
Activated alumina	2.41	Ghorai and Pant. (2005)
Ceramic adsorbent	2.16	Chen et al. (2010)
Algal biosorbent Spirogyra sp.-102	1.27	Mohan et al. (2007)
Activated carbon (Al-C300)	1.10	Ramos et al. (1999)

Chapter 8 Conclusions

Fluoride removal from aqueous solution using natural clay (Kanuma mud) and ceramic materials ($FeSO_4 \cdot 7H_2O$ impregnated; Fe_2O_3 impregnated and iron-aluminum impregnated) were studied in batch and column studies. This study demonstrated the applicability of ceramic materials for removal of fluoride. Moreover, adsorption process for fluoride removal and simultaneous regeneration of these adsorbents were investigated in this research.

8.1. Fluoride removal by Kanuma mud

8.1.1. Batch adsorption process for fluoride removal by Kanuma mud

In the present study, Kanuma mud is used to be the adsorbent and the following conclusion will be made:

1) The adsorption of fluoride by using Kanuma mud is very effective and its adsorption capacity is 1.311mg/g at 5mg/L initial fluoride concentration. That indicates the adsorbent of Kanuma mud is applicable for the removal of fluoride from underground water or drinking water.

2) Among different pH, an optimum fluoride removal was observed in the pH range of 6-8. That pH is very suitable and reasonable for practical application.

3) Some of anions such as carbonate and phosphate ions have shown significant negative effect on fluoride removal by Kanuma mud. There was a sharp decrease in fluoride removal efficiency from 96.98% (blank) to 32.62% and 13.31% in the

presence of CO_3^{2-} and PO_4^{3-}, respectively.

4) Fluoride adsorption was very rapid during the first 30min and after that gradually reached the pseudo-equilibrium value in 60min. Adsorption kinetics followed pseudo-second-order model and that may indicate the process of fluoride adsorption is mainly a chemisorptions process. Besides, fluoride uptake by Kanuma mud is a complex process and intraparticle diffusion plays a significant role in the adsorption process.

5) Freundlich isotherm model can fit the equilibrium data well in this study, whereas the other three isotherm models could not predict the equilibrium data well.

6) Desorption studies showed that the fluoride can be easily desorbed at pH 12, and that indicates the adsorbent can be reused.

7) Briefly, the adsorbent is very cost effective, efficient and novel for the removal of fluoride from underground water or drinking water.

8.1.2. Column adsorption process for fluoride removal by Kanuma mud

In this study, the fluoride adsorption capacity of Kanuma mud was evaluated for fixed-bed column adsorption systems, the conclusions were drawn as follows:

1) The fixed-bed column breakthrough curves were analyzed at different flow rates, bed depth and initial fluoride concentration. Thomas and BDST models were successfully used for predicting breakthrough curves for fluoride removal by a fixed bed of Kanuma mud using different flow rates and bed depths.

2) The F-adsorbed Kanuma mud can be regenerated and reused with minimal loss

of efficiency after three adsorption-desorption cycles.

3) The use of Kanuma mud as an adsorbent for fluoride removal is potentially cost-effective and may provide an alternative method for fluoride removal from contaminated water.

8.2. Fluoride removal by ceramic materials

8.2.1. Fluoride removal by iron-impregnated ceramic adsorbent

In this study, a novel sorbent, ferrous-amended ceramic adsorbent has been prepared and examined for its potential in removing fluoride from aqueous solution. The conclusions were drawn as follows:

1) Its granular structure, high surface area and effective capacity of fluoride removal make the adsorbent a highly potential media to be used in purification of fluoride from water.

2) The adsorption capacity of ceramic adsorbent for fluoride was 2.16 mg/g at 30 °C. The sorption process was fitted well with both the Langmuir and Freundlich isotherm models.

3) Kinetic study results indicate that the adsorption process followed a pseudo-second-order kinetic model.

4) The optimum fluoride removal was observed at pH ranges of 4.0-11.0 indicating that the ceramic adsorbent has promising potential utility in practical application. The fluoride adsorption was reduced in the presence of carbonate, phosphate and sulfate and increased slightly in the presence of chloride and nitrate ions.

5) The ceramic adsorbent also can be regenerated several times with 0.1 M HCl as eluent. Therefore, the new ceramic adsorbent is a promising material for fluoride removal from water environment.

8.2.2. Fluoride removal by comparing different kinds of adsorbents

In the present study, iron-impregnated novel granular ceramic adsorbents with high specific surface areas were synthesized by simple granulation procedure at room temperature. The conclusions were drawn as follows:

1) This study has demonstrated that both GC ($FeSO_4 \cdot 7H_2O$) and GC (Fe_2O_3) adsorbents can be used for fluoride removal from aqueous solution, while GC ($FeSO_4 \cdot 7H_2O$) is more effective for fluoride removal than GC (Fe_2O_3).

2) Maximum adsorption of fluoride on GC ($FeSO_4 \cdot 7H_2O$) and GC (Fe_2O_3) at pH 7.0 and 4.0 were 94.23% and 60.48%, respectively. The equilibrium data of samples fitted well to both Langmuir and Freundlich isotherms.

3) Both of these two granular adsorbents followed second-order kinetics and were governed by intra-particle diffusion model. With the increase in temperature from 303 to 323 K, fluoride removal on these two adsorbents increased indicating combination of physical and chemical adsorption process.

4) The calculated thermodynamic parameters showed that both of the adsorption processes were thermodynamically favorable, spontaneous and endothermic in nature. Moreover, the particle size of these granular ceramics was around 3~5 mm, which would not block the sewer and could be easily separated from water.

5) Therefore, the iron-impregnated granular ceramic is a potential material to be used in practical application of defluoridation from aqueous solution.

8.2.3. Fluoride removal by Fe/Al impregnated ceramics (Knar)

In this study, Al and Fe dispersed in porous granular ceramics were prepared by the impregnation process with aluminum and iron chloride salts followed by a precipitation. The conclusions were drawn as follows:

1) These low-cost adsorbents have shown a good efficiency in fluoride removal from aqueous solution and can be useful for environmental protection purposes.

2) The loading capacity of these prepared adsorbents for fluoride was 1.79 mg/g at room temperature.

3) The optimum fluoride removal was observed at pH ranges of 4.0-9.0 indicating that the adsorbent has promising potential utility in practical application. Carbonate and phosphate ions showed extremely negative effect, nitrate ion showed slightly positive effect while chloride and sulfate ions really did not affect the fluoride removal.

4) The adsorption process was fitted well with both the Freundlich and Langmuir isotherm models. Kinetic study results indicate that the adsorption process followed a pseudo-second-order kinetic model.

5) Therefore, the elaborated porous granular ceramics with mixed aluminum and iron oxides have a good potential by promising environmental materials for fluoride removal from aqueous solution.

8.2.4. Fluoride removal by Fe/Al impregnated ceramics (King Kong)

The iron (III)-aluminum (III) impregnated granular ceramic adsorbent has been synthesized by a simple method and the material is porous with irregular surface morphology. The following conclusions were drawn from the results:

1) The pH_{zpc} was 6.2 ($\pm$ 0.1) for this adsorbent. The fluoride removal efficiency increased with increasing initial solution pH (pH_i) from 2.0 to 4.0, and remained nearly constant up to pH_i 9.0 indicating that the adsorbent has promising potential utility in practical application.

2) The presence of nitrate and sulfate did not interfere much with fluoride adsorption while chloride had a slightly negative influence. However, carbonate and phosphate showed extremely negative effect for fluoride removal efficiency.

3) The equilibrium data described the Langmuir isotherm well, and the monolayer adsorption capacity was 3.38 mg/g.

4) The kinetic data described the pseudo-second-order model very well. Both the intra-particle diffusion and pore diffusion played important roles in fluoride adsorption process by this adsorbent.

5) The elaborated iron (III)-aluminum (III) impregnated granular ceramics have a very good potential by promising environmental materials for fluoride removal from aqueous solution.

References

Apparao B.V., G. Kartikeyan, 1986. Permissible limits of fluoride on in drinking water in India inrural environment. *Int. J. Environ. Protec.* 6 (3), 172-175.

Aldaco R., A. Irabien, P. Luis, 2005. Fluidized bed reactor for fluoride removal. *Chem. Eng. J.* 107, 113-117.

Ayoob S., A.K. Gupta, P.B. Bhakat, V.T. Bhat, 2008. Investigations on the kinetics and mechanisms of sorptive removal of fluoride from water using alumina cement granules. *Chem. Eng. J.* 140, 6-14.

Aksu Z., F. Gonen, 2004. Bisorption of phenol by immobilized activated sludge in a continuous packed bed: prediction of breakthrough curves. *Process Biochem.* 39, 599-613.

Arami M., N.Y. Limaee, N.M. Mahmoodi, N.S. Tabrizi, 2005. Removal of dyes from colored textile wastewater by orange peel adsorbent: equilibrium and kinetic studies. *J. Colloid and Inter. Sci.* 288, 371-376.

Aharoni C., M. Ungarish, 1977. Kinetics of activated chemisorptions, Part-2. Theoretical models. *J Chem Soc., Faraday Trans.* 1: *Phys Chem Condens Phases.* 73 (3), 456-464.

Bulusu K.R., B.N. Pathak, 1980. Discussion on water defluoridation with activated alumina. *J. Environ. Eng. Div.* 106 (2), 466-469.

Bail A.L., C. Jacoboni, M. Lebalc, H. Depape, J.L. Fourquet, 1988. Crystal structure of the metastable form of aluminum trifluoride β-AlF_3 and the gallium and indium homologs. *J. Solid. State. Chem.* 77, 96-101.

Brandt, R.K., M.R. Hughes, L.P. Bourget, K. Truszkowska, R.G. Greenler, 1993. The interpretation of CO adsorbed on Pt/SiO_2 of two different particle-size

distributions. *Surf. Sci.* 286, 15–25.

Barbier J.P., P. Mazounie, 1984. Methods of reducing high fluoride content in drinking water. *Water. Supply.* 2, SS 8/1-4.

Bhargava D.S., D.J. Killedar, 1992. Fluoride adsorption on fishbone charcoal through a moving media adsorber. *Water Res.* 26(6), 781-788.

Biswas K., K. Gupta, A. Goswami, U.C. Ghosh, 2010. Fluoride removal effeiciency from aqueous solution by synthetic iron (III)-aluminum (III)-chromium(III) ternary mixed oxide. *Desalination.* 255, 44-51.

Biswas K., K. Gupta, U.C. Ghosh, 2009. Adsorption of fluoride by hydrous iron(III)-tin (IV) bimetal mixed oxide from the aqueous solutions. *Chem. En. J.* 149, 196-206.

Cao J., Y. Zhao, J.W. Liu, 1997. Brick tea consumption as the cause of dental fluorosis among children from Mongol, Kazak and Yugu populations in China. *Food. Chem. Toxicol.* 35, 827-833.

Culp R., H. Stolenberg, 1958. Fluoride reduction at La Cross, Kan. *J. AWWA.* 50(3), 423-431.

Cengeloglu Y., E. Kir, M. Ersoz, 2002. Removal of fluoride from aqueous solution by using red mud. *Sep. Purif. Technology.* 28, 81-86.

Chutia P., S. Kato, T. Kojima, S. Satokawa, 2009. Arsenic adsorption from aqueous solution on synthetic zeolites. *J. Hazard. Mater.* 162, 440-447.

Chen N., Z.Y. Zhang, C.P. Feng, N. Sugiura, M. Li, R.Z. Chen, 2010. Fluoride removal from water by granular ceramic adsorption. *J. Colloid and Inter. Sci.* 348, 579-584.

Chen N., Z.Y. Zhang, C.P. Feng, N. Sugiura, M. Li, R.Z. Chen, D.R. Zhu, 2010. An excellent fluoride sorption behavior of ceramic adsorbent. *J. Hazard. Mater.*

183, 460-465.

China standard for drinking water quality. 2006. *GB 5749-2006*, Vol. 1.

Carrillo R.J.J., A. Cardona, W.M. Edmunds, 2002. Use of abstraction regime and knowledge of hydrogeological conditions to control high-fluoride concentration in abstracted groundwater: San Luis Potosi basin, Mexico. *J. Hydrol.* 261, 24-47.

Chubar N.I., V.F. Samanidou, V.S. Kouts, G.G. Gallios, V.A. Kanibolotsky, V.V. Strelko, I.Z. Zhuravlev, 2005. Adsorption of fluoride, chloride, bromide and bromated ions on a novel ion exchanger. *J. Colloid and Inter. Sci.* 291, 67-74.

Dieye A., C. Larchet, B. Auclair, C.M. Diop, 1998. Elimination des fluorures parla dialyse ionique croisee. *Eur. Polym.* 34, 67-75.

Das N., P. Pattanaik, Das, 2005. Defluoridation of drinking water using activated titanium rich bauxite. *J. Colloid and Inter. Sci.* 292, 1-10.

Do˘gan M., M. Alkan, A. Türkyilmaz, Y. Özdemir, 2004. Kinetics and mechanism of removal of methylene blue by adsorption onto perlite. *J. Hazard. Mater.* 109, 141-148.

Ding W.M., T. Hairet, X. Huang, 2008. Primary study of fluoride removal from aqueous solution by activated ferric hydroxide, in: *2nd International Conference on Bioinformatics and Biomedical Engineering (ICBBE 08).* 2911-2913.

Daifullah A.A.M., S.M. Yakout, S.A. Elreefy, 2007. Adsorption of fluoride in aqueous solutions using $KMnO_4$-modified activated carbon derived from stem pyrolysis of rich straw. *J. Hazard. Mater.* 147, 633-643.

Eskandarpour A., M.S. Onyango, A. Ochieng, 2008. Removal of fluoride ions from aqueous solution at low pH using schwertmannite. *J. Hazard. Mater.* 152,

571-579.

Eric T.K., A. Véronique, C.P N. Njiki, A. Nathalie, N. Emmanuel, D. André, 2010. Preparation and characterization of charcoals that contain dispersed aluminum oxide as adsorbents for removal of fluoride from drinking water. *Carbon.* 48, 333-343.

Ergun E., A. Tor, Y. Cengeloglu, I. Kocak, 2008. Electrodialytic removal of fluoride from water: Effects of process parameters and accompanying anions. *Sep. Purif. Technol.* 64, 147-153.

Fluorine and fluorides, 1984. Environmental Health Criteria. *IPCS International Programme on Chemical Safety.* 36.

Fan X., D.J. Parker, M.D. Smith, 2003. Adsorption kinetics of fluoride on low cost materials. *Water Res.* 37, 4929-4937.

Freundlich H.M.F., 1906. Über die adsorption in losungen. *Z. Phys. Chem.* 57A, 385-470.

Fuhrman H.G., L.C. Tjell, D. Mcconchie, 2004. Adsorption of arsenic from water using activated neutralized red mud. *Environ. Sci. Technol.* 38, 2428-2434.

Grimaldo M., V.H. Borjaaburto, A.L. Ramirez, 1995. Endemic fluorosis in Sanluis, Potosi, Mexico.1. Identification of risk-factors associated with human exposure to fluoride. *Environ. Res.* 68, 25-30.

Ghorai S., K.K. Pant, 2005. Equilibrium, kinetics and breakthrough studies for adsorption of fluoride on activated alumina. *Sep. Purif. Technol.* 42, 265-271.

Gopal V., K.P. Elango, 2006. Equilibrium, Kinetics and thermodynamic studies of adsorption of fluoride onto plaster of paris. *J. Hazard. Mater.* 141, 98-105.

Gupta V.K., I. Ali, V.K. Saini, 2007. Defluoridation of wastewaters using waste carbon slurry. *Water Res.* 41, 3307-3316.

Hem J.O., 1959. Study and interpretation of chemical characteristics of natural water. U. G. *Geological Survey Water Supply Paper.* 1473.

Hichour M., F. Persin, J. Sandeaux, J. Molenat, C. Gavach, 1999. Water defluoridation by donann dialysis and electrodialysis. *Rev. Sci. Eau.* 12, 671-686.

Hichour M., F. Persin, J. Sandeaux, C. Gavach, 2000. Fluoride removal from waters by Donnan dialysis. *Sep. Purif. Technol.* 18, 1-11.

Hu C.Y., S.L. Lo, W.H. Kuan, Y.D. Lee, 2005. Removal of fluoride from semiconductor wastewater by electrocoagulation-flotation. *Water Res.* 39, 895-901.

Harouiya N., E.H. Oelkers, 2004. An experimental study of the effect of aqueous fluoride on quartz and alkali-feldspar dissolution rates. *Water Res.* 205, 155-167.

Hutchins R.A., 1973. New method simplifies design of activated carbon system. *Chem. Eng.* 80, 133-138.

Ho Y.S., 2006. Review of second-order models for adsorption systems. *J. Hazard. Mater.* 136, 681-689.

Ho Y.S., G. Mckay, 1999. Pseudo-second order model for sorption process. *Process. Biochem.* 34, 451-465.

Ho Y.S., G. Mckay, 1998. Kinetic models for the sorption of dye from aqueous solution by wood. *Pocess. Saf. Environ. Prot.* 76 (B2), 183-191.

Ho Y.S., G. Mckay, 2000. The kinetics of sorption of divalent metal ions onto sphagnum moss peat. *Water Res.* 34, 735-742.

Hiemstra T., W.H.V. Riemsdijk, 2000. Fluoride adsorption on goethite in relatio to different types of surface sites. *J. Colloid and Inter. Sci.* 225, 94-104.

Ikuo A., I. Satoshi, T. Toshimitsu, K. Naohito, N. Takeo, T. Seiki, 2004. Adsorption of fluoride ions onto carbonaceous materials. *J. Colloid and Inter. Sci.* 275, 35-39.

Islam M., R.K. Patel, 2007. Evaluation of removal efficiency of fluoride from aqueous solution using quick lime. *J. Hazard. Mater.* 143, 303-310.

Joshi S.V., S.H. Mehta, A.P. Rao, A.V. Rao, 1992. Estimation of sodium fluoride using HPLC in reverse osmosis experiments. *Water Treat.* 10, 307-312.

Kagne S., S. Jagtap, P. Dhawade, S.P. Kamble, S. Devotta, S.S. Rayalu, 2008. Hydrated cement: A promising adsorbent for the removal of fluoride from aqueous solution. *J. Hazard. Mater.* 154, 88-95.

Khan A.A., P.P. Singh, 1987. Adsorption thermodynamics of carbofuran on Sn (IV) arsenosicicate in H^+, Na^+ and Ca^{2+} forms. *J. Colloid. Surf.* 24, 33-42.

Kumr E., A. Bhatnagar, M. Ji, W. Jung, 2009. Defluoridation from aqueous solution by granular ferric hydroxide (GFH). *Water Res.* 43, 490-498.

King P., N. Rakesh, S. Beenalahari, Y.P. Kumar, V.S.R.K. Prasad, 2007. Removal of lead from aqueous solution using Syzygium cumini L: equilibrium and kinetic studies. *J. Hazard. Mater.* 142, 340-347.

Li H.R., Q.B. Liu, W.Y. Wang, L.S. Yang, Y.H. Li, F.J. Feng, X.Y. Zhao, K. Hou, G. Wang, 2009. Fluoride in drinking water, brick tea infusion and human urine in two countries in Inner Mongolia, China. *J. Hazard. Mater.* 167, 892-895.

Lagergren S., K. Svenska, 1898. About the theory of so called adsorption of soluble substances. *K. Sven. Vetenskapsad. Handl.* 24(4), 1-39.

Langmuir I., 1916. The constitution and fundamental properties of solids and liquids. *J. Am. Chem. Soc.* 38, 2221-2295.

Mira A.K., A. Mishra, 2007. Study of quaternary aquifers in Ganga Plain, India: focus on groundwater salinity, fluoride and fluorosis. *J. Hazard. Mater.* 144, 438-448.

Malde M.K., A. Maage, E. Macha, 1997. Fluoride content in selected food items from five areas in East Africa. *J. Food. Compost. Anal.* 10, 233-245.

Meenakshi, R.C. Maheshwari, 2006. Fluoride in drinking water and its removal. *J. Hazard. Mater.* 137B, 456-463.

Muthukumaran K., N. Balasubramanian, T.V. Ramakrishna, 1995. Removal of fluoride by chemically activated carbon. *Ind. J. Environ. Protec.* 15 (7), 514-517.

Mahramanlioglu M., I. Kizilcikli, I.O. Bicer, 2002. Adsorption of fluoride from aqueous solution by acid treated spent bleaching earth. *J. Fluorine. Chem.* 115, 41-47.

Meenakshi S., C.S. Sundaram, S. Rugmini, 2008. Enhanced fluoride sorption by mechanochemically activated kaolinites. *J. Hazard. Mater.* 153, 164-172.

Min Y., T. Hashimoto, N. Hoshi, H. Myoga, 1999. Fluoride removal in a fixed bed packed with granular calcite. *Water Res.* 33 (16), 3395-3402.

Mckee R., W.S. Johnston, 1999. Removal of fluorides from drinking water using low-cost adsorbent. *Ind. J. Environ. Health.* 41 (1), 53-58.

Meenakshi S., N. Viswanathan, 2007. Identification of selective ion-exchange resin for fluoride sorption. *J. Colloid and Inter. Sci.* 308, 438-450.

Mellah A., S. Chegrouche, 1997. The removal of zinc from aqueous solutions by natural bentonite. *Water Res.* 31, 621-629.

Mitali S., B. Aparna, P.P. Partha, R.S. Asit, 2006. Use of laterite for the removal of fluoride from contaminated drinking water. *J. Colloid and Inter. Sci.* 302,432-441.

Makhni S.S., 1980. The parathyroid in human fluorotic syndrome. *Fluoride.* 13, 17-19.

Maliyekkal S.M., A.K. Sharma, L. Philip, 2006. Manganese-oxide-coated alumina: a promising sorbent for defluoridation of water. *Water Res.* 40, 3497-3506.

Mandal S., S. Mayadevi, 2008. Adsorption of fluoride ions by Zn-Al layered double hydroxides. *Applied. Clay. Sci.* 40, 54-62.

Mandal S., S. Mayadevi, 2009. Defluoridation of water using as-synthesized Zn/Al/Cl anionic clay adsorbent: Equilibrium and regeneration studies. *J. Hazard. Mater.* 167, 873-878.

Murray J.W., W.E. Stumm, 1988. Aquatic surface chemistry: Chemical processes at the particle-water interface. John Wiley & Sons, New York. 52, 1742.

Moore W.J., 1971. Magnetic field effects on the excitation spectra of neutral group II double acceptors in germanium. *J. Phys and Chem. Solids.* 32, 93-102.

Meenakshi V.K., K. Garg, A.M. Renuka, 2004. Groundwater quality in some villages of Haryana, India: focus on fluoride and fluorosis. *J. Hazard. Mater.* 106, 85-97.

Ministry of Health of the People's Republic of China. 2007. *Chinese Health Statistical Digest.* http://www.moh.gov.cn/open/2007tjts/P50.htm.

Mohan S.V., S.V. Ramanaiah, B. Rajkumar, P.N. Sarma, 2007. Removal of fluoride from aqueous phase by biosorption on to algal biosorbent spirogyra sp.-102: sorption mechanism elucidation. *J. Hazard. Mater.* 141, 465-474.

Nawalakhe W.G., D.N. Kulkarni, B.N. Pathak, K.R. Bulusu, 1974. Defluoridation of water with alum. *Ind. J. Environ. Health.* 16 (1).

Ndiaye P.I., P. Moulin, L. Dominguez, J.C. Millet, F. Charbit, 2005. Removal of fluoride from electronic industrial effluent by RO membrane separation. *Desalination.* 173, 25-32.

Onyango M.S., Y. Kojima, O. Aoyi, E.C. Bernardo, H. Matsuda, 2004. Adsorption

equilibrium modeling and solution chemistry dependence of fluoride removal from water by trivalent-cation-exchanged zeolite. *J. Colloid and Inter. Sci.* 279, 341-350.

Oguz E., 2005. Adsorption of fluoride on gas concrete materials. *J. Hazard. Mater.* 117B, 227-233.

Parker C.L., C.C. Fong, 1975. Fluoride removal technology and cost estimates. *Ind. Wastes.* 23-25.

Qaiser S., A.R. Saleemi, M. Umar, 2009. Biosorption of lead from aqueous solution by ficus religiosa leaves: Batch and column study. *J. Hazard. Mater.* 166, 998-1005.

Raichur A.M., M.J. Basu, 2001. Adsorption of fluoride onto mixed rare earth oxides. *Sep. Purif. Technol.* 24, 121-127.

Rai K., M. Agarwal, S.R. Shivastava, S. Das, 2000. Fluoride: diffusive mobility in soil and some remedial measures to control its plant uptake. *Curr. Sci.* 79, 1370.

Rubel J.F., 1983. The removal of excess fluoride from drinking water by the activated alumina method. *Paragon Press. Salt Lake City.* 345.

Ramos R.L., J.O. Turrubiartes, M.A.S. Castillo., 1999. Adsorption of fluoride from aqueous solution on aluminum-impregnated carbon. *Carbon.* 37 (4), 609-617.

Ramos R.L., J.R.R. Mendez, L.A.B. Jacome, M.S.B. Mendoza, 2005. Intraparticle diffusion of cadmium and zinc ions during sorption from aqueous solution on activated carbon. *J. Chem. Technol. Biotechnol.* 580, 924-933.

Reimann C., K. Bjorvatn, B. Frengsta, Z. Melaku, H.R. Tekle, U. Siewers, 2003. Drinking water quality in the Ethiopian section of the East African Rift Valley I—data and health aspects. *Sci. Tot. Environ.* 311, 65–80.

Ruthven D.M., 1984. Principles of sorption and sorption processes. John Wiley &

Sons Publishers, New York, (Chapter 6).

Rude P.D., R.C. Aller, 1993. The influence of Mg^{2+} on the sorption of fluoride by hydrous oxides in seawater. *Am. J. Sci.* 293, 1-24.

Singh R., R.C. Maheshwari R.C., 2001. Defluoridation of drinking water - a review. *Ind. J. Environ. Protec.* 21 (11), 983-991.

Singh G., B. Kumar, P.K. Sen, J. Majumdar, 1999. Removal of fluoride from spent pot liner leachate using ion exchange. *Water. Environ. Res.* 71, 36-42.

Saha S., 1993. Treatment of aqueous effluent for fluoride removal. *Water Res.* 27, 1347-1350.

Sarkar M., A. Banerjee, P.P. Prammanick, A.R. Sarkar, 2006. Use of laterite for the removal of fluoride from contaminated drinking water. *J. Colloid and Inter. Sci.* 302, 432-441.

Sushree S.T., B. Jean-Luc, G. Krishna, 2006. Removal of fluoride from drinking water by adsorption onto alum-impregnated activated alumina. *Sep. Purif. Technol.* 50, 310-317.

Shen F., X. Chen, P. Gao, G. Chen, 2003. Electrochemical removal of fluoride ions from industrial wastewater. *Chem. Eng. Sci.* 58, 987-993.

Sourirajan S., T. Matsurra, 1972. Studies on reverse osmosis for water pollution control. *Water Res.* 6, 1073-1086.

Shihabudheen M., Maliyekkal, S. Sanjay, P. Ligy, M.N. Indumathi, 2008. Enhanced fluoride removal from drinking water by magnesia-amended activated alumina granules. *J. Eng. Chem.* 140, 183-192.

Simons R., 1993. Trace element removal from ash dam waters by nanofiltration and diffusion dialysis. *Desalination.* 89, 325-341.

Sairam S.C., V. Natrayasamy, S. Meenakashi, 2008. Defluoridation of water using

magnesia/ chitosan composite. *J. Hazard. Mater.* 163, 618-624.

Sujana M.G., R.S. Thakur, S.B. Rao, 1998. Removal of fluoride from aqueous solution by using alum sludge. *J. Colloid and Inter. Sci.* 206, 94-101.

Sangi M.R., A. Shahmoradi, J. Zolgharnein, G.H. Azimi, M. Ghorbandoost, 2008. Removal and recovery of heavy metals from aqueous solution using Ulmus carpinifolia and Fraxinus excelsior tree leaves. *J. Hazard. Mater.* 155, 513-522.

Solangi I.B., S. Memon, M.I. Bhanger, 2010. An excellent fluoride sorption behavior of modified amberlite resin. *J. Hazard. Mater.* 176, 186-192.

Stumm W., 1992. Chemistry of the solid-water interface. John Wiley & Sons, Inc, New York.

Sujana M.G., G. Soma, N. Vasumathi, S. Anand, 2009. Studies on fluoride adsorption capacities of amorphous Fe/Al mixed hydroxides from aqueous solutions. *J. Fluorine. Chem.* 130, 749–754.

Sujana M.G., S. Anand, 2010. Iron and aluminum based mixed hydroxides: A novel sorbent for fluoride removal from aqueous solutions. *Applied. Sur. Sci.* 256, 6956-6962.

Suzuki T., M. Kanesato, T. Yokoyama, 1990. Removal of fluorides from aqueous solutions. *Japanese Kokai Tokkyo Koho* (Patent number 02191543).

Tan J.A., 1990. The atlas of endemic diseases and their environments in the People's Republic of China. *Science Press*. Beijing. 156-159.

Tor A., N. Danaoglu, G. Arslan, Y. Cengeloglu, 2009. Removal of fluoride from water by using granular red mud: Batch and column studies. *J. Hazard. Mater.* 164, 271-278.

Tor A., 2007. Removal of fluoride from water using anion-exchange membrane under Donnan dialysis condition. *J. Hazard. Mater.* 141, 814-818.

Tor A., 2006. Removal of fluoride from an aqueous solution by using montmorillonite. *Desalination.* 201, 267-276.

Thomas H.C., 1944. Heterogeneous ion exchange in a flowing system. *J. Am. Chem. Soc.* 66, 1664-1666.

Uddin M.T., M. Rukanuzzaman, M.M.R. Khan, M.A. Islam, 2009. Adsorption of methylene blue from aqueous solution by jackfruit (*Artocarpus heteropyllus*) leaf powder: A fix-bed column study. *J. Environ. Manage.* 90, 3443-3450.

Viswanathan N., S. Meenakshi, 2008. Enhanced fluoride sorption using La(III) incorporated carboxylated chitosan beads. *J. Colloid and Inter. Sci.* 322, 375–383.

World Health Organization (WHO), SDE/WSH/03.04/96, 2004. Fluoride in drinking water background document for development for development of WHO guidelines for drinking water quality. *Fluorine and Fluorides*. Geneva.

World Health Organization (WHO), 1984. Environmental Health Criteria 36, International Programme on Chemical Safety. *Fluorine and Fluorides*. Geneva.

Wang L.F., J.Z. Huang, 1995. Outline of control practice od endemic fluorosis in China. *Soc. Sci. Med.* 41, 1191-1195.

Wang L.F., 1993. Fluorosis and habit of drinking tea in Kazak in Xinjiang. *Chin. J. End. Dis. Bull.* 8, 43.

Wang R.S., H. Li, P. Na, W. Ying, 1995. Study of a new adsorbent for fluoride removal from waters. *Water. Qual. Res. J. Can.* 30 (1), 81-88.

Wang S.X., Z.H. Wang, X.T. Cheng, J. Li, Z.P. Sang, X.D. Zhang, 2007. Arsenic and fluoride exposure in drinking water: children's IQ and growth in Shanyin country, Shanxi province, China. *Environ. Health. Perspect.* 115 (4), 643-647.

Worku N., Z. Feleke, B.S. Chandravanshi, 2007. Removal of excess fluoride from

water using waste residue from alum manufacturing process. *J. Hazard. Mater.* 147, 954-963.

Weber W.J., J.C. Morris, 1963. Kinetics of adsorption on carbon from solution. *J. Sanit. Eng. Div. ASCE.* 89, 31-59.

Wu X., Y. Zhang, X. Dou, M. Yang, 2007. Fluoride removal performance of a novel Fe- Al-Ce trimetal oxide adsorbent. *Chemosphere.* 69 (11), 1758-1764.

Xiong X.Z., J.L. Liu, W.H. He, 2007. Dose-effect relationship between drinking water fluoride levels and damage to liver and kidney functions in children. *Environ. Res.* 103, 112-116.

Xu Y.M., A.R. Ning, J. Zhao, 2001. Preparation and defluoridation performance of activated cerium (Ⅳ) oxide/SiMCM-41 adsorbent in water. *J. Colloid and Inter. Sci.* 235, 66-69.

Yang M., T. Hashimoto, N. Hoshi, H. Myoga, 1999. Fluoride removal in a fixed bed packed with granular calcite. *Water Res.* 33, 3395-3402.

Acknowledgement

I wish to express my sincere appreciation to my academic advisor, Professor Zhenya Zhang, for his guidance, friendship, and encouragement during my studies at Tsukuba University. His professionalism is an excellent example I can follow throughout my career.

I would like to thank the other academic advisors, Associate Professor Yingnan Yang and Professor Norio Sugiura for their supervision, guidance and support during my studies in my research.

I also would like to express my great appreciation to my dissertation committee members, Associate Professor Motoo Utsumi, Professor Norio Sugiura, Associate Professor Yingnan Yang and Professor Yoshiro Higano, for their numerous suggestions, comments, willingness and helpful discussions to serve as my advisory committee members.

Special gratitude is expressed to my mentor, Professor Chuanping Feng, China University of Geosciences (Beijing), China, for his kind assistances and suggestions in both academic concern and daily life.

I would like to truthfully thank Ph. D. Chunyi Zhi in National Institute for Materials Science and Ph.D. Yoshihisa Ohko in National Institute of Advanced Industrial Science and Technology (AIST), for their kind assistances and suggestions in my experiments.

Many friends and fellow students deserve recognition for their direct and indirect

contributions to this dissertation. I wish to express my appreciation to Miao Li, Rongzhi Chen, Yulin Zhou, Yonggang Liu, Dirui Zhu, Ying Zhao, Shuang Zhang, Qinghong Wang, Yu Gao, Xu Guo, Chao Zhao, Ruiqing Li, Qiang Xue, Wei Yang, and many others for their countless assistance during the years of my study here.

I reserve much of my appreciation for my family. This dissertation would not have been completed without their love and support.

This dissertation is dedicated to the people of the world who have devoted their lives to the protection of our environment.